

Research Project Number TPF-5(193) Supplement #78

DEVELOPMENT OF A TRANSITION BETWEEN FREE-STANDING AND REDUCED-DEFLECTION PORTABLE CONCRETE BARRIERS – PHASE I

Submitted by

Mojdeh Asadollahi Pajouh, Ph.D.
Post-Doctoral Research Associate

Jennifer D. Schmidt, Ph.D., P.E.
Research Assistant Professor

Robert W. Bielenberg, M.S.M.E., E.I.T.
Research Engineer

Ronald K. Faller, Ph.D., P.E.
Research Associate Professor
MwRSF Director

MIDWEST ROADSIDE SAFETY FACILITY

Nebraska Transportation Center
University of Nebraska-Lincoln
130 Whittier Research Center
2200 Vine Street
Lincoln, Nebraska 68583-0853
(402) 472-0965

Submitted to

WISCONSIN DEPARTMENT OF TRANSPORTATION

4802 Sheboygan Avenue
Madison, Wisconsin 53707

MwRSF Research Report No. TRP-03-366-17

August 8^{Deve}, 2017

TECHNICAL REPORT DOCUMENTATION PAGE

1. Report No. TRP-03-366-17	2.	3. Recipient's Accession No.	
4. Title and Subtitle Development of a Transition Between Free-Standing and Reduced-Deflection Portable Concrete Barriers – Phase I		5. Report Date August 8Deve, 2017	
7. Author(s) Asadollahi Pajouh, M., Schmidt, J.D., Bielenberg, R.W., and Faller, R.K.		8. Performing Organization Report No. TRP-03-366-17	
9. Performing Organization Name and Address Midwest Roadside Safety Facility (MwRSF) Nebraska Transportation Center University of Nebraska-Lincoln 130 Whittier Research Center 2200 Vine Street Lincoln, Nebraska 68583-0853		10. Project/Task/Work Unit No.	
12. Sponsoring Organization Name and Address Wisconsin Department of Transportation 4802 Sheboygan Avenue Madison, Wisconsin 53707		11. Contract © or Grant (G) No. TPF-5(193) Supplement #78	
15. Supplementary Notes		13. Type of Report and Period Covered Final Report: 2014 – 2017	
16. Abstract <p>The objective of this research effort was to develop a <i>Manual for Assessing Safety Hardware 2016</i> (MASH) Test Level 3 (TL-3) transition between the recently developed non-anchored, reduced-deflection, F-shape, Portable Concrete Barrier (PCB) system and free-standing, F-shape PCB segments. The reduced-deflection PCB system consisted of a cap plate bolted across the PCB joint and continuous tubes running along the sides of the barriers, which was successfully crash tested under MASH 2016 TL-3. A transition was developed between the reduced-deflection PCB and free-standing PCB systems through engineering analysis and LS-DYNA computer simulation. First, the continuous steel tubes in the reduced-deflection system were tapered down to match the surface of the free-standing PCB segments at a 1:6 lateral-to-longitudinal rate to reduce the potential for vehicle snag. An HSS 3½x3½x⅜ steel tube was added between adjacent PCB segments at the base of two joints upstream from the reduced-deflection system to improve transition performance. Simulations were performed to determine the critical impact points (CIP) for full-scale crash testing of the selected design. It was recommended to conduct three full-scale crash tests, two tests with test designation no. 3-21 with a 2270P pickup truck vehicle, and one test with test designation no. 3-20 using an 1100C passenger car to evaluate the system. For test designation no. 3-21, two impact locations were deemed critical, one at 4.3 ft (1.3 m) upstream from the transition joint (i.e., upstream from the end of the free-standing PCB and upstream from the reduced-deflection PCB system), which is the MASH 2016 recommended CIP, and one at 55.7 ft (17 m) upstream from the transition joint. For test designation no. 3-20, the CIP was recommended to be 3.6 ft (1.1 m) upstream from the transition joint.</p>		14. Sponsoring Agency Code	
17. Document Analysis/Descriptors Highway Safety, Roadside Appurtenances, MASH, Computer Simulation, LS-DYNA, Temporary Concrete Barrier, Portable Concrete Barrier, Reduced Deflection, Transition		18. Availability Statement No restrictions. Document available from: National Technical Information Services, Springfield, Virginia 22161	
19. Security Class (this report) Unclassified	20. Security Class (this page) Unclassified	21. No. of Pages 59	22. Price

DISCLAIMER STATEMENT

This report was completed with funding from the Wisconsin Department of Transportation. The contents of this report reflect the views and opinions of the authors who are responsible for the facts and the accuracy of the data presented herein. The contents do not necessarily reflect the official views or policies of the Wisconsin Department of Transportation. This report does not constitute a standard, specification, regulation, product endorsement, or an endorsement of manufacturers.

ACKNOWLEDGEMENTS

The authors wish to acknowledge several sources that made a contribution to this project: (1) Wisconsin Department of Transportation for funding this project and (2) the Holland Computing Center at the University of Nebraska for the high-performance computing resources.

Acknowledgement is also given to the following individuals who made a contribution to the completion of this research project.

Midwest Roadside Safety Facility

J.D. Reid, Ph.D., Professor
J.C. Holloway, M.S.C.E., E.I.T., Test Site Manager
K.A. Lechtenberg, M.S.M.E., E.I.T., Research Engineer
S.K. Rosenbaugh, M.S.C.E., E.I.T., Research Engineer
C.S. Stolle, Ph.D., Research Assistant Professor
A.T. Russell, B.S.B.A., Shop Manager
S.M. Tighe, Laboratory Mechanic
D.S. Charroin, Laboratory Mechanic
M.A. Rasmussen, Laboratory Mechanic
E.W. Krier, Laboratory Mechanic
Undergraduate and Graduate Research Assistants

Wisconsin Department of Transportation

Jerry Zogg, P.E., Chief Roadway Standards Engineer
Erik Emerson, P.E., Standards Development Engineer
Rodney Taylor, P.E., Roadway Design Standards Unit Supervisor

TABLE OF CONTENTS

TECHNICAL REPORT DOCUMENTATION PAGE	i
DISCLAIMER STATEMENT	ii
ACKNOWLEDGEMENTS	iii
TABLE OF CONTENTS.....	iv
LIST OF FIGURES	vi
LIST OF TABLES	viii
1 INTRODUCTION	1
1.1 Background and Problem Statement.....	1
1.2 Objective	3
1.3 Scope.....	3
2 LITERATURE REVIEW	4
2.1 NCHRP Report 350 PCB Testing.....	4
2.2 MASH 2009 PCB Testing	5
2.2.1 Free-Standing F-Shape PCB	5
2.2.2 Transition from Temporary to Permanent Median Barrier (MwRSF).....	6
2.2.3 Transition from Pinned PCB to Rigid Concrete Barrier (TTI)	7
2.3 Termination of Box Beam in Roadside Systems	9
2.4 Other Horizontal Flares in Barrier Systems.....	11
3 TRANSITION DESIGN AND ANALYSIS	13
3.1 Design Criteria	13
3.2 Design Concepts	13
4 TEST REQUIREMENTS AND EVALUATION CRITERIA	16
4.1 Test Requirements	16
4.2 Evaluation Criteria	16
5 LS-DYNA MODEL.....	18
5.1 PCB Model.....	18
5.2 Reduced-Deflection Steel Components Model.....	18
5.3 Baseline model.....	21
6 SIMULATIONS WITH SLOPED TUBES	25
6.1 Sloped Tubes Model	25
6.2 Simulation of Sloped Tube Model with Different Impact Points	25
7 SIMULATION OF PROPOSED TRANSITION DESIGN MODIFICATIONS	30
7.1 Evaluation Criteria	30
7.2 Tube Spacer Added at Joint No. 1	30
7.3 Tube Spacers Added at Joints Nos. 1 and 2.....	36

7.3.1 Single Tubes with Increased Thickness 38
7.3.2 Simulations of Dual Tubes..... 40
7.3.3 Selected Design Modification..... 43

8 DETERMINATION OF CRITICAL IMPACT POINTS 45
8.1 Determination of CIPs – Test Designation No. 3-21 45
8.2 Determination of CIP – Test Designation No. 3-20 51
8.3 MASH 2016 TL-3 Test Matrix for Evaluation of Transition 53

9 SUMMARY, CONCLUSIONS, AND RECOMMENDATIONS 54

10 REFERENCES 57

LIST OF FIGURES

Figure 1. WisDOT Modified Reduced-Deflection Portable Concrete Barrier [4].....2
Figure 2. Free-standing F-Shape PCB to Rigid Barrier Transition [8].....4
Figure 3. Temporary Concrete Barrier to Permanent Concrete Barrier Transition, Test Nos. TCBT-1 and TCBT-2 [10].....7
Figure 4. Transition Design for Anchored Temporary Barrier to Rigid Concrete Barrier [11].....8
Figure 5. Layout of Transition Design for Anchored Temporary Barrier to Rigid Concrete Barrier [11].....9
Figure 6. BEAT-SSCC Configuration [12-14]10
Figure 7. State of New York Standard Details for Box-Beam to Concrete Parapet Transition [16-17]11
Figure 8. Tapered Concrete Bridge Parapets [18]12
Figure 9. Tubes Tapered Down to Reduced-Deflection PCB Segments Surface.....14
Figure 10. Details of Tubes Tapered Down to Reduced-Deflection PCB Segment Surface.....15
Figure 11. Joint Spacer (Steel Tube) at Transition Joint15
Figure 12. F-shape PCB Barrier Model19
Figure 13. Sequential Photographs: Simulation of Test No. 2214TB-2.....20
Figure 14. Test No. RDTCB-1 Model22
Figure 15. Test No. RDTCB-2 Final Barrier Model.....23
Figure 16. Sequential Photographs: Baseline Simulation of Test No. RDTCB-224
Figure 17. Simulated Tubes Tapered Along Reduced-Deflection PCB Segments’ Surface25
Figure 18. Simulated Tubes Tapered Along Reduced-Deflection PCB Segments’ Surface26
Figure 19. Simulated Vehicle Snag on “Knee” in Transition Region – Impact Point 225.6 in. (5,730 mm) Upstream from Transition Joint.....28
Figure 20. Simulated Vehicle Damage Caused by “Knee” – Impact Point 225.6 in. (5,730 mm) Upstream from Transition Joint28
Figure 21. Sequential Photographs: Impact Point at 225.6 in. (5,730 mm) Upstream from Transition Joint (Left) and Impact Point at 351.6 in. (8,930 mm) Upstream from Transition Joint (Right).....29
Figure 22. Transition with Single Steel Tube at Joint No. 1.....31
Figure 23. Steel Tube Model – HSS 3½x3½x¼31
Figure 24. Crushed Steel Tube at Joint No. 1 After Impact: (a) Tube on Ground, (b) Tube Raised ½ in.....32
Figure 25. Simulated Cases with One Tube at Joint No. 1– Impact Points.....33
Figure 26. Knee Contact on Vehicle Door– Impact Point 225.6 in. (5,730 mm) Upstream from Transition Joint.....34
Figure 27. Sequential Photographs: Impact Point at 225.6 in. (5,730 mm) Upstream from Transition Joint with One Steel Tube35
Figure 28. Single Steel Tube Added at Joint Nos. 1 and 236
Figure 29. Simulated Cases with Tube at Joints Nos. 1 and 2 – Impact Points.....37
Figure 30. (a) Tube Added at Joint No. 1, (b) Tube Added at Joint Nos. 1 and 2 – Impact Point 351.6 in. (8,930 mm) Upstream from Transition Joint.....38
Figure 31. (a) HSS 3½x3½x¼ Tube Added at Joint Nos. 1 and 2, (b) HSS 3½x3½x¾ Tube Added at Joint Nos. 1 and 2 – Impact Point 225.6 in. (5,730 mm) Upstream from Transition Joint39

Figure 32. Single Tube HSS 3½x3½x¾ Added at Joint Nos. 1 and 2 – After Impact39

Figure 33. Dual Tubes – HSS 3½x3½x¼ Tube with HSS 2½x2½x¼ Tube Inside Added at Joint Nos. 1 and 2.....40

Figure 34. Dual Tubes – Stack of Two HSS 3½x1½x¼ Tubes Added at Joint Nos. 1 and 241

Figure 35. Modified Transition Design: (a) HSS 3½x3½x¼ Tube Added, (b) HSS 3½x3½x¼ Tube with HSS 2½x2½x¼ Tube Inside, and (c) Stack of Two HSS 3½x1½x¼ Tubes Added at Joint Nos. 1 and 2 – Impact Point 225.6 in. (5,730 mm) Upstream from Transition Joint42

Figure 36. Single Tube HSS 3½x3½x¾ Added at Joint Nos. 1 and 2.....44

Figure 37. Simulated Cases with Tube at Two Joints Nos. 1 and 2 – Impact Points45

Figure 38. Vehicle Snag on Box Tubes Along Reduced-Deflection PCB – Impact Point 4.3 ft (1.3 m) Upstream from Transition Joint.....46

Figure 39. Knee Contact – Impact Point 669.3 in. (17,000 mm) Upstream from Transition Joint.....47

Figure 40. Sequential Photographs: Impact at MASH 2016-Recommended CIP 4.3 ft (1.3 m) Upstream from Transition Joint – 2270P Vehicle.....49

Figure 41. Sequential Photographs: Impact at MASH 2016-Recommended CIP 669.3 in. (17,000 mm) Upstream from Transition Joint – 2270P Vehicle50

Figure 42. Sequential Photographs: Impact Point at 3.6 ft (1.1 m) Upstream from Transition Joint.....52

Figure 43. Recommended CIPs – 3.6 ft (1.1 m) Upstream from Transition Joint for 1100C Vehicle Testing (Blue Arrow) and 4.3 ft and 55.7 ft (1.3 m and 17 m) upstream from Transition joint for 2270P Vehicle Testing (Red Arrows).....56

LIST OF TABLES

Table 1. F-Shape PCB Deflections6
Table 2. MASH 2016 TL-3 Crash Test Conditions for Transitions16
Table 3. MASH 2016 Evaluation Criteria for Transitions.....17
Table 4. Comparison of Reduced-Deflection PCB System Test and Simulation.....21
Table 5. Summary of Simulation Results – Only Tapered Tubes, No Transition in Stiffness.....27
Table 6. Summary of Simulation Results – Tube on Ground and Raised Tube.....32
Table 7. Summary of Simulation Results – One Steel Tube at Base of Joint No. 133
Table 8. Summary of Simulation Results – Single Steel Tube at Base of Joint Nos. 1 and 2.....37
Table 9. Summary of Simulation Results – Impact Point 225.6 in. (5,730 mm) Upstream
from Transition Joint – Single and Dual Tubes.....43
Table 10. Summary of Simulation Results – HSS 3½x3½x¾ Single Tube at Joints Nos. 1
and 2.....48
Table 11. Summary of Simulation Results – Thick Single Tube and Dual Tubes.....51
Table 12. MASH 2016 TL-3 Test Matrix for Evaluation of Transition53

1 INTRODUCTION

1.1 Background and Problem Statement

Portable concrete barriers (PCBs) are often used in applications where it is desired that their deflection during vehicular impacts be limited, such as on bridge decks and in some work-zones. The Wisconsin Department of Transportation (WisDOT) currently employs the F-shape PCB design previously developed by the Midwest Roadside Safety Facility (MwRSF) [1-4]. However, this system has large deflections which may restrict it from being used in limited-sized construction zones.

WisDOT desired a concept for reducing barrier deflections without the need for additional tie-down anchors and that could be retrofitted to their current PCB with minimal modification. MwRSF recently completed a research effort to develop and test a new, low-deflection system that utilized the F-shape PCB without anchorage to the roadway surface [5, 6].

The initial system design consisted of a cap plate bolted across the PCB joint and continuous tubes running along the sides of the barriers. It was anticipated that the combination of the steel cap and tubes would be effective in limiting barrier deflection through composite action. Further, the continuous tubes would interlock with a vehicle's sheet metal and provide increased vehicle stability by presenting a more vertical barrier face. Full-scale crash test no. RDTCB-1 was conducted on the initial low-deflection PCB design, with the back of the PCB system offset 24 in. (610 mm) away from the edge of a simulated bridge deck. Test no. RDTCB-1 consisted of a 4,998-lb (2,267-kg) pickup truck impacting the low-deflection PCB system at a speed of 63.6 mph (102.4 km/h) and at an angle of 24.9 degrees. The impacting vehicle was safely and smoothly redirected in the test, and all of the barrier segments were safely retained on the edge of the bridge deck. The peak dynamic lateral deflection of the barrier system was 43.0 in. (1,092 mm), which represented a 46 percent reduction in deflection as compared to the free-standing, F-shape PCB crash testing under *Manual for Assessing Safety Hardware 2016* (MASH) Test Level 3 (TL-3) [7].

Following the crash test of the initial low-deflection PCB system, design modifications were proposed and investigated to further reduce dynamic system deflections. The proposed design modifications included: (1) increased barrier-to-ground friction; (2) increased tube thickness; (3) increased cap thickness; (4) reduced joint gap tolerance; and (5) additional attachment points for the tubes to the PCB segments. An LS-DYNA model of the low-deflection PCB system in test no. RDTCB-1 was created and validated, and this model was used to evaluate the proposed design modifications. The simulation results and input from the sponsor led to the selection of additional attachment points between the tubes and the PCB to further stiffen the barrier system. Test no. RDTCB-2 was conducted to evaluate the modified barrier system.

The modified system consisted of a cap plate bolted across the PCB joint, continuous tubes running along the sides of the barriers, and the additional attachment points, as shown in Figure 1. Full-scale crash test no. RDTCB-2 was conducted on the final iteration of the low-deflection PCB with the back of the PCBs offset 24 in. (610 mm) away from the edge of a simulated bridge deck. Test no. RDTCB-2 consisted of a 4,978-lb (2,258-kg) pickup truck impacting the low-deflection PCB system at a speed of 64.8 mph (104.3 km/h) and at an angle of 25.4 degrees. The impacting vehicle was safely and smoothly redirected in the test, and all of the barrier segments were safely retained on the edge of the bridge deck. The peak dynamic lateral deflection of the barrier system

was 40.7 in. (1,034 mm), which represented a 49 percent reduction in deflection as compared to the free-standing, F-shape PCB under MASH 2016 crash testing.



Figure 1. WisDOT Modified Reduced-Deflection Portable Concrete Barrier [5]

This research project focused on the design and evaluation of the length-of-need of the new, low-deflection PCB system. However, additional considerations must be taken into account when implementing the barrier system outside the length-of-need, including within transitions to other barrier systems. The design of transitions to other barrier systems, including free-standing, F-shape PCB segments, was outside the scope of this original study and would require further research to design and evaluate. A new transition between the reduced-deflection PCB system and free-standing F-shape PCB would need to consider several factors. First, the deflections of the two systems vary by approximately 50 percent. Thus, a stiffness transition may be needed to prevent barrier pocketing and provide safe and stable vehicle redirection. Second, the horizontal steel tubes of the reduced-deflection system would need to be tapered down to match the surface of the free-standing PCB segments in a manner that reduces the potential for vehicle snag without inducing vehicle climb or instability. Thus, a need exists to develop and evaluate a crashworthy transition between the new reduced-deflection system and free-standing PCB segments.

1.2 Objective

The objective of this research effort was to develop a MASH 2016 TL-3 transition between the recently-developed, non-anchored, reduced-deflection, F-shape PCB system and free-standing, F-shape PCB segments. The research effort focused on development of a design that safely transitioned between two barrier systems with varying deflections while maintaining vehicle stability. The design focused on minimizing the length of the transition and additional hardware components.

1.3 Scope

The Phase I research effort to design and evaluate a MASH 2016 TL-3 transition between the recently-developed, non-anchored, reduced-deflection, PCB system and free-standing, F-shape PCB segments consisted of a literature review, concept development, computer simulation, and a summary report. The research effort began with a brief literature search to review previous transitions for PCB systems as well as termination and transition elements used for box-beam guardrail and steel tube bridge rail transitions. This information provided insight on potential transition designs and methods for safely tapering and terminating horizontal steel tubes.

Following the literature search, transition design concepts were brainstormed and developed. The transition design concepts were evaluated based on potential safety performance, ease of installation, and length. The most promising design concepts were submitted to the sponsor for review and comment, and design revisions were made based on state feedback. LS-DYNA simulations were used to evaluate selected design concepts according to their safety performance. Validated models of the reduced-deflection and free-standing PCB systems from previous research were used in the LS-DYNA analysis. The computer simulation analysis began with the simplest, sponsor-favored design concepts, and complexity was added as needed to improve safety performance. After a transition design was developed to meet the MASH 2016 TL-3 impact criteria, a simulation study was performed to determine critical impact points (CIPs) for full-scale crash testing. A summary report of the research was completed detailing the literature search, computer simulation modeling, and recommendations for full-scale crash testing.

2 LITERATURE REVIEW

2.1 NCHRP Report 350 PCB Testing

An F-shape PCB is used by WisDOT and a number of other states. It was developed through the Midwest States Pooled Fund Program [1-4]. This PCB system consists of a 32-in. (813-mm) tall x 22½-in. (572-mm) wide x 12½-ft (3.8-m) long F-shape concrete barrier segment with a pin-and-loop type connection. The barrier has been tested to TL-3 under the National Cooperative Highway Research Program (NCHRP) Report 350 [1, 2, 8]. In the NCHRP Report 350 crash testing program, test no. ITMP-2 demonstrated that the F-shape PCB was capable of safely redirecting a 4,409-lb (2,000-kg) vehicle (designated 2000P) when impacted at a speed of 62.3 mph (100.3 km/h) and an angle of 27.1 degrees [1]. The maximum dynamic deflection of the PCB system in test no. ITMP-2 was 45.3 in. (1,151 mm).

Two anchored variations of the F-shape temporary concrete barrier system were tested under NCHRP Report 350 TL-3 [9]. In test no. FTB-1, three 1½-in. (38-mm) x 36-in. (914-mm) steel pins anchored the front face of each barrier segment through a 2-in. (51-mm) asphalt pad on soil. A 2000P pickup truck impacted the barrier system according to NCHRP Report 350 test designation no. 3-11, and the test was acceptable according to the safety performance criteria. The maximum dynamic deflection was 21.8 in. (554 mm) at the top of the barriers, and all of the barriers in the system were safely restrained on the asphalt road surface.

The second variation was transitioning from completely free-standing temporary concrete barriers to a rigid barrier through a pinned-barrier transition. Four transition barriers were pinned in the layout shown in Figure 2 with 1½-in. (38-mm) x 38½-in. (978-mm) steel pins anchored the front face of each barrier segment through a 2-in. (51-mm) asphalt pad on soil. In addition, either 10-gauge or nested 12-gauge thrie beam should be bolted across both sides of the joint between the pinned barriers and the rigid barrier system in order to reduce the potential for vehicle snag at the joint. In test no. FTB-2, a 2000P pickup truck impacted the first transition barrier (with only one asphalt pin) according to NCHRP Report 350 test designation no. 3-21, and the test was acceptable according to the safety performance criteria. The maximum dynamic deflection was 18.4 in. (467 mm) at the top of the barriers.

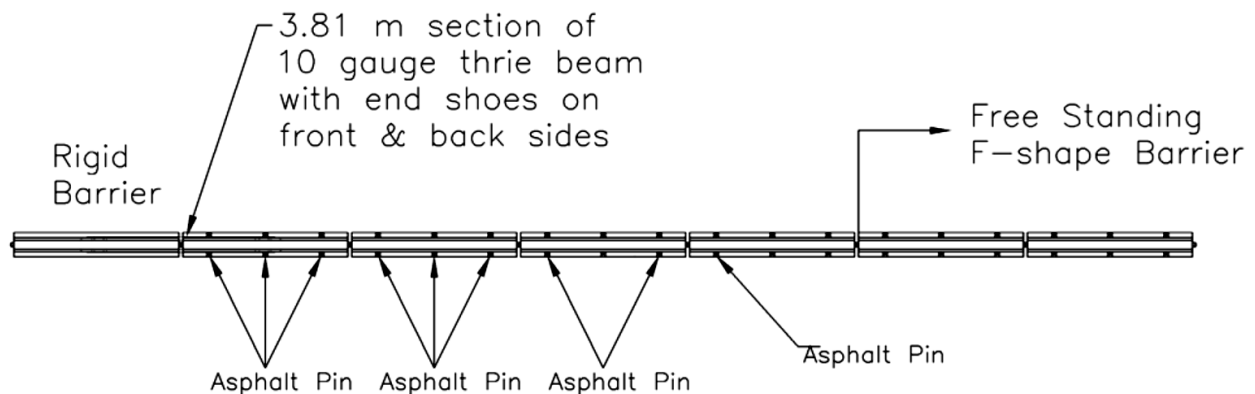


Figure 2. Free-standing F-Shape PCB to Rigid Barrier Transition [9]

2.2 MASH 2009 PCB Testing

2.2.1 Free-Standing F-Shape PCB

Two full-scale crash tests were conducted on the F-shape PCB during the development of the MASH 2009 safety requirements in NCHRP Project No. 22-14 [1, 4, 10]. Note that for this system, there is no difference between the MASH 2009 and MASH 2016 test evaluation criteria. The MASH 2009 testing used a 5,000-lb (2,268-kg) pickup truck rather than the 4,409-lb (2,000 kg) pickup truck specified in NCHRP Report 350. In test no. 2214TB-1, the F-shape PCB was impacted with a 2002 GMC 2500 ¾-ton, single-cab pickup truck with a mass of 5,000 lb (2,268 kg) at a speed of 61.8 mph (99.5 km/h) and at an angle of 25.7 degrees [1]. The PCB system safely redirected the impacting vehicle with a maximum lateral dynamic barrier deflection of 56.7 in. (1,440 mm). Significant vehicle climb was observed during test no. 2214TB-1. It should be noted that the vehicle used in this test had a center of gravity (CG) lower than desired for use in MASH 2009, and subsequent testing with a higher CG vehicle was recommended.

A second test of the F-shape PCB was then conducted using a 2002 Dodge Ram 1500 Quad Cab pickup truck with a mass of 5,000 lb (2,268 kg) [4]. Test no. 2214TB-2 consisted of the 2270P vehicle impacting the PCB system at a speed of 62.0 mph (99.8 km/h) and at an angle of 25.4 degrees. The PCB system safely redirected the impacting vehicle with a maximum lateral dynamic barrier deflection of 79.6 in. (2,022 mm).

Free-standing PCB deflections were significantly higher when testing was conducted with the 2270P vehicle under the MASH 2009 criteria as opposed to testing conducted with the 2000P vehicle under the NCHRP Report 350 criteria. PCB deflections increased 25 to 76 percent when the F-shape PCB was tested under MASH 2009 impact criteria, as shown in Table 1. This increase in deflection was due to a couple of factors: (1) higher vehicle mass induced more inertia and higher load transfer; (2) higher vehicle stability encouraged less climb and less vehicle rotation, which allowed the vehicle to directly load the barrier longer. In test no. 2214TB-2, the vehicle was engaged with the barrier for a longer period of time. Thus, it was believed a combination of increased kinetic energy, inertial transfer, and increased vehicle interaction with the barrier led to large barrier deflections.

There were two successful MASH 2009 TL-3 crash tests on the low-deflection PCB system, which consisted of a cap plate bolted across the PCB joint and continuous tubes running along the sides of the barriers, as mentioned previously. Test no. RDTCB-1 consisted of a 4,998-lb (2,267-kg) pickup truck impacting the low-deflection PCB system at a speed of 63.6 mph (102.4 km/h) and at an angle of 24.9 degrees [5]. The peak dynamic lateral deflection of the barrier system was 43 in. (1,092 mm).

Full-scale crash test no. RDTCB-2 was conducted on the final iteration of the low-deflection PCB with the back of the PCBs offset 24 in. (610 mm) away from the edge of a simulated bridge deck. Test no. RDTCB-2 consisted of a 4,978-lb (2,258-kg) pickup truck impacting the low-deflection PCB system at a speed of 64.8 mph (104.3 km/h) and at an angle of 25.4 degrees [5]. The peak dynamic lateral deflection of the barrier system was 40.7 in. (1,034 mm).

Table 1. F-Shape PCB Deflections

Test No.	Variation	Vehicle	Mass lb (kg)	Speed mph (km/h)	Angle deg.	Impact Severity kip-ft (kJ)	Dynamic Deflection in. (mm)	Static Deflection in. (mm)
ITMP-2	Free-standing	2000P	4,420 (2,005)	62.3 (100.3)	27.1	119.1 (161.5)	45.3 (1,151)	44.9 (1,140)
2214TB-2	Free-standing	2270P	5,000 (2,268)	62.0 (99.8)	25.4	118.0 (160.0)	79.6 (2,022)	73.0 (1,854)
RDTCB-1	Free-standing with Tubes	2270P	4,998 (2,267)	63.6 (102.4)	24.9	119.8 (162.4)	43.0 (1,092)	41.5 (1,054)
RDTCB-2	Free-standing with Tubes	2270P	4,978 (2,258)	64.8 (104.3)	25.4	128.6 (174.4)	40.7 (1,034)	39.5 (1,003)

2.2.2 Transition from Temporary to Permanent Median Barrier (MwRSF)

An approach transition was designed between free-standing, F-shape temporary concrete barriers and a permanent concrete median barrier [11]. The 42-in. (1,067-mm) tall, California single-slope, concrete median barrier was found to be most critical due to its height as compared to the F-shape temporary concrete barrier. The researchers utilized a combination of free-standing and tied-down Kansas Temporary F-shape Barriers, nested thrie beam on each side of the barriers for the transition to the single-slope permanent barrier, and transition cap, as shown in Figure 3.

Two full-scale vehicle crash tests were performed on the system under MASH 2009 safety requirements. In crash test no. TCBT-1, a 5,006-lb (2,271-kg) pickup truck impacted the temporary barriers 56 $\frac{3}{8}$ in. (1,432 mm) upstream from the permanent barrier at a speed of 62.4 mph (100.7 km/h) and an angle of 24.7 degrees. Crash test no. TCBT-2 was performed using a 4,990-lb (2,263-kg) pickup truck, which impacted the temporary barriers 54 ft - 6 $\frac{3}{4}$ in. (16.6 m) upstream from the permanent barrier at a speed of 62.2 mph (100.1 km/h) and an angle of 26.2 degrees. Both tests were determined to be acceptable according to the MASH 2009 TL-3 evaluation criteria.



Figure 3. Temporary Concrete Barrier to Permanent Concrete Barrier Transition, Test Nos. TCBT-1 and TCBT-2 [11]

2.2.3 Transition from Pinned PCB to Rigid Concrete Barrier (TTI)

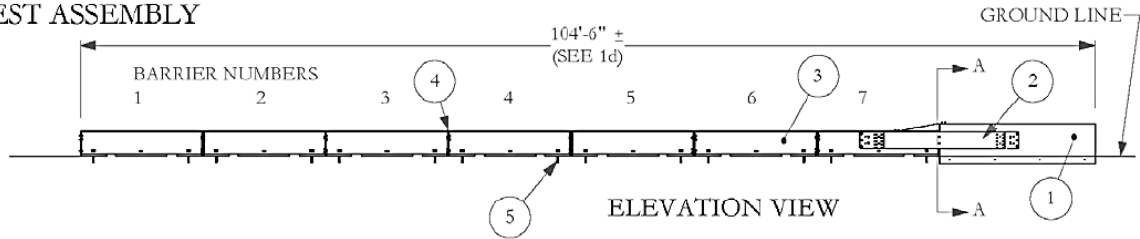
The Texas A&M Transportation Institute (TTI) developed a transition from the pinned-down F-shape temporary concrete barrier to a permanent concrete barrier [12]. The transition was crash tested under MASH 2009 TL-3 criteria using a 32-in. (813-mm) tall, pinned-down (with angled pins), anchored F-shape temporary concrete barrier connected to a 42-in. (1,067-mm) tall, single-slope, concrete median barrier. The transition consisted of a 12-gauge (2.7-mm) thrie beam connected to the traffic-side face of the barriers, a 1/8-in. (3-mm) thick steel cap attached to the top of the F-shape and single-slope barriers, and a 1/4-in. (6-mm) thick steel plate fastened to the non-traffic side faces of the barriers. The cap transitioned 10 in. (254 mm) vertically over a longitudinal length of 48 in. (1,219 mm) from a 32-in. (813-mm) tall F-shape barrier to the 42-in. (1,067-mm) tall, single-slope barrier, as shown in Figures 4 and 5.

The transition for the anchored temporary barrier to rigid concrete barrier safely redirected the 2270P vehicle and performed acceptably to MASH 2009 criteria test designation no. 3-21. Maximum dynamic deflection and permanent set of the transition were 5.7 in. (145 mm) and 2.5 in. (64 mm), respectively.

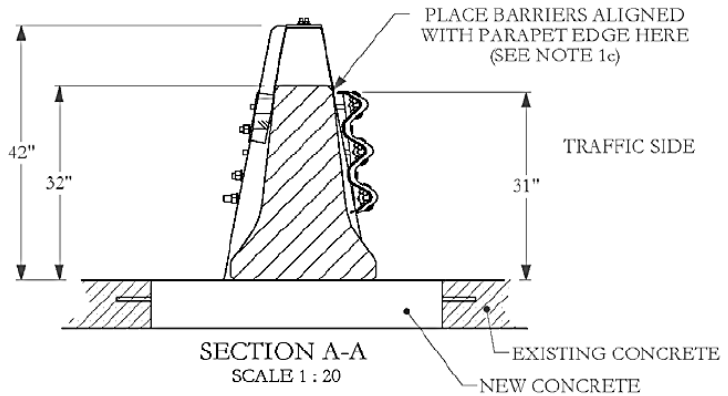


Figure 4. Transition Design for Anchored Temporary Barrier to Rigid Concrete Barrier [12]

TEST ASSEMBLY



PARTS LIST		
#	PART NAME	QTY.
1	SSCB Parapet	1
2	Nested Thrie-beam assembly	1
3	Pinned-Down F-Shape Barrier, 12.5'	7
4	Connection Pin	6
5	Anchor Pin, Ø1-1/2"	14
6	Transition Cap	1
7	Hilti Anchor, HAS-E #00385424	4
8	Field Side Connection Strap	1
9	Wood Block Spacer	1
10	Bolt, 5/8 x 4 carriage	1
11	Nut, 5/8 hex	1
12	Bolt, 7/8 x 14 hex	3
13	Bolt, 7/8 x 16 hex	3
14	Bolt, 7/8 x 18 hex	2
15	Bolt, 7/8 x 20 hex	1
16	Bolt, 7/8 x 22 hex	1
17	Nut, 7/8 heavy hex	10
18	Washer, 7/8 flat hardened	20



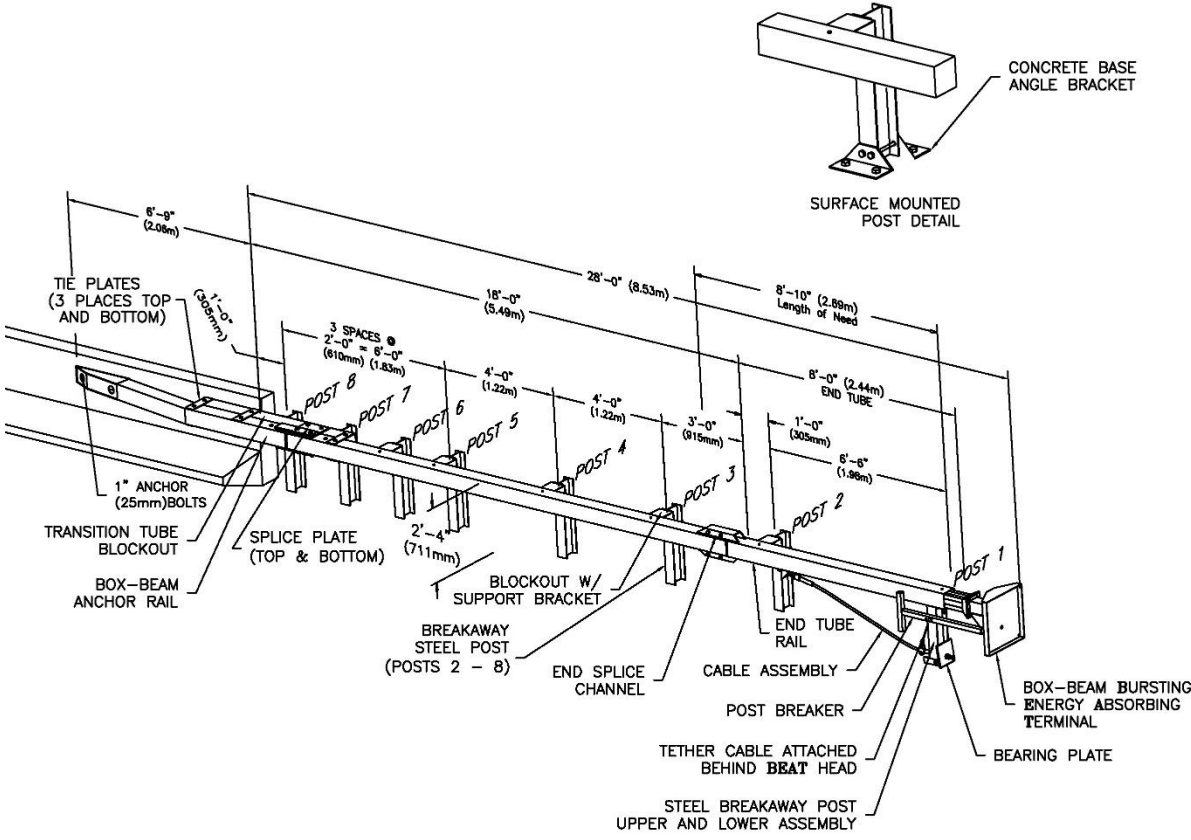
- 1a. All Ø7/8 bolts are ASTM A325 or A449.
- 1b. All fabricated steel parts are A36 unless otherwise noted.
- 1c. Barriers are pinned to 8" thick concrete, with one pin at each end on the traffic side.
- 1d. 16' SSCB Parapet and seven 12.5' F-Shape Barriers with ≈2" space between them.
- 1e. Hilti Anchor, HAS is Ø1/2" x 6-1/2".

		Roadside Safety and Physical Security Division - Proving Ground	
Project	405160-34	Pin-down to Rigid Transition	
Drawn By	GES	Scale 1:150	Sheet 1 of 13 Installation
Approved:			Date:
Nauman Sheikh:			2012-07-25

Figure 5. Layout of Transition Design for Anchored Temporary Barrier to Rigid Concrete Barrier [12]

2.3 Termination of Box Beam in Roadside Systems

Previous designs exist to taper box-beam guardrail to a concrete barrier. The box-beam burster, energy-absorbing, single-sided crash cushion (BEAT-SSCC) includes a configuration with 6-in. x 6-in. (152-mm x 152-mm) box-beam tapered to a concrete barrier, as shown in Figure 6 [13-15]. The last 7 in. (178 mm) is tapered at a 1:2.14 lateral-to-longitudinal rate. The upstream tube is tapered at a 1:6 lateral-to-longitudinal rate until connecting to 6-in. x 6-in. (152-mm x 152-mm) box beam with no taper. This crash cushion was successfully evaluated with a 2000P pickup truck in test no. SSC-4 in the reverse direction (impacting the tapered tube section at 20-degree angle) according to NCHRP Report 350 test no. 3-39. A very similar connection with the same taper rate was utilized in a Wyoming Department of Transportation transition design from a box-beam guardrail to a permanent concrete barrier [16].



- NOTES:
 1. SYSTEM CAN BE INSTALLED WITH GROUND MOUNTED POSTS IN THE SOIL OR SURFACE MOUNTED POSTS WITH ANCHOR BOLTS.
 SCI13a Driven Posts
 SCI13b Surface Mounted Posts
 2. CAN BE ATTACHED TO SAFETY SHAPE BARRIER OR VERTICAL WALL.



Figure 6. BEAT-SSCC Configuration [13-15]

The State of New York Department of Transportation developed standard plans for their box-beam guardrail to concrete parapet transition, as shown in Figure 7 [17-18]. The 6-in. x 6-in. (152-mm x 152-mm) box beam rail is tapered to the face of the concrete barrier over 3 ft (914 mm) at a 1:6 lateral-to-longitudinal rate.

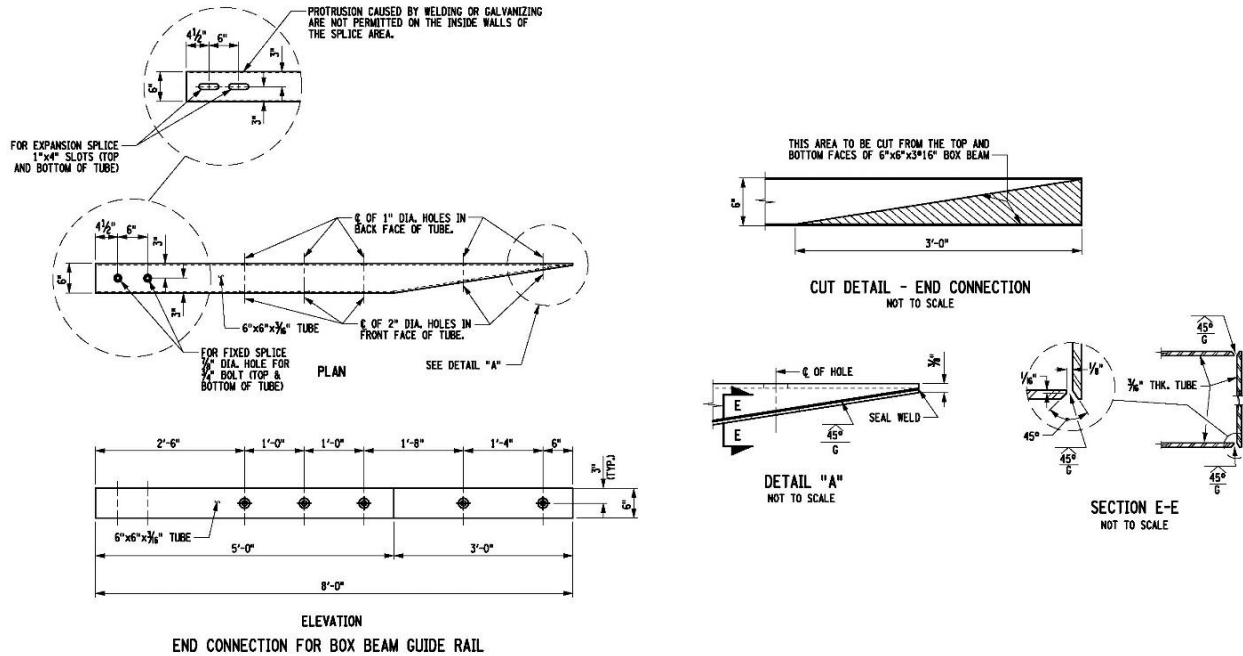


Figure 7. State of New York Standard Details for Box-Beam to Concrete Parapet Transition [17-18]

2.4 Other Horizontal Flares in Barrier Systems

In January 1988, the Federal Highway Administration (FHWA) provided recommendations on commonly used flare rates of concrete bridge rails [19]. Two examples of concrete bridge parapets had a 1:4 lateral-to-longitudinal flare rate, as shown in Figure 8.

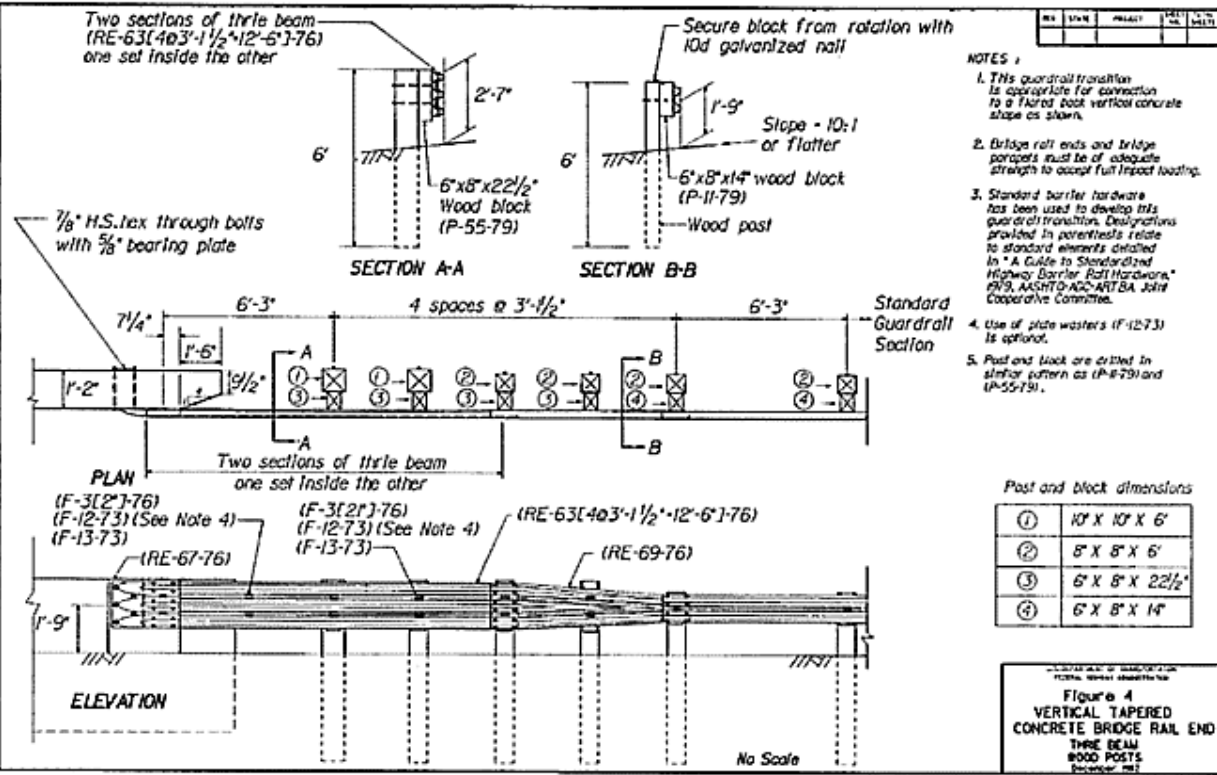
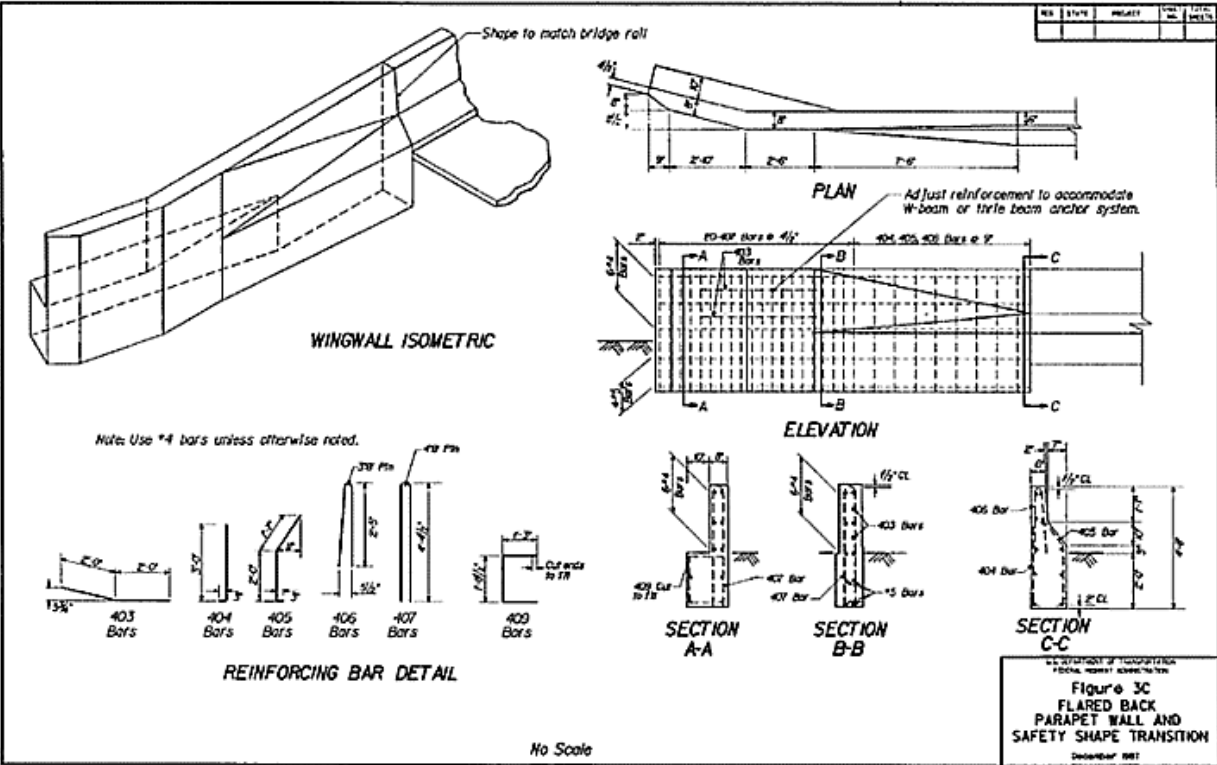


Figure 8. Tapered Concrete Bridge Parapets [19]

3 TRANSITION DESIGN AND ANALYSIS

3.1 Design Criteria

Prior to developing design concepts for a transition between the reduced-deflection PCB and free-standing PCB, the following design criteria were identified:

1. Design concepts should meet MASH 2016 TL-3 safety performance criteria.
2. The dynamic deflection of the transition system should range between deflections found for the reduced-deflection system (40.7 in. (1,034 mm)) and the free-standing PCB system (79.6 in. (2,022 mm)).
3. The transition design requires minimal modification to the barrier. This system should not include modifications to the pin-and-loop connection.
4. The concepts' fabrication and installation should be easy.
5. The length of the transition and the required hardware should be minimized.

These criteria were considered during the development of transition design concepts. The deflections of the reduced-deflection PCB and free-standing PCB systems vary by approximately 50 percent. No stiffness transition is desired for ease of installation. However, a stiffness transition may be necessary in order to prevent barrier pocketing and provide safe and stable vehicle redirection. Concepts with and without a stiffness transition were considered.

3.2 Design Concepts

First, it was anticipated that the sharp, blunt ends of the HSS $5 \times 5 \times \frac{3}{16}$ continuous tubes running along the sides of the reduced-deflection PCB segments would increase the potential for vehicle snag. The researchers recommended that the HSS $5 \times 5 \times \frac{3}{16}$ tubes be tapered down to match the PCB surface. As previously noted in the literature review, several existing designs use tapered box beam ends to match the face of a concrete barrier. The BEAT-SSCC utilized a two-stage end taper with 1:2.14 and 1:6 lateral-to-longitudinal flare rates, which was successfully crash tested to NCHRP Report 350 criteria with a 2000P pickup truck [13-15]. Similarly, in a Wyoming Department of Transportation transition design, the box-beam guardrail ends were tapered to match a concrete barrier at the same rates. In the State of New York Department of Transportation transition design from a box-beam guardrail to a concrete parapet, the box-beam rail was tapered to match the concrete barrier at a 1:6 lateral-to-longitudinal rate. Other lateral-to-longitudinal flare rates utilized in roadside barriers vary from 1:4 to 1:10. In the current transition design, it was recommended to initially taper the HSS $5 \times 5 \times \frac{3}{16}$ tubes to the concrete segments at a 1:6 lateral-to-longitudinal rate, as shown in Figures 9 and 10. The drawings do not depict the final transition design.

The design modification of tapering tubes at a 1:6 lateral-to-longitudinal rate with no incremental transition in stiffness was the first concept evaluated. If an incremental transition in stiffness was necessary, the researchers further brainstormed a number of ideas to improve the transition performance from the reduced-deflection PCB to the free-standing PCB. The concepts were grouped into four main categories based on the mechanism for mitigating significant changes in stiffness between adjacent barrier segments. The four concept categories for the transition were as follows:

1. Reduction of Joint Tolerance in Transition Region – Reduction in the tolerance or gaps in the barrier joints such that the barrier segments engage each other more rapidly during impact to avoid “knee-shape” contact between the vehicle and the barrier segments.
2. Composite Action – Development of tension and compression loads across the barrier joints in the transition region in order to develop moment continuity in the adjacent barrier segments in transition region.
3. Increased Barrier-to-Ground Friction – Increasing friction between barrier and roadway surface in the transition region.
4. Increased Barrier Mass of Free-Standing Segment – Adding mass or ballast to the free-standing barrier segment adjacent to the transition joint in order to provide increased inertial and friction resistance to motion.

Following the review of the design concepts, it was concluded that the concept of reducing joint tolerance by adding a joint spacer (e.g., a steel tube) would be a simple yet functional option if a transition in stiffness was required. An example of a joint spacer is shown in Figure 11.

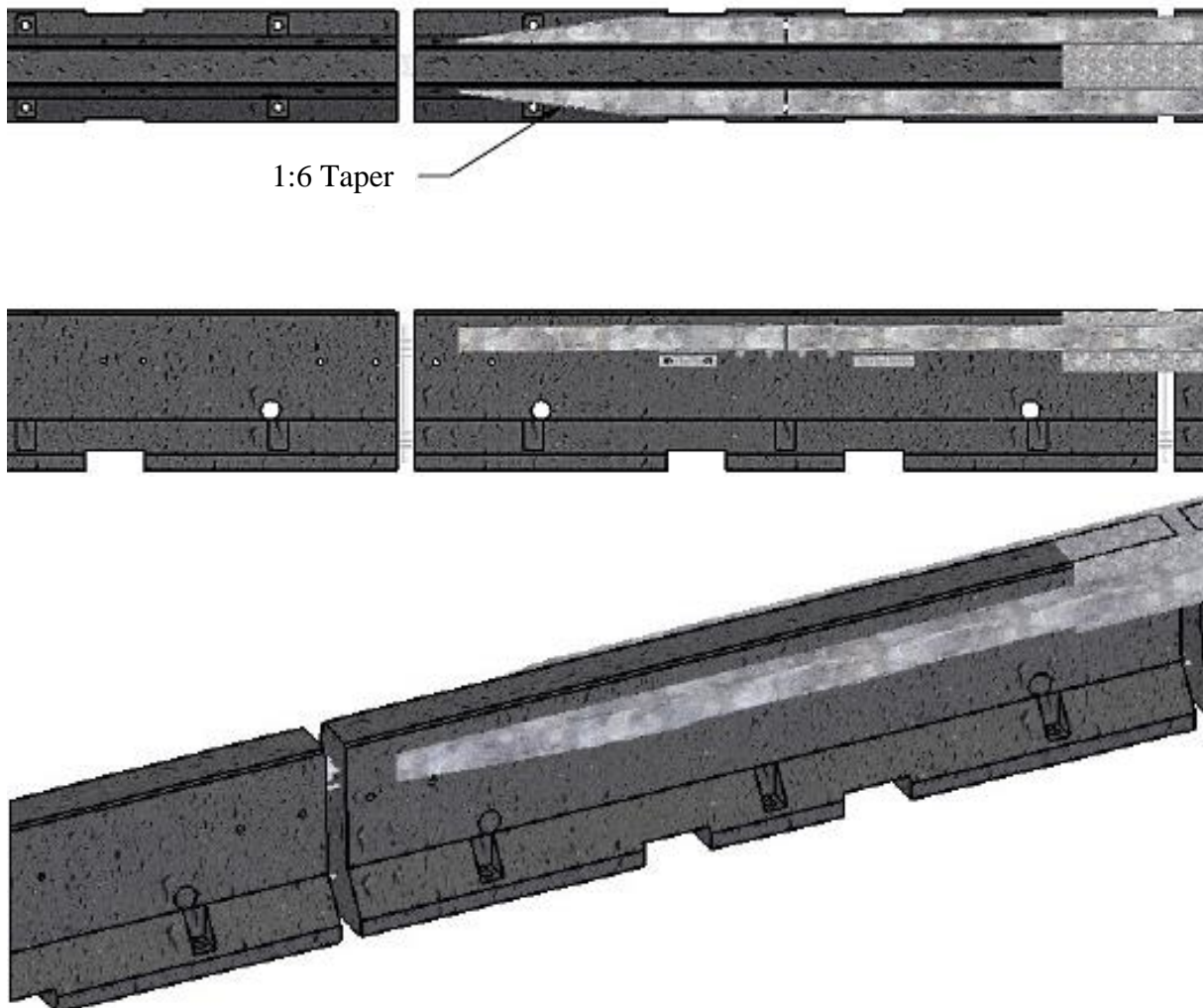


Figure 9. Tubes Tapered Down to Reduced-Deflection PCB Segments Surface

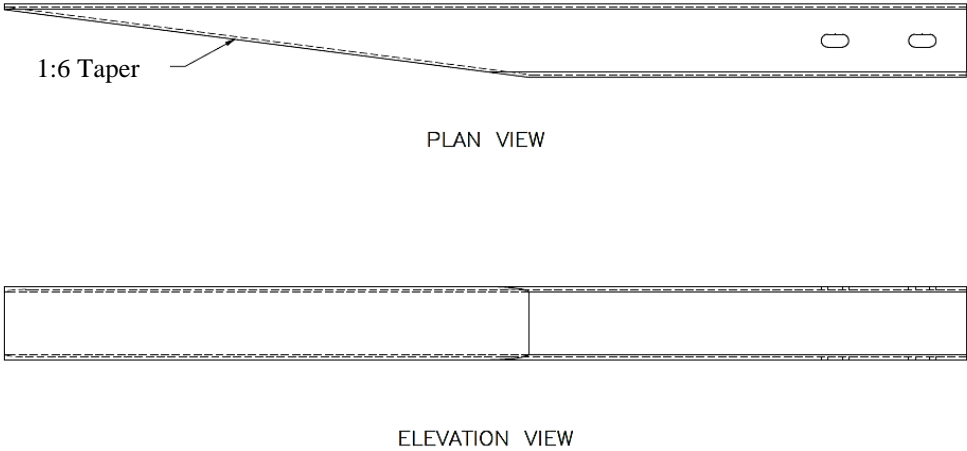


Figure 10. Details of Tubes Tapered Down to Reduced-Deflection PCB Segment Surface

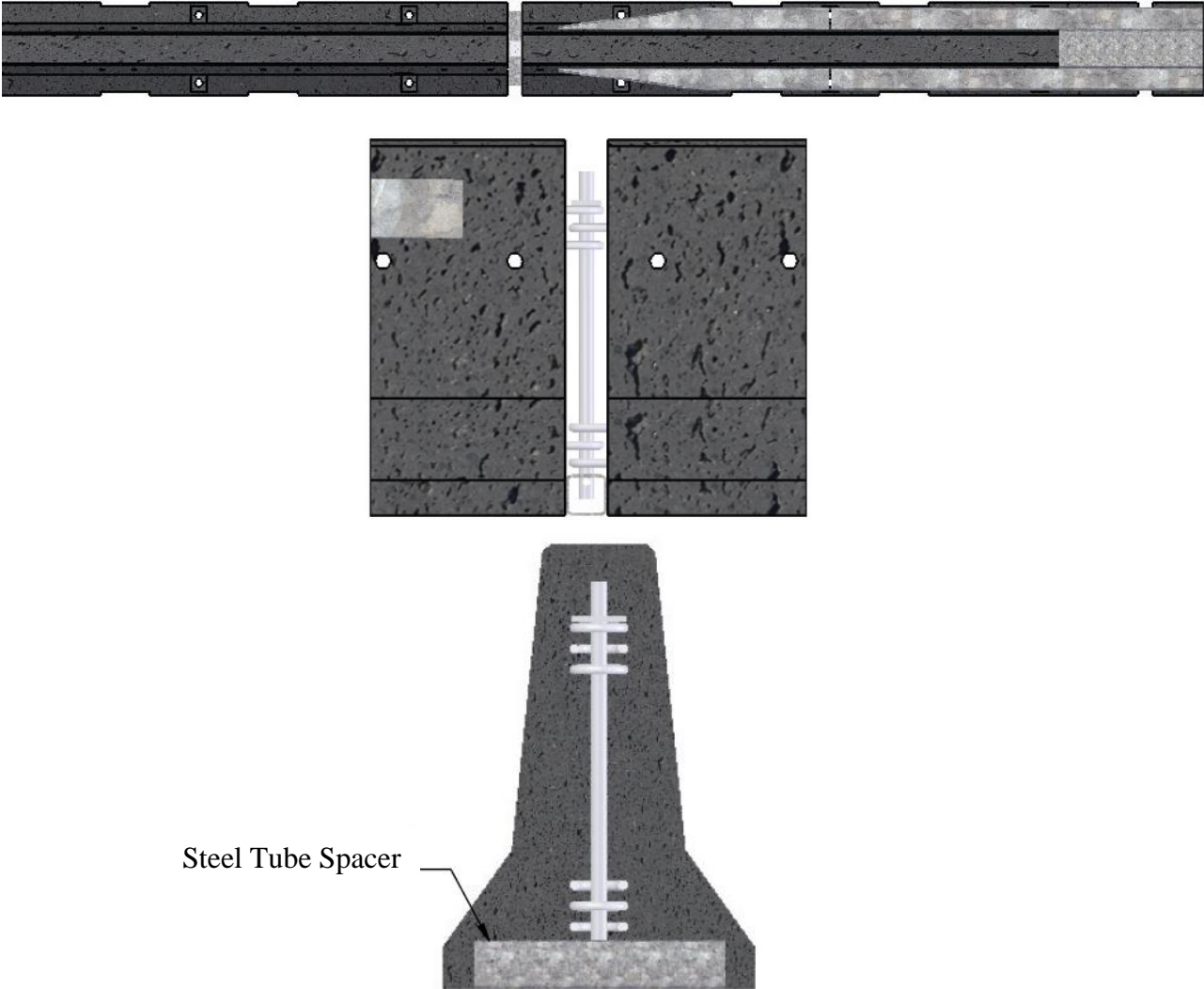


Figure 11. Joint Spacer (Steel Tube) at Transition Joint

4 TEST REQUIREMENTS AND EVALUATION CRITERIA

4.1 Test Requirements

Transitions, including those between free-standing PCBs and reduced-deflection PCBs, must satisfy impact safety standards in order to be declared eligible for federal reimbursement by the FHWA for use on the National Highway System (NHS). For new hardware, these safety standards consist of the guidelines and procedures published in MASH 2016 [7]. According to TL-3 of MASH 20016, transitions must be subjected to two full-scale vehicle crash tests, as summarized in Table 2. Note that there is no difference between MASH 2009 and MASH 2016 evaluation criteria for this system.

Table 2. MASH 2016 TL-3 Crash Test Conditions for Transitions

Test Article	Test Designation No.	Test Vehicle	Vehicle Weight lb (kg)	Impact Conditions		Evaluation Criteria ¹
				Speed mph (km/h)	Angle deg.	
Transitions	3-20	1100C	2,425 (1,100)	62 (100)	25	A,D,F,H,I
	3-21	2270P	5,000 (2,268)	62 (100)	25	A,D,F,H,I

¹ Evaluation criteria explained in Table 3.

4.2 Evaluation Criteria

Evaluation criteria for full-scale vehicle crash testing are based on three appraisal areas: (1) structural adequacy; (2) occupant risk; and (3) vehicle trajectory after collision. Criteria for structural adequacy are intended to evaluate the ability of the transition to contain and redirect impacting vehicles. In addition, controlled lateral deflection of the test article is acceptable. Occupant risk evaluates the degree of hazard to occupants in the impacting vehicle. Post-impact vehicle trajectory is a measure of the potential of the vehicle to result in a secondary collision with other vehicles and/or fixed objects, thereby increasing the risk of injury to the occupants of the impacting vehicle and/or other vehicles. These evaluation criteria are summarized in Table 3 and defined in greater detail in MASH 2016.

In lieu of conducting full-scale crash tests to evaluate the initial design concepts, a computer simulation effort was conducted and the results were evaluated according to MASH 2016 test designation nos. 3-20 and 3-21 evaluation criteria.

Table 3. MASH 2016 Evaluation Criteria for Transitions

Structural Adequacy	A. Test article should contain and redirect the vehicle or bring the vehicle to a controlled stop; the vehicle should not penetrate, underide, or override the installation although controlled lateral deflection of the test article is acceptable.		
Occupant Risk	D. Detached elements, fragments or other debris from the test article should not penetrate or show potential for penetrating the occupant compartment, or present an undue hazard to other traffic, pedestrians, or personnel in a work zone. Deformations of, or intrusions into, the occupant compartment should not exceed limits set forth in Section 5.2.2 and Appendix E of MASH 2016.		
	F. The vehicle should remain upright during and after collision. The maximum roll and pitch angles are not to exceed 75 degrees.		
	H. Occupant Impact Velocity (OIV) (see Appendix A, Section A5.2.2 of MASH 2016 for calculation procedure) should satisfy the following limits:		
	Occupant Impact Velocity Limits		
	Component	Preferred	Maximum
Longitudinal and Lateral	30 ft/s (9.1 m/s)	40 ft/s (12.2 m/s)	
I. The Occupant Ridedown Acceleration (ORA) (see Appendix A, Section A5.2.2 of MASH 2016 for calculation procedure) should satisfy the following limits:	Occupant Ridedown Acceleration Limits		
Component	Preferred	Maximum	
Longitudinal and Lateral	15.0 g's	20.49 g's	

5 LS-DYNA MODEL

5.1 PCB Model

The LS-DYNA computer simulation model of the F-shape temporary concrete barrier was based on a model developed previously at MwRSF for determining the deflection of tied-down, F-shape barrier systems [11, 20]. The model consisted of the F-shape barrier, the end connection loops, and the connection pins, as shown in Figure 12. The main body of the F-shape barrier model was created using shell elements with a rigid material definition. The rigid material definition allowed the proper mass and rotational inertias to be defined for the barrier even though it was essentially hollow. The barrier segments were assigned a mass of 4,976 lb (2,257 kg) based on measurements taken from actual barrier segments. The rotational inertias were determined based on SolidWorks models of the PCB segment. The SolidWorks models used tended to overestimate the mass and rotational inertia of the PCB segment as the solid model included the mass of the concrete body and the reinforcing steel, but did not account for the volume of concrete lost due to the reinforcing steel. Thus, the rotational inertias determined by the software were scaled down based on the ratio of the actual measured mass of the barrier segment to the software-estimated mass of the segment. The use of the shell elements improved the overall contact of the barrier and the vehicle. In addition, the use of shell elements made it easier to fillet the corners and edges of the barrier. By rounding off the barrier edges, the edge contacts and penetrations were reduced, thus further improving the contact interface.

The loops in the barrier model were also modified to match the current configuration, which consisted of two sets of three rebar loops. The connection loops were modeled with a rigid material as previous testing of the barrier in various configurations showed little to no deformation of the connection loops. The connection pin was modeled with the MAT_PIECEWISE_LINEAR_PLASTICITY material in LS-DYNA with the appropriate properties for ASTM A36 steel. The barrier system model incorporated a total of sixteen barrier segments for a total barrier length of 200 ft (61.0 m).

The simulated F-shape barrier model was impacted under the MASH 2016 TL-3 impact conditions for test designation no. 3-11. It was then compared to actual tests on free-standing, F-shape barriers (test no. 2214TB-2) to ensure that it provided reasonable estimates of the barrier deflection prior to implementing deflection-limiting concepts. Details of the comparison can be found in Bielenberg et al. [5]. Sequential photographs of the baseline simulation for test no. RDTCB-2 are shown in Figure 13.

5.2 Reduced-Deflection Steel Components Model

The PCB model geometry was modified to add holes for the reduced-deflection steel component connections [5]. A simulation model of test no. RDTCB-1, as shown in Figure 14, was constructed to serve as a baseline for comparison of proposed design modifications for further reducing the deflections of the PCB system. The steel cap across the barrier joint and the steel tubes on the side of the barrier were added using shell elements.

MAT_24_PIECEWISE_LINEAR_PLASTICITY was used to define the steel material properties for these components. The tubes were welded to the cap using constrained nodal rigid bodies to create a simplified weld. The connection hardware, including the bolts, nuts, and splice

plates were modeled explicitly in the model. Bolt preload was achieved using the INITIAL_STRESS_SECTION command in LS-DYNA.

The baseline model was simulated for a 2270P vehicle impacting the system with the same impact conditions as test no. RDTCB-1. Thus, the Chevy Silverado model impacted the barrier system at a speed of 63.6 mph (102.4 km/h) and an angle of 24.9 degrees. The vehicle model used for the simulation was the Chevy Silverado Version 3 (v3) model developed at the National Crash Analysis Center (NCAC). The vehicle impacted the system 4.3 ft (1.3 m) upstream from the center of the joint between the eighth and ninth barrier segments. Comparison of the simulation results with full-scale crash test no. RDTCB-1 found that the model provided good correlation with the full-scale test and was appropriate for use in evaluation of the deflection-limiting mechanisms. Details of the comparison can be found in Bielenberg et al. [5].

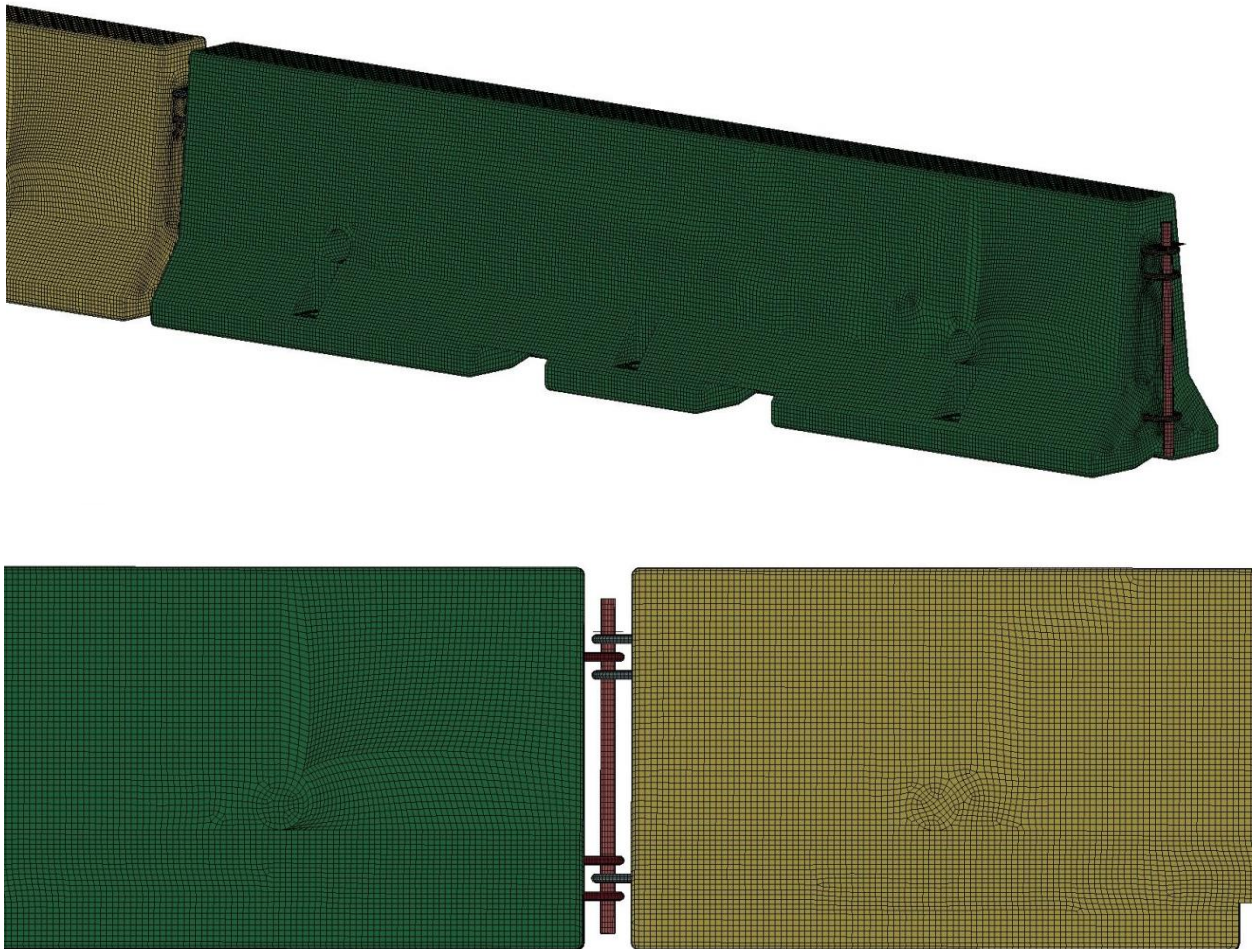


Figure 12. F-shape PCB Barrier Model

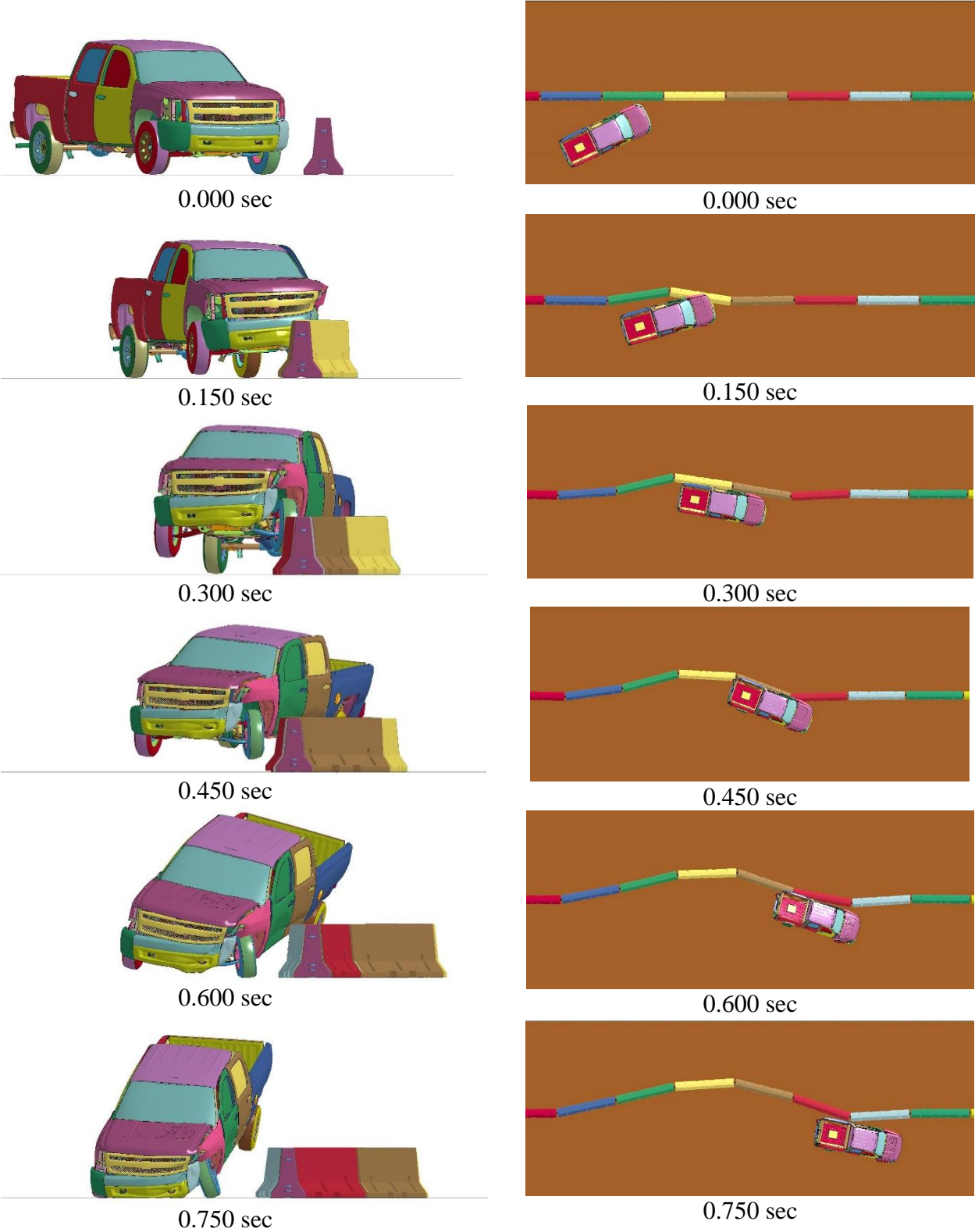


Figure 13. Sequential Photographs: Simulation of Test No. 2214TB-2

The additional attachment points that were utilized in test no. RDPCB-2 were incorporated into the model with $\frac{3}{8}$ -in. (10-mm) thick and 12-in. (305-mm) long steel brackets that were welded on the top and bottom of the steel tubes on each side of the splice at the center of the length of the PCB segment. These angles were bolted through the barrier, similar to the other bolted connections in the model, as shown in Figure 15.

Initial simulations of test no. RDTCB-2 demonstrated significantly lower deflections than the full-scale test. The discrepancy between the physical test and the model was attributed largely to the concrete damage and fracture observed in the test which was not reproduced in the rigid PCB model as it could not fracture. As a compromise, the simulation model of test no. RDTCB-2 was modified to reduce the barrier-to-ground friction coefficient of 0.4 to 0.24 to reproduce the dynamic barrier deflections observed in the full-scale test. The results from this model estimated a dynamic lateral barrier deflection of 41.1 in. (1,044 mm). This value correlated very well with the 39.5 in. (1,003 mm) permanent set deflection and 40.7 in. (1,034 mm) dynamic lateral barrier deflection from test no. RDTCB-2. Complete details of the simulations can be found in Bielenberg et al. [5].

5.3 Baseline model

The previously-developed model of the low-deflection, PCB system was further calibrated by modeling an impact with the Chevrolet Silverado Version 2 (v2) pickup truck originally developed by NCAC [21]. The Silverado v2 has a softer tire and no steering defined, whereas the Silverado v3 has a harder tire with steering defined. The barrier geometry and parameters remained the same as in the previous model. A summary of the results from numerical simulation and test no. RDTCB-2 is shown in Table 4. Sequential photographs of the baseline simulation for test no. RDTCB-2 are shown in Figure 16.

Table 4. Comparison of Reduced-Deflection PCB System Test and Simulation

Evaluation Parameters	Max. Dynamic Deflection in. (mm)	Max. Roll Angle (deg.)	Max. Pitch Angle (deg.)	Max. Yaw Angle (deg.)	Long. ORA (g's)	Lateral ORA (g's)	Long. OIV ft/s (m/s)	Lateral OIV ft/s (m/s)
Test No. RDTCB-2	40.7 (1,034)	11.8	6.3	35.1	5.6	8.5	12.5 (3.8)	21.3 (6.5)
Simulation	39.7 (1,008)	9.9	8.5	32.9	7.0	11.0	16.4 (5.0)	19.7 (6.0)

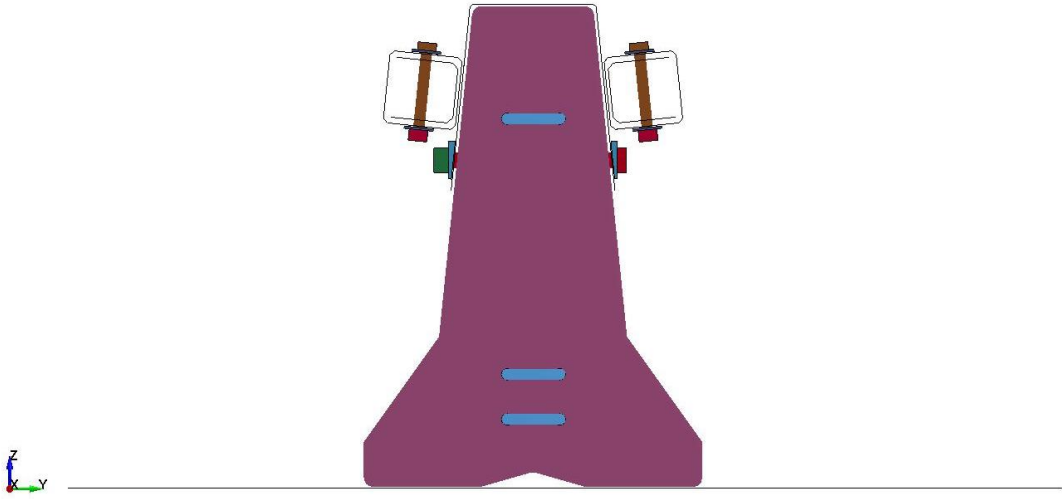
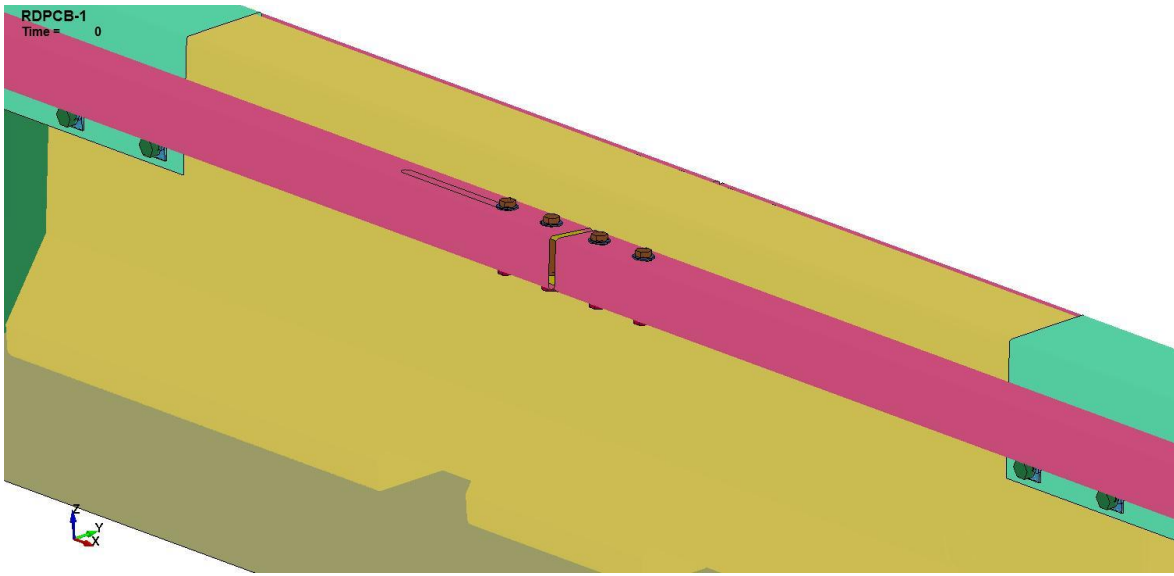
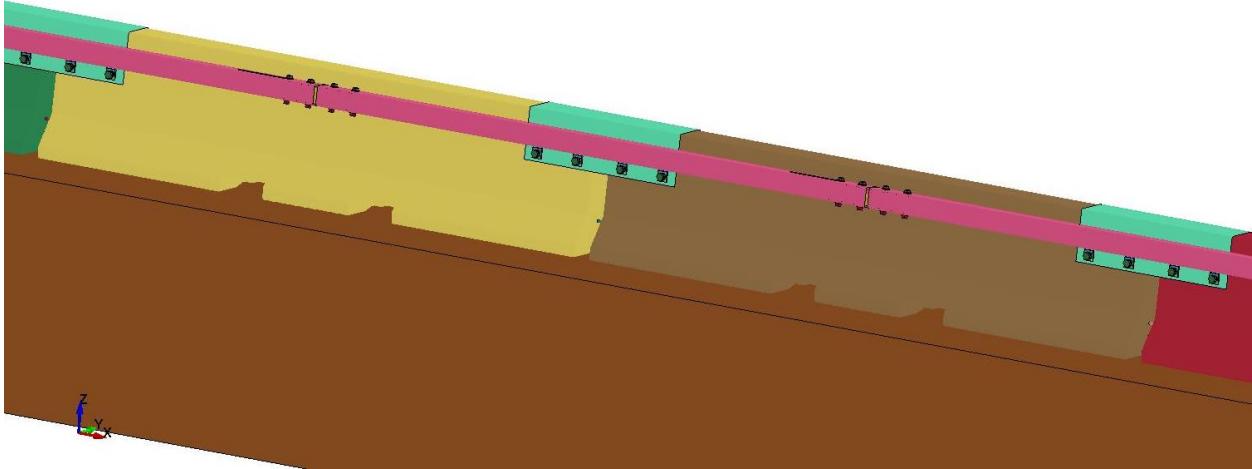


Figure 14. Test No. RDTCB-1 Model

Comparison of the simulation results with full-scale crash test no. RDTCB-2 found that the model provided good correlation with the full-scale test and was appropriate for use in evaluation of the transition. As shown in Table 4, LS-DYNA simulation tended to predict slightly larger lateral and longitudinal ORAs as compared to the crash testing results, which may be due to lack of failure in the wheel, tire, and suspension model assembly. In addition, as noted previously, the coefficient of friction between the barriers and ground was decreased from 0.4 to 0.24 to accurately model deflections, which were inaccurate due to the lack of concrete material failure in the model. Since the impacts in the transition region would be upstream from the reduced-deflection PCB system, a coefficient of friction of 0.40 was utilized, which was previously used to accurately model freestanding PCB deflections. However, it was noted that the deflections in the model just upstream from the reduced-deflection PCB system may be lower than what would actually occur. This discrepancy was considered throughout the analysis.

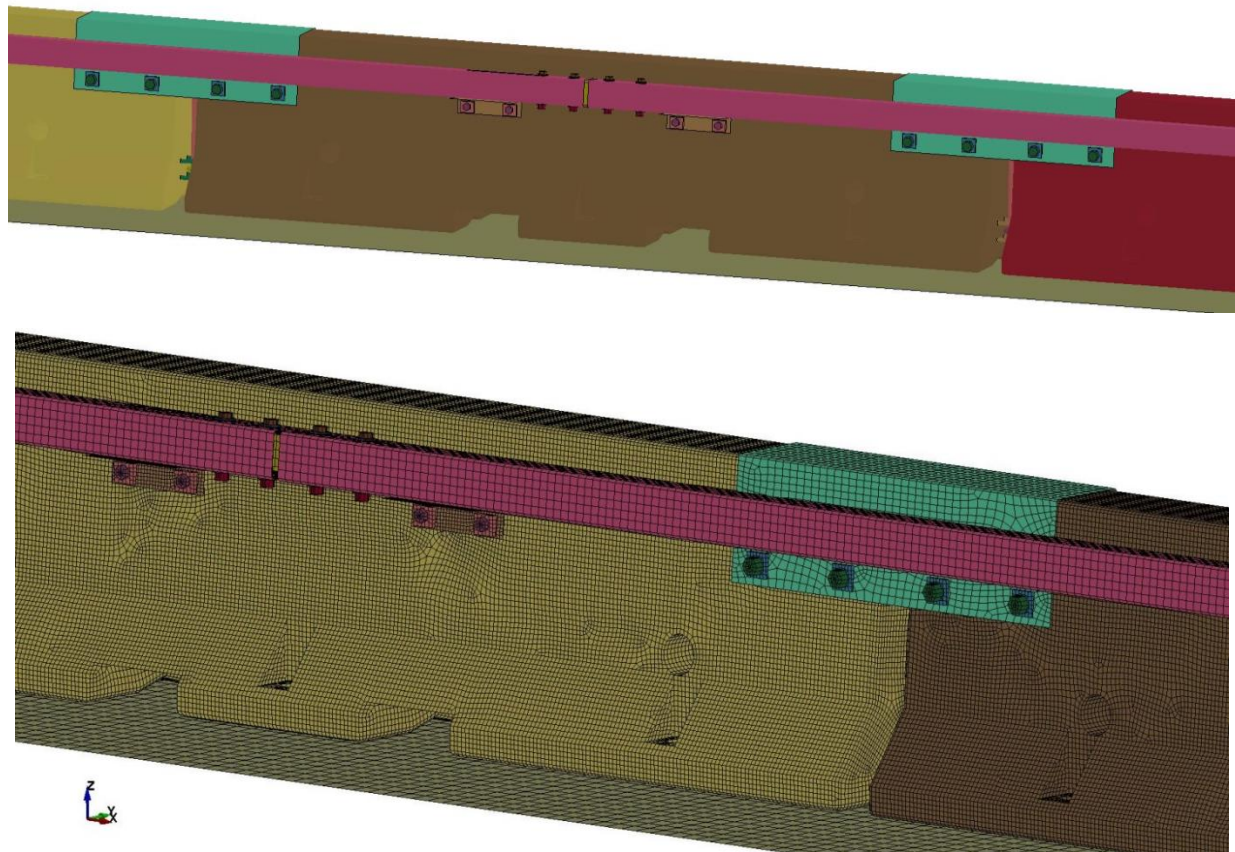


Figure 15. Test No. RDTCB-2 Final Barrier Model

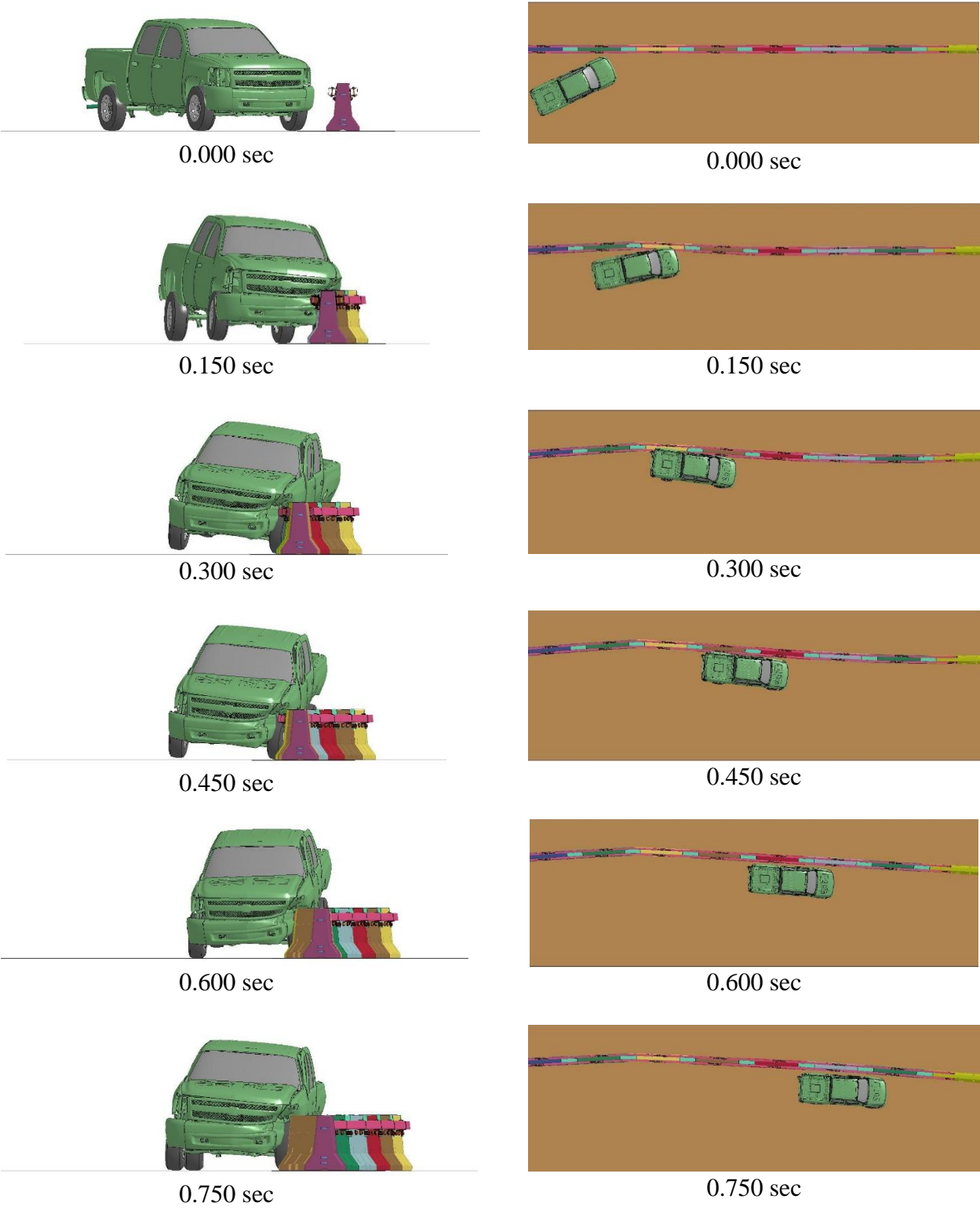


Figure 16. Sequential Photographs: Baseline Simulation of Test No. RDTCB-2

6 SIMULATIONS WITH SLOPED TUBES

6.1 Sloped Tubes Model

As previously discussed, the end section of the HSS 5x5x³/₁₆ continuous tubes running along the sides of the reduced-deflection PCB segments could pose vehicle snag risk. Thus, the tubes along the reduced-deflection PCB segments were tapered down to the PCB surface upstream from the joint between the free-standing and reduced-deflection PCB systems at a 1:6 lateral-to-longitudinal rate over a 30-in. (762-mm) length. Computer simulations of the barrier with only the tapered tubes and no transition in the barrier stiffness were evaluated to the MASH 2016 safety performance criteria. The tapered tube model is shown in Figure 17.

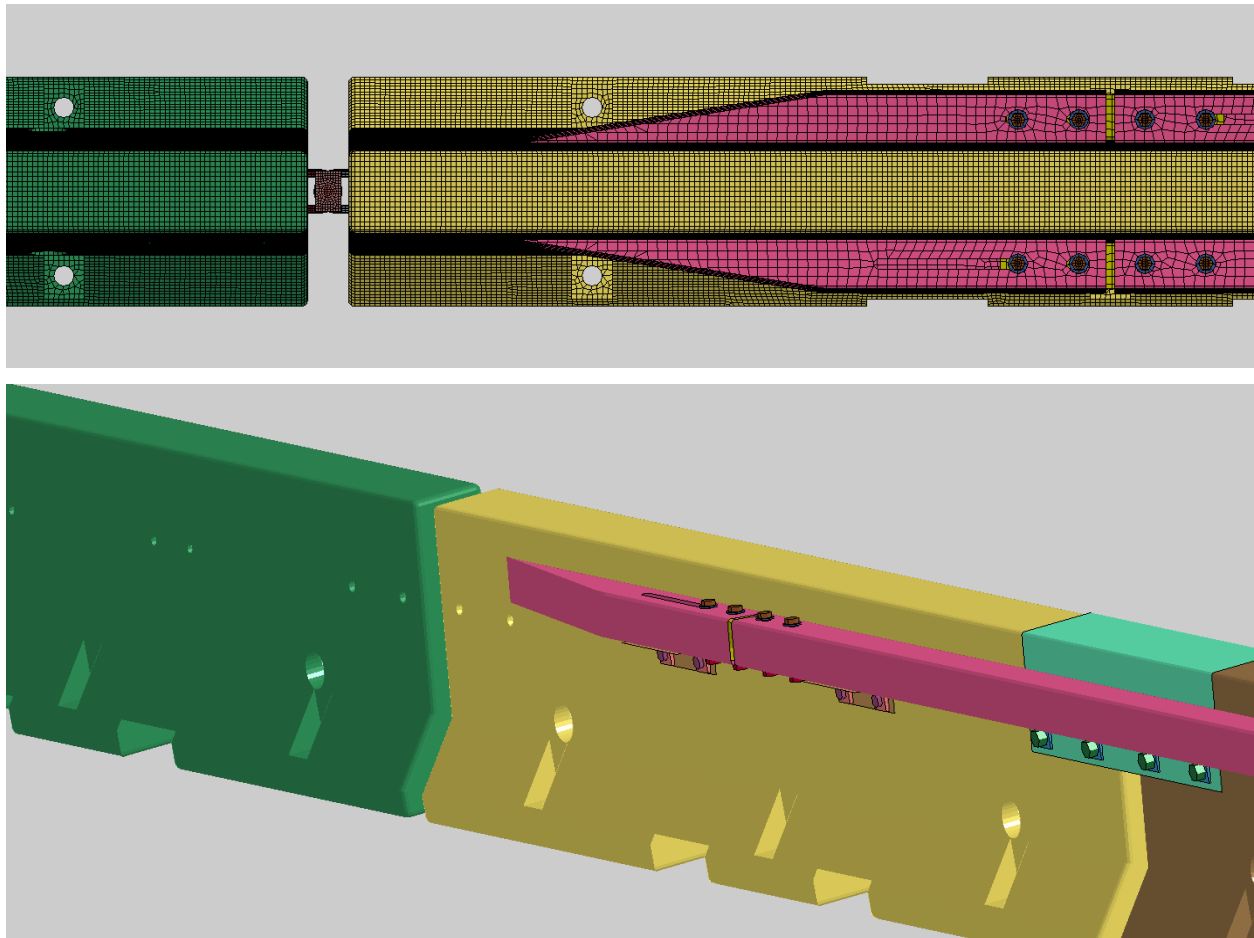


Figure 17. Simulated Tubes Tapered Along Reduced-Deflection PCB Segments' Surface

6.2 Simulation of Sloped Tube Model with Different Impact Points

Several impact points upstream from the joint between the reduced-deflection PCB system and the free-standing PCB (Joint no. 1), as shown in Figure 18 and Table 5, were simulated using the 2270P Silverado model. Initially the impact points were picked every 39.4 in. (1,000 mm), while more impact points with a 7.8-in. (200-mm) increment were selected in the critical regions. The simulation results are summarized in Table 5. The simulations ended early with impact points

194.1 and 202.0 in. (4,930 and 5,130 mm) upstream from the transition joint due to numerical instability errors and low occupant risk values.

With no transition in the barrier stiffness, several impact points including 178.3 in., 194.1 in., 202.0 in., 225.6 in., 272.8 in., and 351.6 in. (4,530 mm, 4,930 mm, 5,130 mm, 5,730 mm, 6930 mm, and 8,930 mm) upstream from the transition joint had a predominant “knee-shape” that formed in the system and contacted the impact-side door, as shown in Figure 19. For example, the simulated vehicle damage due to the vehicle snag on the knee for the case with a 225.6 in. (5,730 mm) impact point is shown in Figure 20. Sequential photographs for the simulations with the “knee” hitting the vehicle’s side-door are shown in Figure 21. This knee contact did not appear to be critically detrimental to the vehicle or the barrier performance in the simulations. However, the impact of the knee into the vehicle’s door has been shown to increase vehicle instability in previous PCB tests. In test no. NELON-2, which was a modified MASH 2009 test designation no. 3-37 on the end of the length-of-need of a 100-ft (30.5-m) long PCB installation, the vehicle had a roll angle in excess of 75 degrees and failed to meet MASH 2009 safety criteria [22]. A knee formed in the system, which extended forward laterally from the original barrier line and impacted the vehicle’s door. The knee contact accentuated vehicle roll and likely contributed to the excessive roll angle. This excessive roll was not captured in computer simulations of the system. Since the same barrier model was used in this research project, attention was paid to the indications of knee formation and vehicle’s door impact.

Other safety measures, including occupant risk values, barrier deflection, vehicle roll and pitch angles, and vehicle climb did not appear critical. As noted previously, LS-DYNA tends to predict larger lateral and longitudinal ORAs as compared to the crash testing results, likely due to lack of failure in the wheel, tire, and suspension model assembly. Therefore, the lateral ORAs that were larger than the MASH 2016 limit (20.49 g’s) (including impact points 115.4, 123.2, 131.1, 139.0, 217.7 in. (2,930, 3,130, 3,330, 3,530, and 5,530 mm) upstream from the transition joint) would likely be below the MASH 2016 limit in an actual crash test. In the simulations with impact points just upstream from Joint no. 1, the truck model’s fender and door contacted the tapered tube and caused vehicle damage. The tapered tube was fixed to the PCB model and could not separate from the barrier. However, the actual connection may have some flexibility and allow the truck fender to get between the tapered tubes and PCB face. Thus, there was potential for vehicle snag on tapered box tube ends along the reduced-deflection PCB when impacted at the points upstream from transition joint.

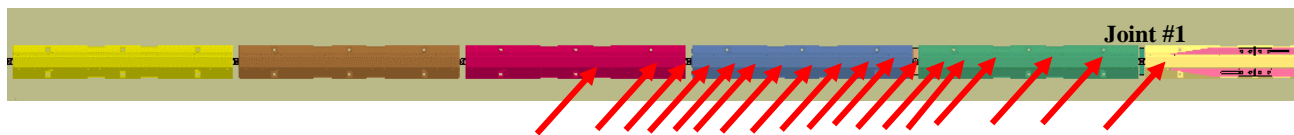


Figure 18. Simulated Tubes Tapered Along Reduced-Deflection PCB Segments’ Surface

Table 5. Summary of Simulation Results – Only Tapered Tubes, No Transition in Stiffness

Simulation No.	Impact Point in. (mm) US or DS Joint No. 1	Lat. OIV ft/s (m/s)	Long. OIV ft/s (m/s)	Lat. ORA g's	Long. ORA g's	Roll deg.	Pitch deg.	Lateral Barrier Deflection in. (mm)	Increase in Vertical Bumper Height in. (mm)
1	24.8 (630) downstream	-18.4 (-5.6)	-19.4 (-5.9)	-10.3	-6.4	-8.1	9.6	61.0 (1,549)	1.4 (36)
2	36.6 (930) upstream	-19.7 (-6.0)	-21 (-6.4)	-14.7	-6.6	-9.7	9.5	64.7 (1,643)	5.6 (142)
3	76.0 (1,930) upstream	-18.7 (-5.7)	-15.1 (-4.6)	-14.6	-9.8	-15.2	10.1	61.1 (1,552)	6.9 (175)
4	115.4 (2,930) upstream	-20.0 (-6.1)	-13.1 (-4.0)	-20.9	-5.3	-18.0	12.1	53.6 (1,361)	9.3 (236)
5	123.2 (3,130) upstream	-20.0 (-6.1)	-13.8 (-4.2)	-21.3	5.4	-17.9	11.7	52.4 (1,331)	10.3 (262)
6	131.1 (3,330) upstream	-20.3 (-6.2)	-14.1 (-4.3)	-20.5	-4.5	-17.4	13.1	58.4 (1,483)	10.1 (257)
7	139.0 (3,530) upstream	-20.3 (-6.2)	-14.4 (-4.4)	-20.6	-5.0	-15.8	13.1	59.5 (1,511)	10.3 (262)
8	146.9 (3,730) upstream	-20.0 (-6.1)	-14.1 (-4.3)	-19.2	-5.0	-17.5	10.8	60.0 (1,524)	9.4 (239)
9	154.7 (3,930) upstream	-19.4 (-5.9)	-16.4 (-5.0)	-16.5	-9.9	-16.3	12.3	60.4 (1,534)	24.6 (625)
10	162.6 (4,130) upstream	-18.7 (-5.7)	-16.4 (-5.0)	-16.7	-6.6	-14.8	10.1	62.7 (1,593)	25.3 (643)
11	170.5 (4,330) upstream	-18.7 (-5.7)	-16.4 (-5.0)	-15.5	-5.3	-14.7	11.7	64.2 (1,631)	19.4 (493)
12	178.3 (4,530) upstream	-18.0 (-5.5)	-15.7 (-4.8)	-16.4	-9.3	-8.5	11.3	45.2 (1,148)	11.9 (302)
13	186.2 (4,730) upstream	-18.4 (-5.6)	-16.4 (-5.0)	-15.1	-6.3	-15.3	12.8	62.2 (1,580)	17.8 (452)
14*	194.1 (4,930) upstream	-19.4 (-5.9)	-16.1 (-4.9)	-5.3	-5.9	-4.4	5.8	36.8 (919)	11.3 (287)
15*	202.0 (5,130) upstream	-17.1 (-5.2)	-14.8 (-4.5)	-6.7	-4.8	-5.9	4.5	36.2 (935)	9.2 (234)
17	217.7 (5,530) upstream	-16.4 (-5.0)	-13.8 (-4.2)	-20.4	-7.9	-24.4	21.2	62.8 (1,595)	5.3 (135)
18	225.6 (5,730) upstream	-16.7 (-5.1)	-10.2 (-3.1)	-19.0	-8.3	-23.1	9.4	65.3 (1,659)	6.1 (155)
19	233.5 (5,930) upstream	-18.7 (-5.7)	-11.8 (-3.6)	-12.7	-7.5	-23.8	10.3	65.2 (1,656)	7.3 (185)
20	272.8 (6,930) upstream	-19.7 (-6.0)	-13.8 (-4.2)	-18.4	-4.9	-19.8	15.9	69.6 (1,768)	9.6 (244)
21	312.2 (7,930) upstream	-19.4 (-5.9)	-17.1 (-5.2)	-10.2	-4.1	-12.4	18.8	80.1 (2,035)	25.8 (655)
22	351.6 (8,930) upstream	-17.4 (-5.3)	-15.1 (-4.6)	-13.5	-6.14	-16.5	13.2	74.1 (1,882)	7.9 (201)

* Simulation terminated early due to numerical instabilities

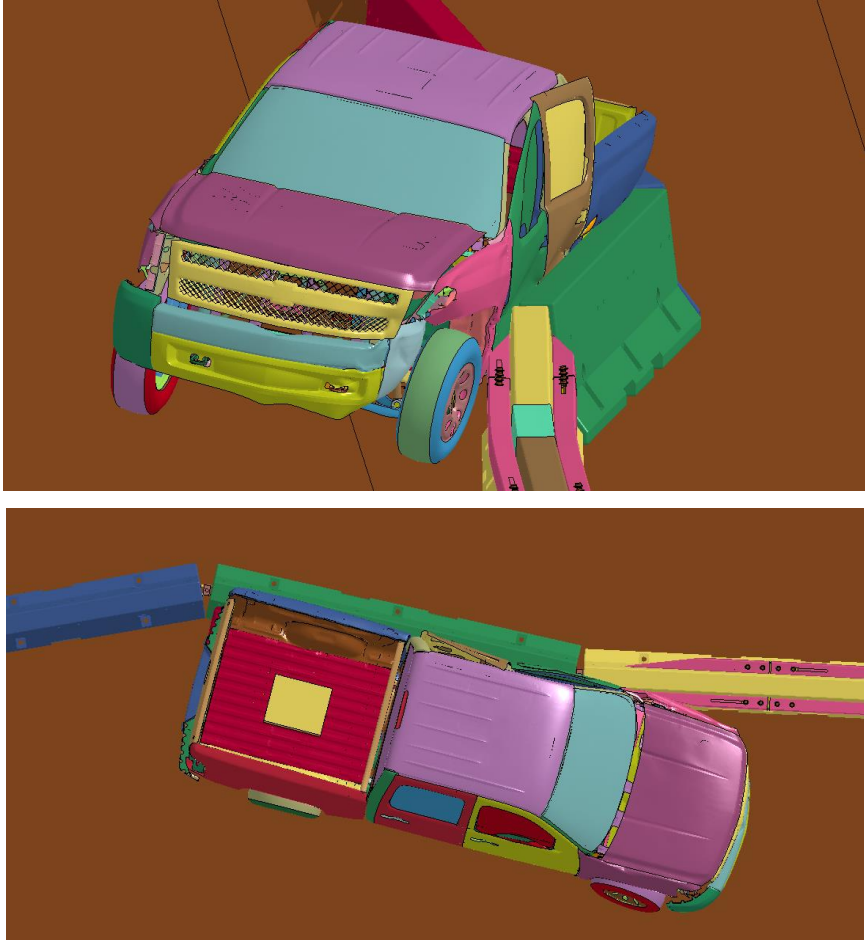


Figure 19. Simulated Vehicle Snag on “Knee” in Transition Region – Impact Point 225.6 in. (5,730 mm) Upstream from Transition Joint

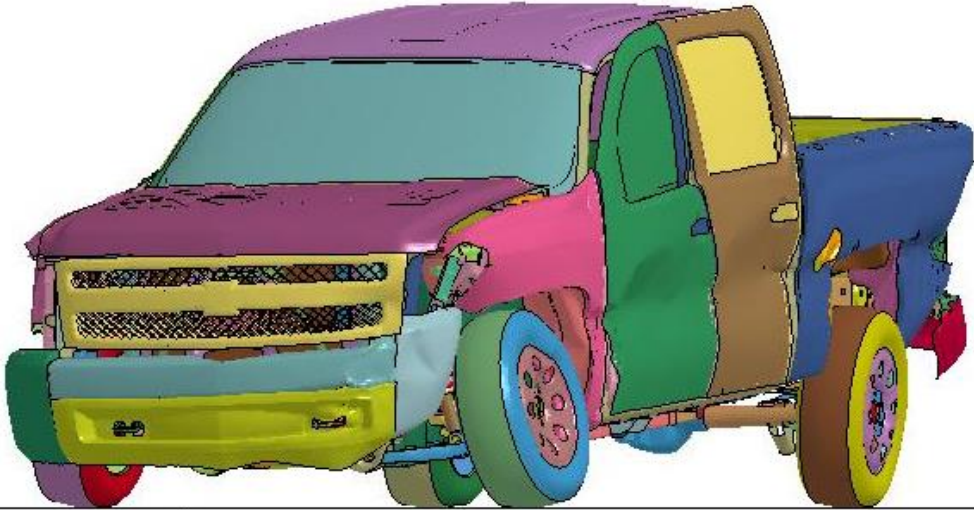
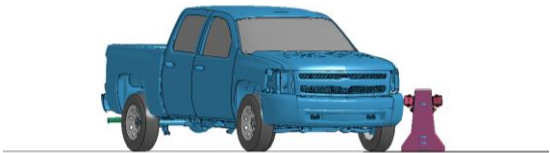


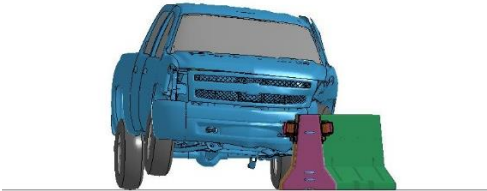
Figure 20. Simulated Vehicle Damage Caused by “Knee” – Impact Point 225.6 in. (5,730 mm) Upstream from Transition Joint



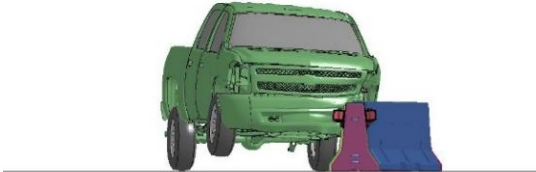
0.000 sec



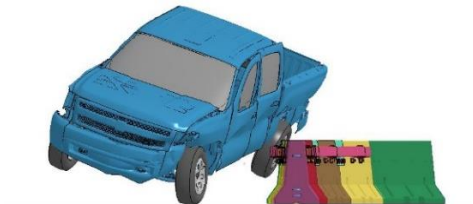
0.000 sec



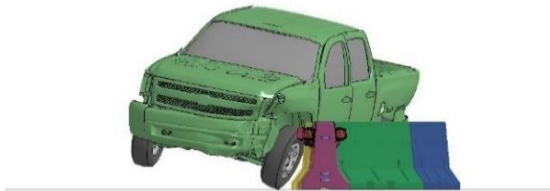
0.200 sec



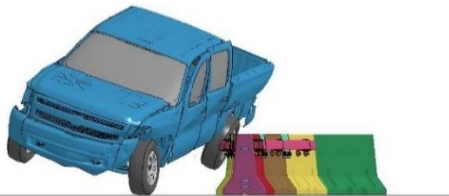
0.200 sec



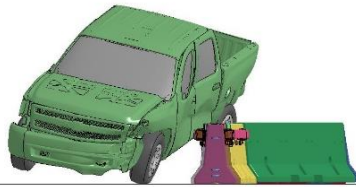
0.400 sec



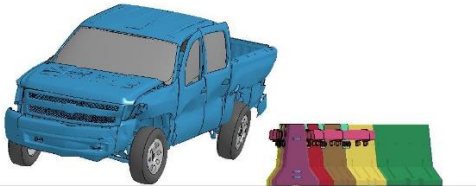
0.400 sec



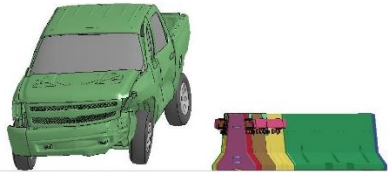
0.600 sec



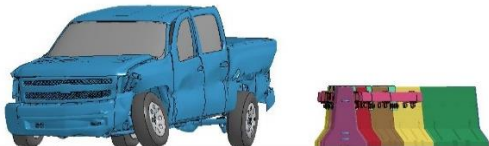
0.600 sec



0.800 sec



0.800 sec



1.000 sec



1.000 sec

Figure 21. Sequential Photographs: Impact Point at 225.6 in. (5,730 mm) Upstream from Transition Joint (Left) and Impact Point at 351.6 in. (8,930 mm) Upstream from Transition Joint (Right)

7 SIMULATION OF PROPOSED TRANSITION DESIGN MODIFICATIONS

For simulated impacts on the free-standing PCB adjacent to the reduced-deflection PCB, it was noted that a “knee” formed in the system, which contacted the vehicle’s door and could increase the potential for vehicle instability. In order to mitigate this concern and provide a smooth and safe transition in barrier stiffness, several design modifications were considered, as discussed in Chapter 3. The concept of reducing joint tolerance by adding a steel tube spacer was preferred as it was a simple option for resolving the safety concerns in the transition area, as shown in Figure 11. Thus, an investigation was conducted using LS-DYNA computer simulation [20] to evaluate the effects of adding steel tubes at the joints on the transition performance during an impact. Joint spacers with various configurations, stiffnesses, and strengths were added to an LS-DYNA model of a free-standing PCB system connected to a reduced-deflection PCB in order to evaluate impact performance.

The design modifications were evaluated based on safety performance, ease of installation, and minimizing the length of the transition and additional hardware components. LS-DYNA simulations were performed to evaluate the selected design concepts according to MASH 2016 safety performance criteria.

7.1 Evaluation Criteria

In addition to MASH 2016 safety performance criteria, including vehicle stability (roll and pitch) and occupant risk measures, other concerns including vehicle snag (knee hitting door), vehicle climbing, and barrier deflection were also considered. Thus, these criteria were evaluated in each simulation.

Euler angles, including roll, pitch, and yaw angles, were used to evaluate vehicle stability. Roll and pitch angles should not exceed 75 degrees according to MASH 2016 [7]. Occupant risk measures, which evaluate the degree of hazard to the occupants in the impacting vehicle, included the longitudinal and lateral OIV as well as longitudinal and lateral ORA. According to MASH 2016, longitudinal and lateral OIV should fall below the maximum allowable value of 40.0 ft/s (12.2 m/s). MASH 2016 also states that longitudinal and lateral ORAs should fall below the maximum allowable value of 20.49 g’s [7]. The vehicle bumper climb, which can be an indicator of vehicle instability, was also examined. In addition, the barrier dynamic deflection was measured in each simulation. System and vehicle damage were also considered. In order to identify the concern of “knee” hitting the vehicle door, the forward deflection of barrier segments was measured and the PCB and door contact was closely monitored.

7.2 Tube Spacer Added at Joint No. 1

Initially, an 18-in. (457-mm) long HSS 3½x3½x¼ steel tube spacer was modeled and added at the base of Joint no. 1 (i.e., the transition joint between the reduced-deflection PCB and the free-standing PCB) in order to add a transition in the barrier stiffness, as shown in Figure 22. The nominal PCB gap distance was 4 in. ±0.5 in. (102 mm ±13 mm). Thus, an HSS 3½x3½x¼ would properly fit in the gap. In order to pass the connection pin through the tube, a 2-in. (51-mm) diameter hole was created on the top surface of the tube, as shown in Figure 23. In addition, the tube was raised ½ in. (13 mm) in the simulations in order to account for the rounded edges on the PCB model, which were necessary to prevent numerical instabilities. When the tube was on the

ground, the rounded edges on the PCB model caused the tube to crush asymmetrically, as shown in Figure 24a. In reality, the concrete segments do not have rounded edges and the tube would crush symmetrically, as shown in Figure 24b. Thus, raising the tube ½ in. (13 mm) would allow the tube to crush similarly to an actual test. A comparison between the simulation results with the tube spacer on the ground and the tube spacer raised is shown in Table 6. As shown in Table 6, raising the tube ½ in. (13 mm) did not significantly affect the simulation results.

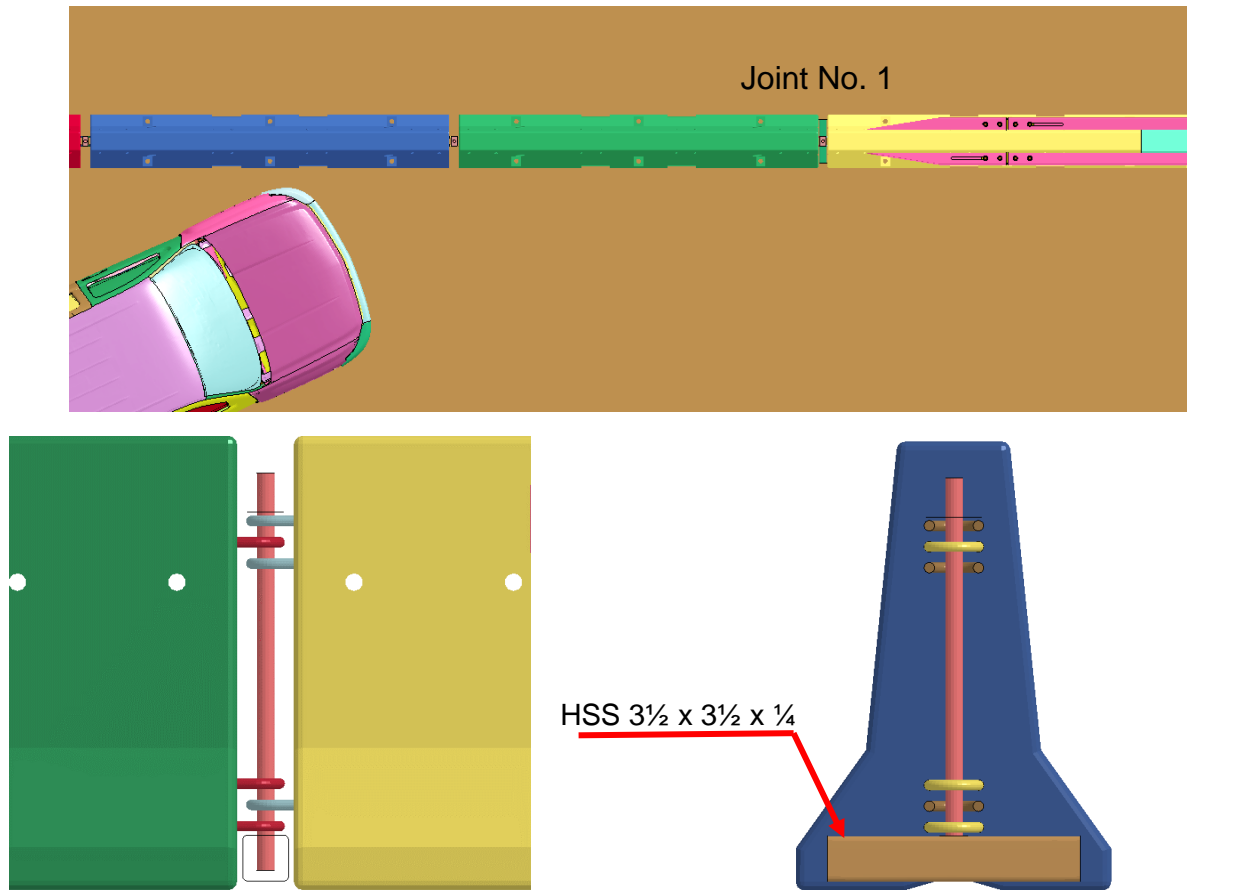


Figure 22. Transition with Single Steel Tube at Joint No. 1

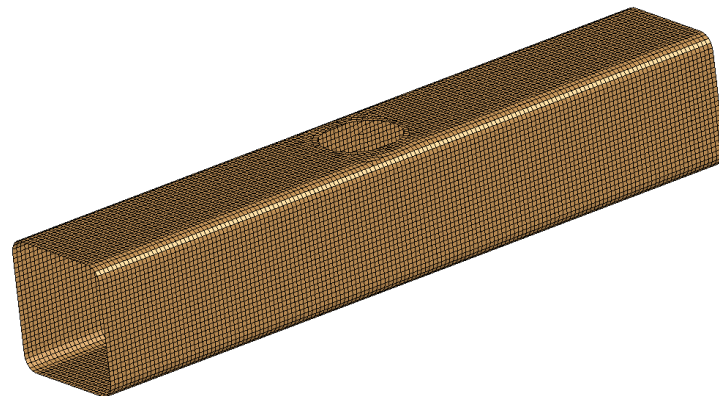
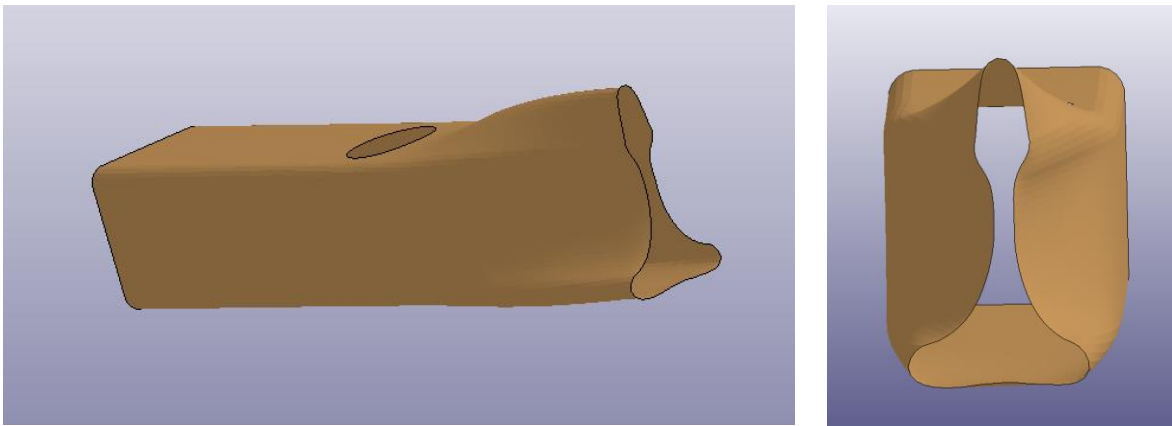


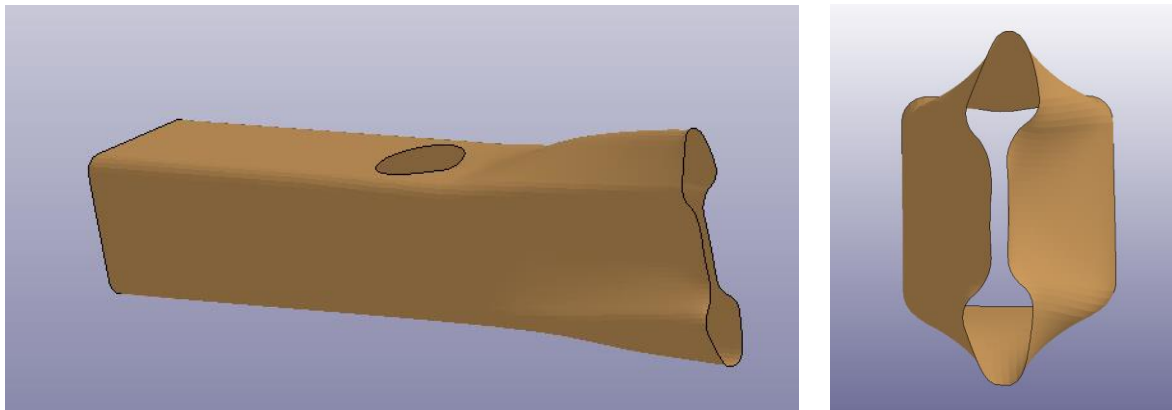
Figure 23. Steel Tube Model – HSS 3 1/2 x 3 1/2 x 1/4

Table 6. Summary of Simulation Results – Tube on Ground and Raised Tube

Simulation No.	Lat. OIV ft/s (m/s)	Long. OIV ft/s (m/s)	Lat. ORA g's	Long. ORA g's	Roll deg.	Pitch deg.	Lat. Barrier Deflection in. (mm)	Increase in Vertical Bumper Height in. (mm)
Case with Tube on Ground	-17.4 (-5.3)	-10.5 (-3.2)	-16	-8.3	15.4	12.7	74.7 (1,897)	6.9 (175)
Case with Raised Tube	-17.4 (-5.3)	-10.5 (-3.2)	-17.6	-9.9	18.7	12	75.5 (1,918)	6.3 (160)



(a)



(b)

Figure 24. Crushed Steel Tube at Joint No. 1 After Impact: (a) Tube on Ground, (b) Tube Raised ½ in.

A number of simulations were conducted using the 2270P pickup truck impacting the system with one tube at Joint no. 1 (i.e., the transition joint between the reduced-deflection PCB and the free-standing PCB) with different impact points, as shown in Figure 25. The simulation results with one steel tube at the base of Joint no. 1 and with no tube spacer are shown in Table 7.

Table 7. Summary of Simulation Results – One Steel Tube at Base of Joint No. 1

Impact Point in. (mm) Upstream Joint No. 1	Tube Location	Lat. OIV ft/s (m/s)	Long. OIV ft/s (m/s)	Lat. ORA g's	Long. ORA g's	Roll deg.	Pitch deg.	Lateral Barrier Deflection in. (mm)	Increase in Vertical Bumper Height in. (mm)
194.1 (4,930)	Joint No. 1	-17.7 (-5.4)	-16.1 (-4.9)	-16.8	-5.5	-13.7	12.5	64.3 (1,633)	12.2 (310)
	None *	-17.7 (-5.4)	-16.1 (-4.9)	-5.3	-5.9	-4.4	5.8	36.8 (935)	11.3 (287)
202.0 (5,130)	Joint No. 1	-17.1 (-5.2)	-15.1 (-4.6)	-17.8	-5.5	-15.6	11.8	61.9 (1,572)	6.7 (170)
	None *	-17.1 (-5.2)	-14.8 (-4.5)	-6.7	-4.8	-5.9	4.5	36.2 (919)	9.2 (234)
209.8 (5,330)	Joint No. 1	-16.1 (-4.9)	-16.1 (-4.9)	-18.0	-6.2	-20.9	11.9	65.9 (1,674)	7.8 (198)
	None	-16.1 (-4.9)	-16.1 (-4.9)	-19.8	-6.8	-23.2	29.1	63.8 (1,621)	7.0 (178)
217.7 (5,530)	Joint No. 1	-16.1 (-4.9)	-13.5 (-4.1)	-20.9	-6.0	-24.1	9.4	65.5 (1,664)	5.7 (145)
	None	-16.1 (-4.9)	-13.8 (-4.2)	-20.4	-7.9	-24.4	21.2	62.8 (1,595)	5.3 (135)
225.6 (5,730)	Joint No. 1	-17.4 (-5.3)	-10.5 (-3.2)	-20.6	-10.6	-21.9	10.9	64.1 (1,628)	6.2 (157)
	None	-16.7 (-5.1)	-9.8 (-3.0)	-19.0	-8.3	-23.1	9.4	65.3 (1,659)	6.1 (155)
312.2 (7,930)	Joint No. 1	-19.4 (-5.9)	-16.7 (-5.1)	-11.0	3.8	-17.1	17.6	79.2 (2,012)	24.9 (632)
	None	-19.4 (-5.9)	-17.1 (-5.2)	-10.2	-4.1	-12.4	18.8	80.1 (2,035)	25.8 (655)
351.6 (8,930)	Joint No. 1	-17.4 (-5.3)	-15.4 (-4.7)	-14.8	-5.9	-14.6	12.6	76.8 (1,951)	8.3 (211)
	None	-17.4 (-5.3)	-15.1 (-4.6)	-13.5	-6.1	-16.5	13.2	74.1 (1,882)	7.9 (201)

* Simulation terminated early due to numerical instabilities

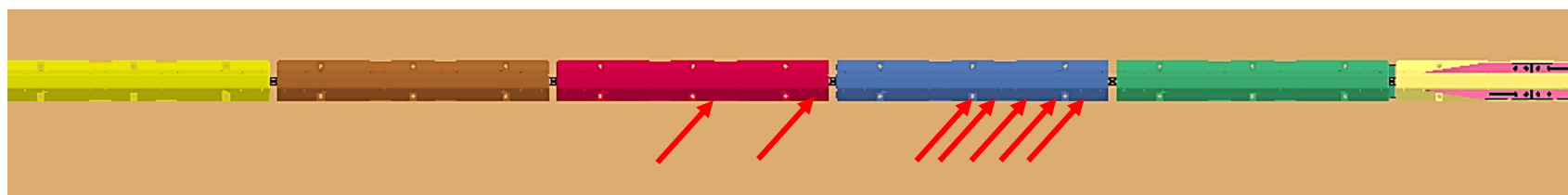


Figure 25. Simulated Cases with One Tube at Joint No. 1– Impact Points

Adding a single tube at the base of Joint no. 1 improved the transition behavior slightly in terms of knee formation and contact with the vehicle's side. However, this concern was not completely resolved. In a number of cases, including the impact points 202.0, 217.7, and 225.6 in. (5,130, 5,530, and 5,730 mm) upstream from the transition joint, the knee formed and hit the vehicle door. The knee contact on the vehicle door and propensity for instability with the impact point at 225.6 in. (5,730 mm) upstream from the transition joint is shown in Figure 26. Additional sequential photographs of this simulation are shown in Figure 27.

In the cases with one tube spacer, the occupant risk values and the roll and pitch angles did not change significantly. In most of the cases with one tube, a slight increase in barrier deflection of approximately 2 in. (51 mm) was observed. In these simulations, the steel tube joint spacer was completely crushed. This behavior itself was not of concern. Stiffer tubes may help prevent the knee from forming and providing smoother redirection.

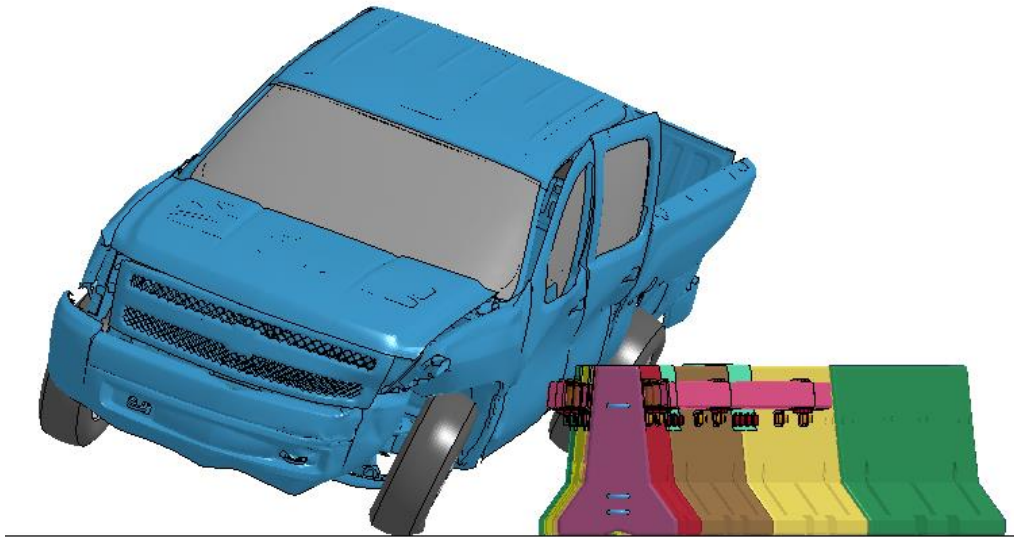


Figure 26. Knee Contact on Vehicle Door– Impact Point 225.6 in. (5,730 mm) Upstream from Transition Joint

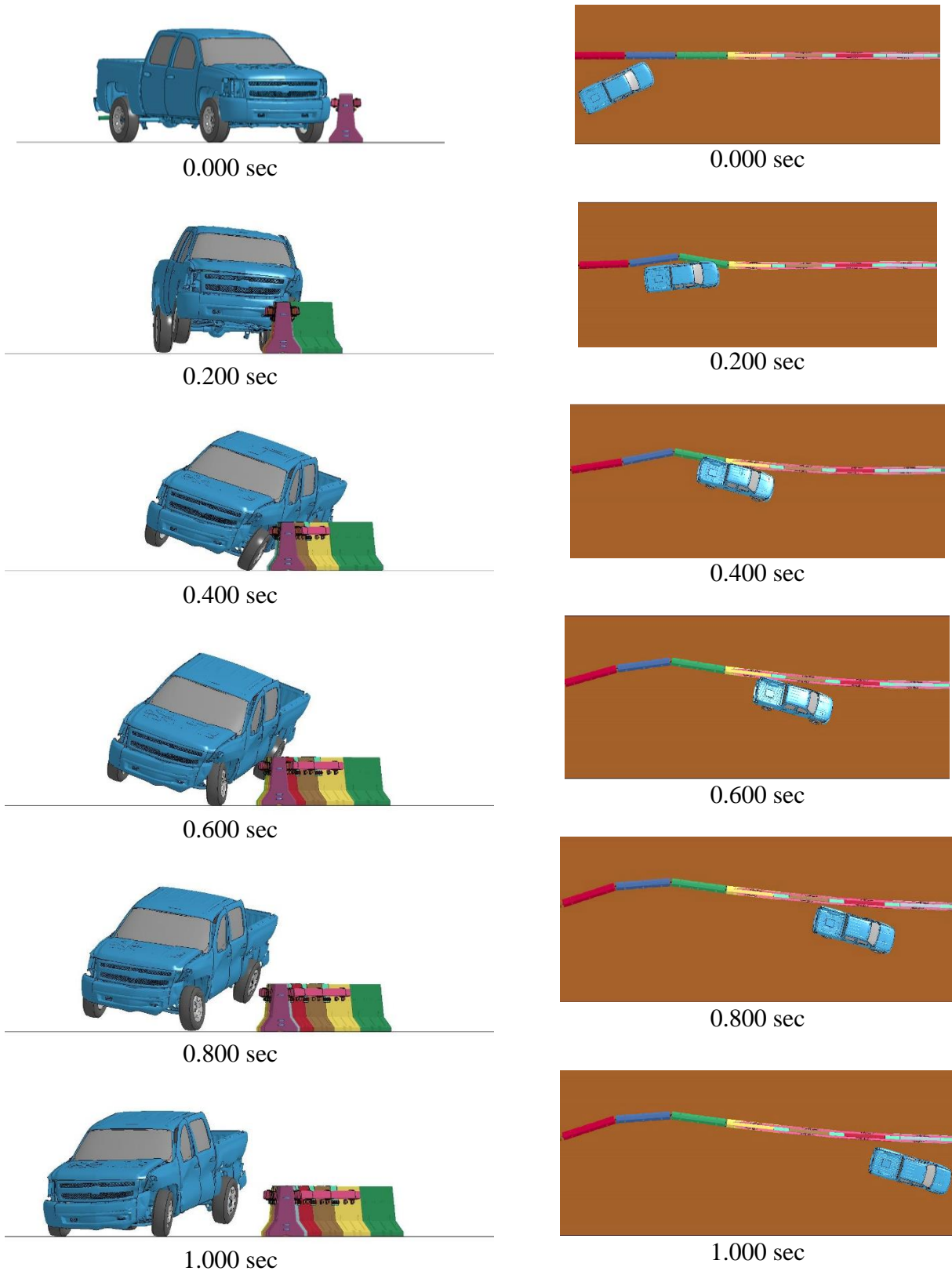


Figure 27. Sequential Photographs: Impact Point at 225.6 in. (5,730 mm) Upstream from Transition Joint with One Steel Tube

7.3 Tube Spacers Added at Joints Nos. 1 and 2

After it was determined that adding a single HSS 3½x3½x¼ tube at one joint (Joint no. 1) improved the vehicle and barrier performance, another tube (HSS 3½x3½x¼) was added at the base of the next joint upstream from the previous joint with a tube spacer. Thus, a total of two joints had a tube spacer, as shown in Figure 28. A number of simulations were conducted with the 2270P pickup truck model impacting the system with one tube at Joint nos. 1 and 2 at different impact points. A summary of simulation results with one steel tube at the base of Joint nos. 1 and 2 and one steel tube at the base of Joint no. 1 is shown in Table 8.

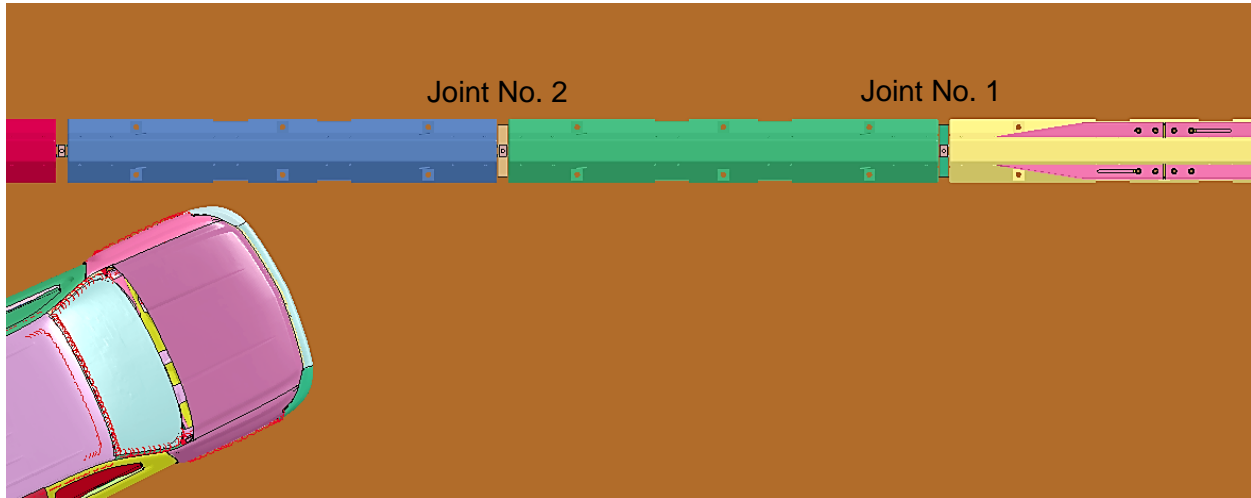


Figure 28. Single Steel Tube Added at Joint Nos. 1 and 2

The simulations with tubes at two joints had lateral ORA values 10 to 20 percent less than the simulations with a tube at one joint. Adding tubes at two joints created a smoother redirection as more barrier segments were engaged throughout the impact. In most of the simulations, including impact points at 224.4, 217.7, 312.2, and 351.6 in. (5,700, 5,530, 5,730, 7,930, and 8,930 mm) upstream from the transition joint, the roll angle decreased with tubes at two joints. The vehicle snag and knee hitting the vehicle's door were less pronounced in the simulations with one tube at two joints as compared to one tube at one joint. An example comparison of simulations with a tube at one joint and a tube at two joints is shown in Figure 30. The deflection of the system increased approximately 10 in. (254 mm), but it was still in desired deflection range. In the simulations with tubes at two joints, the crushing of tubes was moderate.

Utilizing stiffer tubes at two joints would further decrease the potential for vehicle snag, decrease ORAs, provide smoother vehicle redirection, and mitigate knee and door contact concerns. Thus, various alternatives, including utilizing thicker tubes (HSS 3½x3½x¾ tubes), utilizing two tubes with different sizes (HSS 3½x3½x¼ tube with HSS 2½x2½x¼ tube inside), and utilizing a stack of two tubes (HSS 3½x1½x¼ tube at the base and HSS 3½x1½x¼ tube on top) at Joint nos. 1 and 2 were investigated through simulations, as described in the following sections. The simulations included a 2270P vehicle model impacting the concrete barriers 225.6 in. (5,730 mm) upstream from the transition joint to evaluate and compare the effectiveness of different stiffer tubes configurations with the same impact conditions and impact location.

Table 8. Summary of Simulation Results – Single Steel Tube at Base of Joint Nos. 1 and 2

Impact Point in. (mm) Upstream Joint No. 1	Tube Location	Lat. OIV ft/s (m/s)	Long. OIV ft/s (m/s)	Lat. ORA g's	Long. ORA g's	Roll deg.	Pitch deg.	Lateral Barrier Deflection in. (mm)	Increase in Vertical Bumper Height in. (mm)
194.1 (4,930)	Joint No. 1	-17.7 (-5.4)	-16.1 (-4.9)	-16.8	-5.5	-13.7	12.5	64.3 (1,633)	12.2 (310)
	Joint Nos. 1 and 2	-18.4 (-5.6)	-16.1 (-4.9)	-15	-5.8	-15.2	12.2	74.7 (1,897)	10.8 (274)
202.0 (5,130)	Joint No. 1	-17.1 (-5.2)	-15.1 (-4.6)	-17.8	-5.5	-15.6	11.8	61.9 (1,572)	6.7 (170)
	Joint Nos. 1 and 2	-17.4 (-5.3)	-14.1 (-4.3)	-16.9	-4.8	-16.8	10.2	74.0 (1,880)	9.4 (239)
209.8 (5,330)	Joint No. 1	-16.1 (-4.9)	-16.1 (-4.9)	-18.0	-6.2	-20.9	11.9	65.9 (1,674)	7.8 (198)
	Joint Nos. 1 and 2	-16.4 (-5.0)	-14.1 (-4.3)	-17.6	-5.1	-17.6	9.9	75.6 (1,920)	5.4 (137)
217.7 (5,530)	Joint No. 1	-16.1 (-4.9)	-13.5 (-4.1)	-20.9	-6.0	-24.1	9.4	65.5 (1,664)	5.7 (145)
	Joint Nos. 1 and 2	-16.4 (-5.0)	-13.1 (-4.0)	-17.8	-5.1	-16.3	12.1	77.4 (1,966)	6.3 (160)
225.6 (5,730)	Joint No. 1	-17.4 (-5.3)	-10.5 (-3.2)	-20.6	-10.6	-21.9	10.9	64.1 (1,628)	6.2 (157)
	Joint Nos. 1 and 2	-17.7 (-5.4)	-10.5 (-3.2)	-17.7	-9.9	-18.7	11.9	75.5 (1,918)	6.3 (160)
312.2 (7,930)	Joint No. 1	-19.4 (-5.9)	-16.7 (-5.1)	-11.0	3.8	-17.1	17.6	79.2 (2,011)	24.9 (632)
	Joint Nos. 1 and 2	-19.0 (-5.8)	-16.7 (-5.1)	-11.1	-4.0	-12.8	17.6	83.1 (2,111)	25.4 (645)
351.6 (8,930)	Joint No. 1	-17.4 (-5.3)	-15.4 (-4.7)	-14.8	-5.9	-14.6	12.6	76.8 (1,951)	8.3 (211)
	Joint Nos. 1 and 2	-16.7 (-5.1)	-15.7 (-4.8)	-12.6	-6.3	-12.7	7.0	59.5 (1,511)	11.3 (287)

37

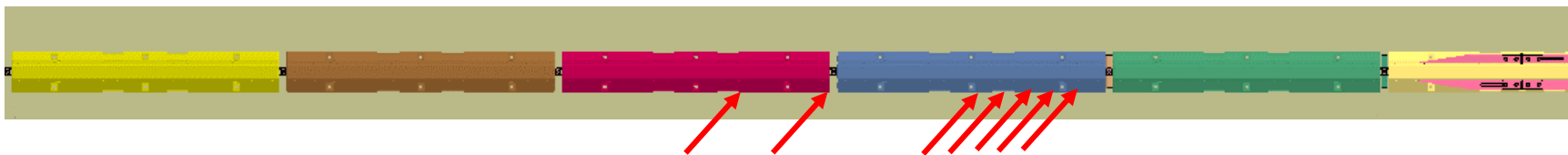


Figure 29. Simulated Cases with Tube at Joints Nos. 1 and 2 – Impact Points

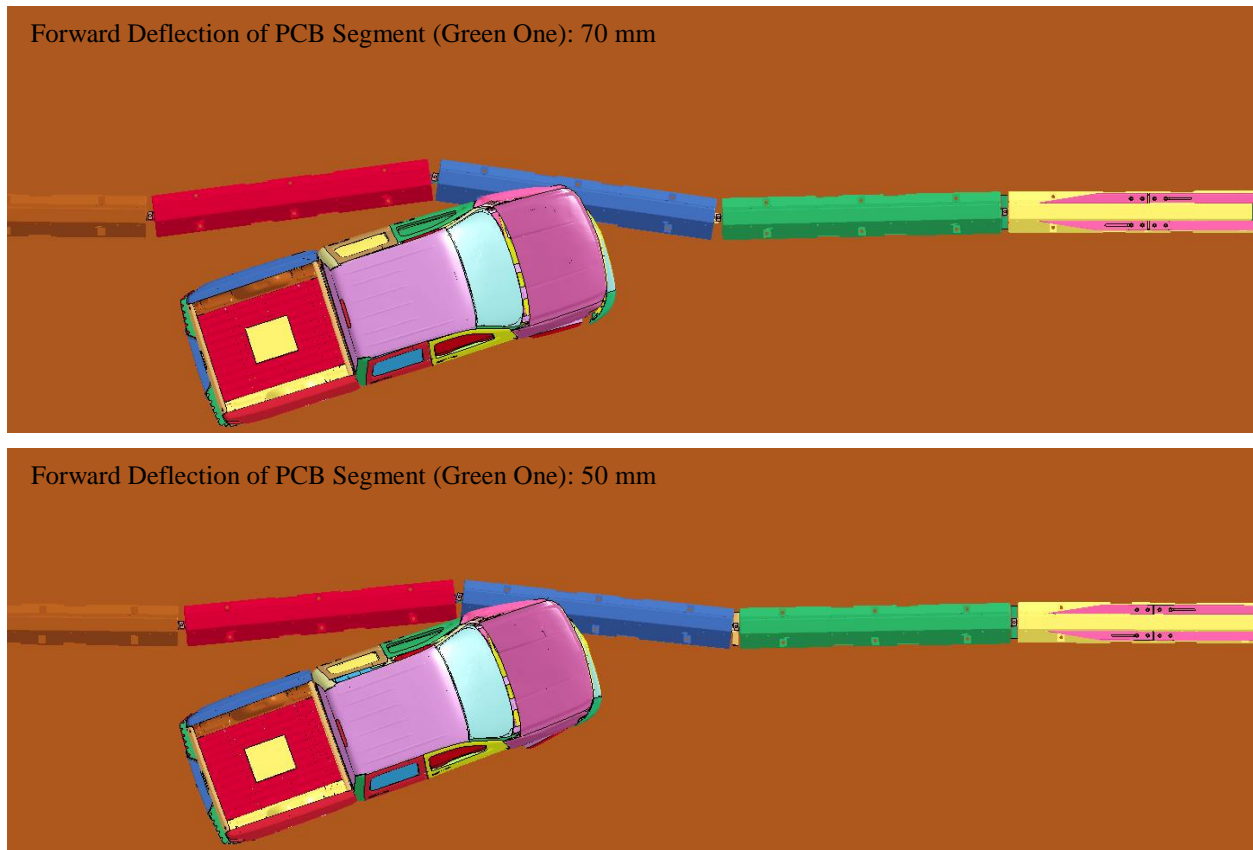


Figure 30. (a) Tube Added at Joint No. 1, (b) Tube Added at Joint Nos. 1 and 2 – Impact Point 351.6 in. (8,930 mm) Upstream from Transition Joint

7.3.1 Single Tubes with Increased Thickness

The simplest alternative to stiffen the tube spacer was to increase the tube thickness. Computer simulations were performed with $\frac{3}{8}$ -in. (10-mm) thick steel tubes at joint nos. 1 and 2. The transition performance was significantly improved. In most of the simulations with different impact points, the concern of knee contact with the door was resolved. As shown in Figure 31 and by comparing the cases with an impact point 225.6 in. (5,730 mm) upstream from the transition joint, one HSS $3\frac{1}{2} \times 3\frac{1}{2} \times \frac{3}{8}$ tube at two joints indicated less knee contact with the door as compared to the one HSS $3\frac{1}{2} \times 3\frac{1}{2} \times \frac{1}{4}$ tube at two joints. A comparison between these simulations with $\frac{1}{4}$ -in. and $\frac{3}{8}$ -in. (6-mm and 10-mm) thick tubes with an impact point of 225.6 in. (5,730 mm) upstream from the transition joint is shown in Table 9. The occupant risk values, roll and pitch angles, and vehicle bumper climb slightly increased with the $\frac{3}{8}$ -in. (10-mm) thick tube. However, these values were still within the acceptable MASH 2016 limits. The dynamic deflection of the system decreased from 75.5 in. (1,918 mm) with $\frac{1}{4}$ -in. (6-mm) thick tubes to 56.1 in. (1,425 mm) with $\frac{3}{8}$ -in. (10 mm) thick tubes. The tubes were partially crushed.



(a)



(b)

Figure 31. (a) HSS $3\frac{1}{2} \times 3\frac{1}{2} \times \frac{1}{4}$ Tube Added at Joint Nos. 1 and 2, (b) HSS $3\frac{1}{2} \times 3\frac{1}{2} \times \frac{3}{8}$ Tube Added at Joint Nos. 1 and 2 – Impact Point 225.6 in. (5,730 mm) Upstream from Transition Joint

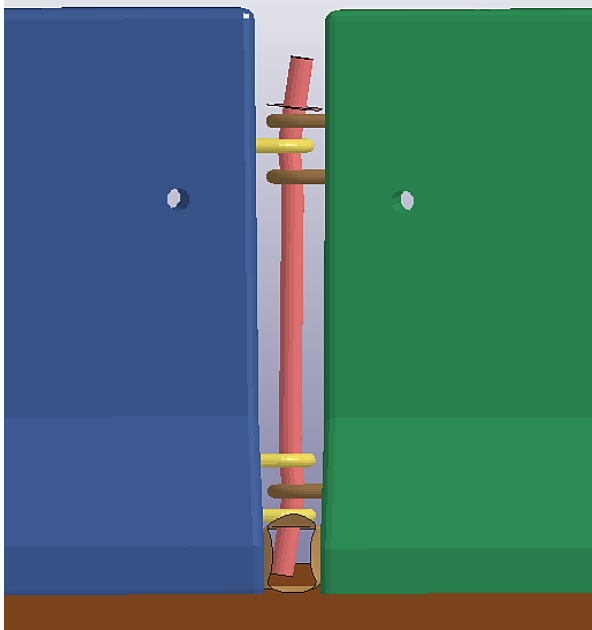


Figure 32. Single Tube HSS $3\frac{1}{2} \times 3\frac{1}{2} \times \frac{3}{8}$ Added at Joint Nos. 1 and 2 – After Impact

7.3.2 Simulations of Dual Tubes

Another stiffened transition design utilized an HSS $3\frac{1}{2} \times 3\frac{1}{2} \times \frac{1}{4}$ tube with an HSS $2\frac{1}{2} \times 2\frac{1}{2} \times \frac{1}{4}$ tube inside, as shown in Figure 33. The other dual tube alternative with an HSS $3\frac{1}{2} \times 1\frac{1}{2} \times \frac{1}{4}$ tube at the base and another HSS $3\frac{1}{2} \times 1\frac{1}{2} \times \frac{1}{4}$ tube on top was also evaluated through simulations, as shown in Figure 34. A comparison between the cases with single and dual tubes with an impact point of 225.6 in. (5,730 mm) upstream from the transition joint is shown in Table 9. Both dual tube alternatives indicated an improved performance in terms of knee and door contact as compared to a single HSS $3\frac{1}{2} \times 3\frac{1}{2} \times \frac{1}{4}$ tube. As shown in Figure 35, the knee was much less prominent than observed for the single HSS $3\frac{1}{2} \times 3\frac{1}{2} \times \frac{1}{4}$ tube simulation. The occupant risk values, roll and pitch angles, and vehicle bumper climbing were similar to the single $\frac{3}{8}$ -in. thick tube option and were within the acceptable MASH 2016 limits. The dynamic deflection of the system decreased from 75.5 in. (1,918 mm) with $\frac{1}{4}$ -in. (6-mm) thick tubes to 60 in. (1,524 mm) and 58.8 in. (1,494 mm) with concentric dual tubes and stack of two tubes at Joint nos. 1 and 2, respectively. The dual tubes were also partially crushed.

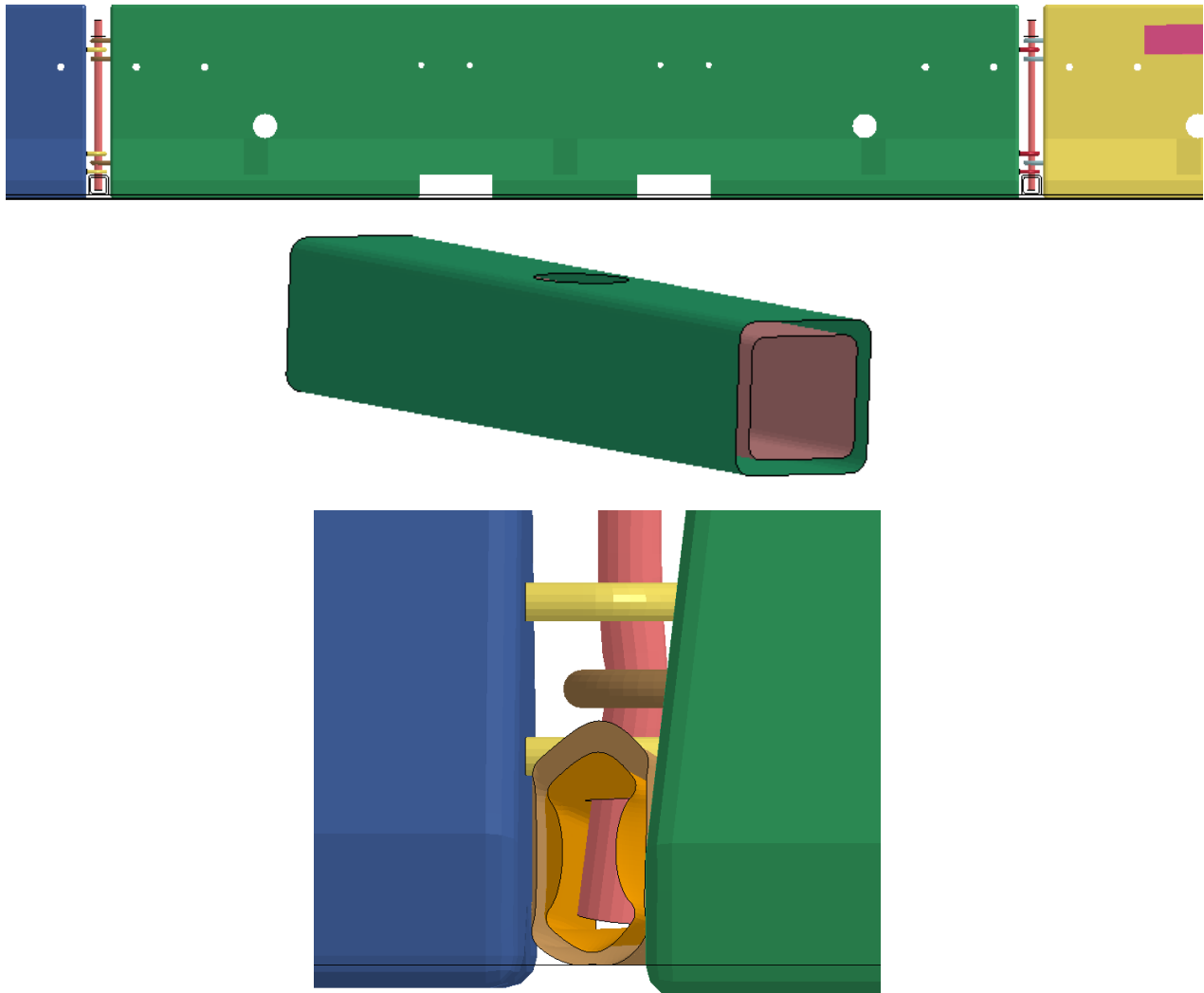


Figure 33. Dual Tubes – HSS $3\frac{1}{2} \times 3\frac{1}{2} \times \frac{1}{4}$ Tube with HSS $2\frac{1}{2} \times 2\frac{1}{2} \times \frac{1}{4}$ Tube Inside Added at Joint Nos. 1 and 2

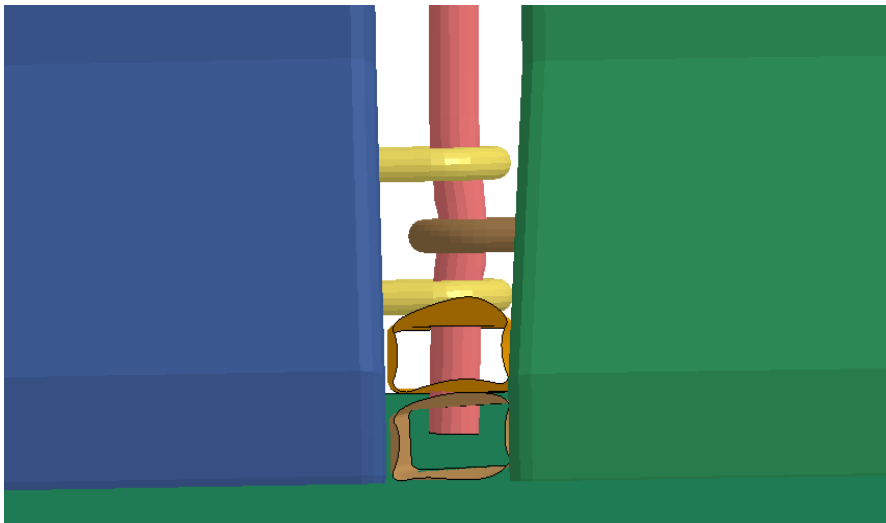
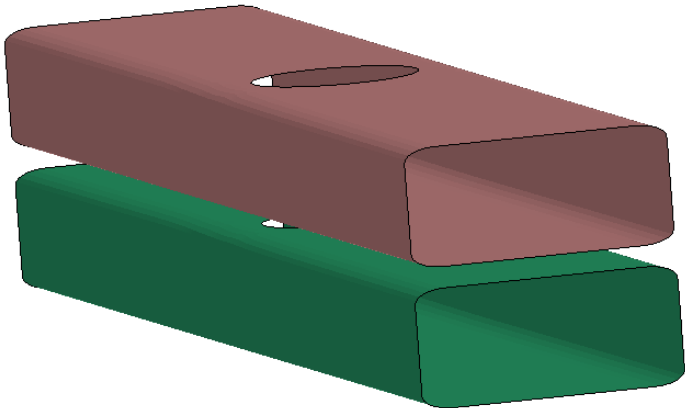
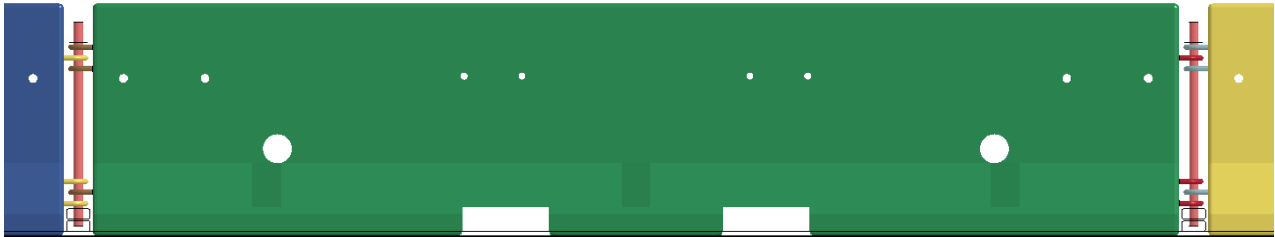
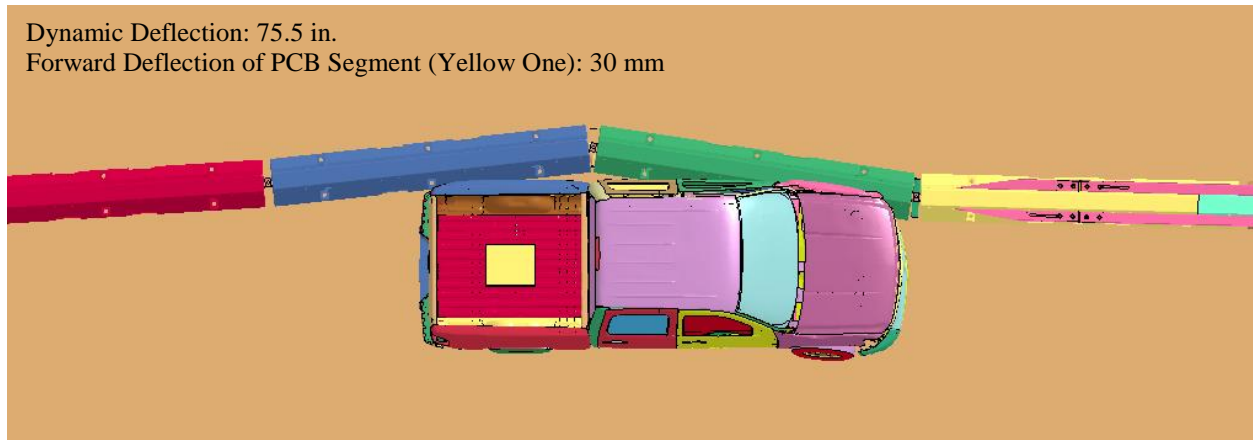
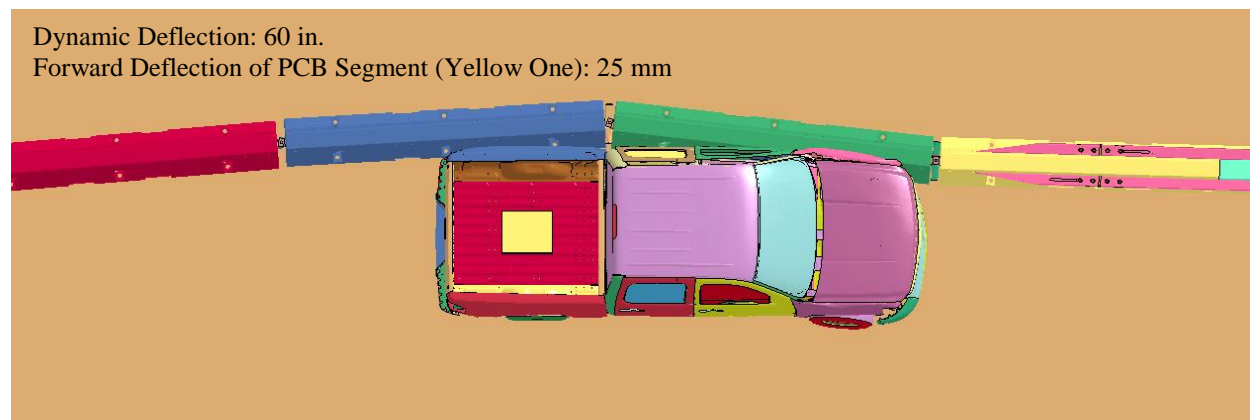


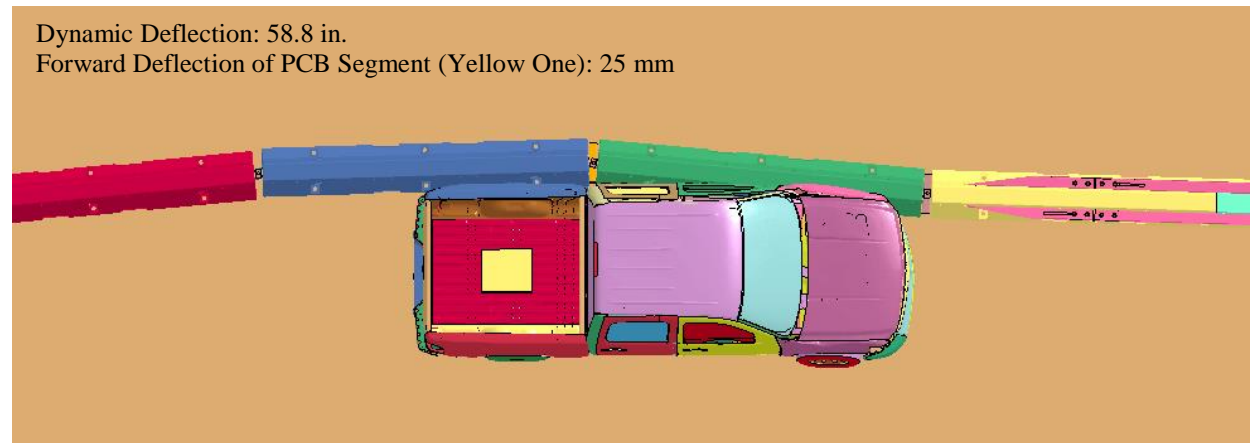
Figure 34. Dual Tubes – Stack of Two HSS 3½x1½x ¼ Tubes Added at Joint Nos. 1 and 2



(a)



(b)



(c)

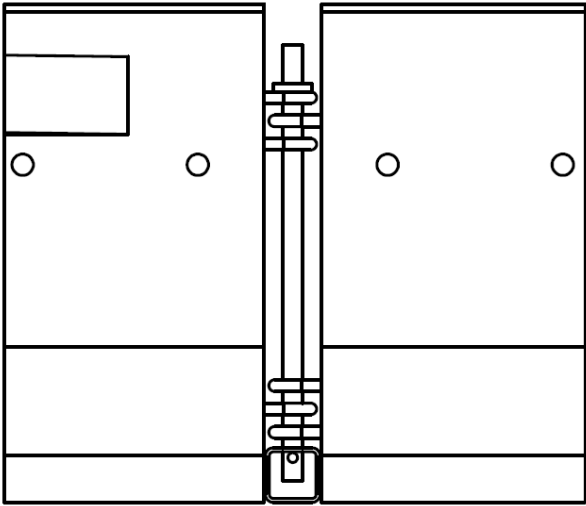
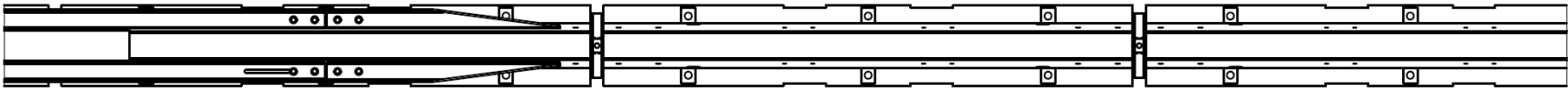
Figure 35. Modified Transition Design: (a) HSS $3\frac{1}{2} \times 3\frac{1}{2} \times \frac{1}{4}$ Tube Added, (b) HSS $3\frac{1}{2} \times 3\frac{1}{2} \times \frac{1}{4}$ Tube with HSS $2\frac{1}{2} \times 2\frac{1}{2} \times \frac{1}{4}$ Tube Inside, and (c) Stack of Two HSS $3\frac{1}{2} \times 1\frac{1}{2} \times \frac{1}{4}$ Tubes Added at Joint Nos. 1 and 2 – Impact Point 225.6 in. (5,730 mm) Upstream from Transition Joint

Table 9. Summary of Simulation Results – Impact Point 225.6 in. (5,730 mm) Upstream from Transition Joint – Single and Dual Tubes

Simulation	Lat. OIV ft/s (m/s)	Long. OIV ft/s (m/s)	Lat. ORA g's	Long. ORA g's	Roll deg.	Pitch deg.	Lat. Barrier Deflection in. (mm)	Increase in Vertical Bumper Height in. (mm)
Single ¼-in. (6-mm) Tube	-17.7 (-5.4)	-10.5 (-3.2)	-17.7	-9.9	-18.7	11.9	75.5 (1,918)	6.3 (160)
Single ⅜-in. (10-mm) Tube	-18.4 (-5.6)	-12.1 (-3.7)	-19.2	-10.4	-17.6	12.4	56.1 (1,425)	7.2 (183)
Dual Tubes – Concentric	-17.7 (-5.4)	-10.8 (-3.3)	-19.8	-10.5	-18.0	12.5	60.0 (1,524)	7.1 (180)
Dual Tubes – Stacked	-18.7 (-5.7)	-13.8 (-4.2)	-18.5	-13.4	19.1	12.5	58.8 (1,494)	7.5 (191)

7.3.3 Selected Design Modification

All three alternatives indicated a promising improvement in vehicle and barrier performance in terms of decreased potential for vehicle snag, decreased ORAs, smoother vehicle redirection, and mitigation of knee contact. It was recommended to pursue the option of thicker tubes – one HSS 3½x3½x⅜ at the two joints upstream from the reduced-deflection system due to its ease of fabrication and installation. Details of this concept design are shown in Figure 36.



HSS 3 1/2"x3 1/2"x3/8"
[89x89x10]

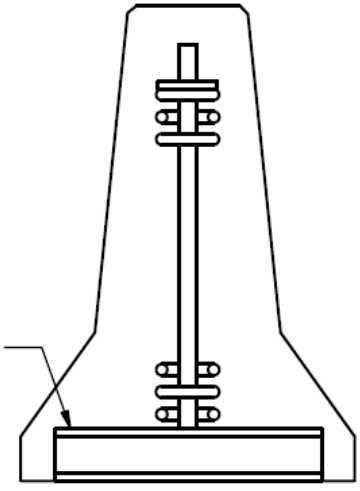


Figure 36. Single Tube HSS 3 1/2x3 1/2x3/8 Added at Joint Nos. 1 and 2

8 DETERMINATION OF CRITICAL IMPACT POINTS

As previously discussed, it was recommended to pursue the option of thicker tubes, one HSS $3\frac{1}{2} \times 3\frac{1}{2} \times \frac{3}{8}$ at the base of two joints upstream from the reduced deflection system, due to its ease of fabrication and installation. Further simulations were performed to determine the CIPs for full-scale crash testing of the selected design. Computer simulations were performed on the selected design modifications with different impact points upstream from the transition joint, and the results are discussed in the subsequent sections.

8.1 Determination of CIPs – Test Designation No. 3-21

In order to identify the CIPs for test designation no. 3-21 upstream from the stiffness transition, pickup truck impacts on the barrier were simulated using a single HSS $3\frac{1}{2} \times 3\frac{1}{2} \times \frac{3}{8}$ tube at the base of two joints located upstream from the reduced-deflection system. The impact points, ranging from 17.7 in. to 820.9 in. (450 mm to 20,850 mm) upstream from Joint no. 1, as shown in Figure 37 and Table 10, covered both regions with stiffness changes, one from the reduced-deflection PCB to the transition section and the other from the transition section to the free-standing PCB. A summary of the simulation results with thicker tubes (i.e., $\frac{3}{8}$ -in. (10-mm) thick tubes) with different impact points is shown in Table 10.

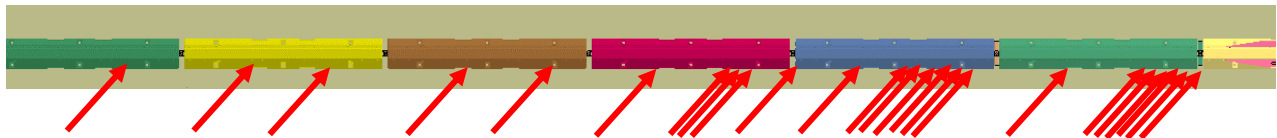


Figure 37. Simulated Cases with Tube at Two Joints Nos. 1 and 2 – Impact Points

MASH 2016 recommends an impact point 4.3 ft (1.3 m) upstream from a joint between PCB segments to investigate the potential for vehicle snag. The dynamic deflection of the system with the impact point of 4.3 ft (1.3 m) upstream from the transition joint was 53 in. (1,346 mm), which ranged between the deflection of the reduced-deflection PCB (40.7 in. (1,034 mm)) and the deflection of the free-standing PCB (79.6 in. (2,022 mm)). The pickup truck fender contacted the box beam and indicated a potential for vehicle snag on the tapered box tube ends along the reduced-deflection PCB at an impact point 4.3 ft (1.3 m) upstream from transition joint, as shown in Figure 38. In the simulations, the tapered tubes were constrained to the PCB segments. Although the box-beam tube connection to the PCB has not been designed, tubes may flex away from the PCB segments and induce increased potential for vehicle snag under the end of the tapered tubes. Other measures, including occupant risk values, roll and pitch angles, and bumper climb, were acceptable.

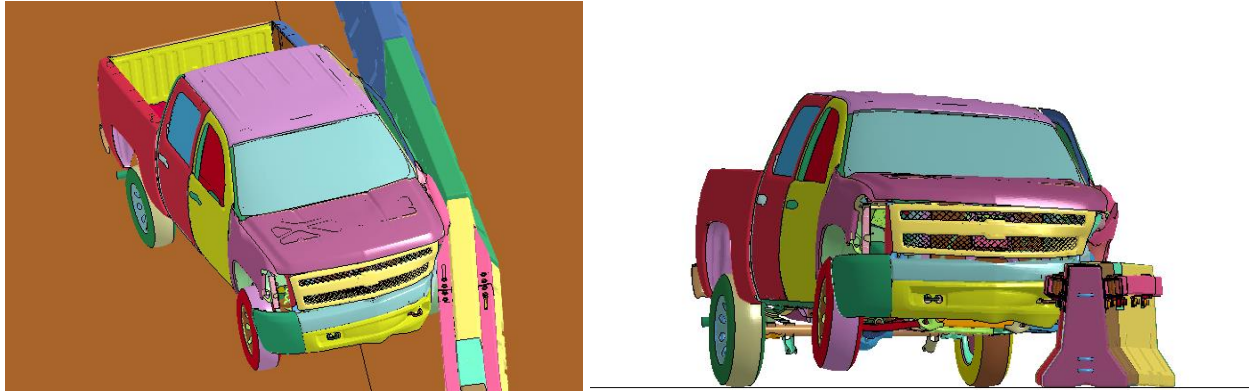


Figure 38. Vehicle Snag on Box Tubes Along Reduced-Deflection PCB – Impact Point 4.3 ft (1.3 m) Upstream from Transition Joint

As shown in Table 10, the impact points farther upstream from the reduced-deflection system, including 352.0 in. (8,940 mm) through 820.9 in. (20,850 mm), had larger deflections and behaved more like the free-standing PCB system. One of the design criteria was to ensure that barrier deflections range between those observed for the reduced-deflection system (40.7 in. (1,034 mm)) and the free-standing PCB system (79.6 in. (2,022 mm)). In the impact points, including 499.2 in. (12,680 mm) through 820.9 in. (20,850 mm), barrier deflections exceeded the free-standing PCB deflection (i.e., > 79.6 in. (2,022 mm)). The increased deflections may be due to the proximity of the impact points to the upstream end of barrier model. Since the barrier model ends were not anchored, vehicle impacts close to the upstream barrier end may cause larger deflections.

In the simulation of the impact point at 820.9 in. (20,850 mm) upstream from the transition joint, the vehicle impact was 410 in. (10,405 mm) away from the end of the barrier model. As such, there was a possibility that the short distance between the impact point and the barrier end would affect the results (i.e., PCB deflections and the knee formation). In the simulation of this impact point, three identical concrete segments were added to the barrier model. The results of the longer barrier with impact point at 820.9 in. (20,850 mm) are provided in Table 10. Based on this numerical study, a minimum of eight barriers would be needed upstream the transition joint.

In addition, the impact points farther upstream, including 511.8 in. (13,000 mm) through 820.9 in. (20,850 mm), generally had larger roll and pitch angles. Two impact points, 590.6 in. (15,000 mm) and 744.1 in. (18,900 mm), indicated relatively high lateral ORAs (22.5 g's). However, as previously noted, LS-DYNA simulation tends to over-predict lateral ORA, as the back of the pickup truck model appears to be stiffer than actual pickup truck test vehicles. Therefore, these ORAs were not a concern. The impact points, including 669.3, 744.1, and 820.9 in. (17,000, 18,900, and 20,850 mm) upstream from the transition joint, showed potential concern for the PCB knee contacting the vehicle's door. In these impacts, one of the PCB segments upstream from the transition joint deflected forward and hit the vehicle's door. In simulations of these impact points (669.3, 744.1, and 820.9 in. (17,000, 18,900, and 20,850 mm) upstream from the transition joint), the maximum forward deflection of the PCB segments, that formed the knee and contacted the vehicle, was measured 9, 2, and 7 in. (228, 51, and 180 mm), respectively.

In the simulations, the PCB-knee contact was closely examined to determine the most critical cases. The impact point at 669.3 in. (17,000 mm) upstream from the transition joint had a

maximum forward deflection of a PCB segment of 9 in. (228 mm), a maximum roll angle of 18.5 degrees, a dynamic deflection of 83 in. (2,108 mm), and the PCB knee contacted the vehicle's door. Note that knee contact, as shown in Figure 39, did not seem aggressive in the simulations. However, there may be a need to evaluate this impact condition and evaluate the risk of vehicle instability due to the knee contact, based on previous PCB crash testing with a knee forming between adjacent PCBs and the highest roll angle. Thus, a CIP for 2270P vehicle crash testing under designation no. 3-21 was recommended to be 669.3 in. (17,000 mm) upstream from the transition joint. Sequential photographs for the simulation with an impact point at 4.3 ft (1.3 m) and 669.3 in. (17,000 mm) upstream from transition joint are shown in Figures 40 and 41, respectively.

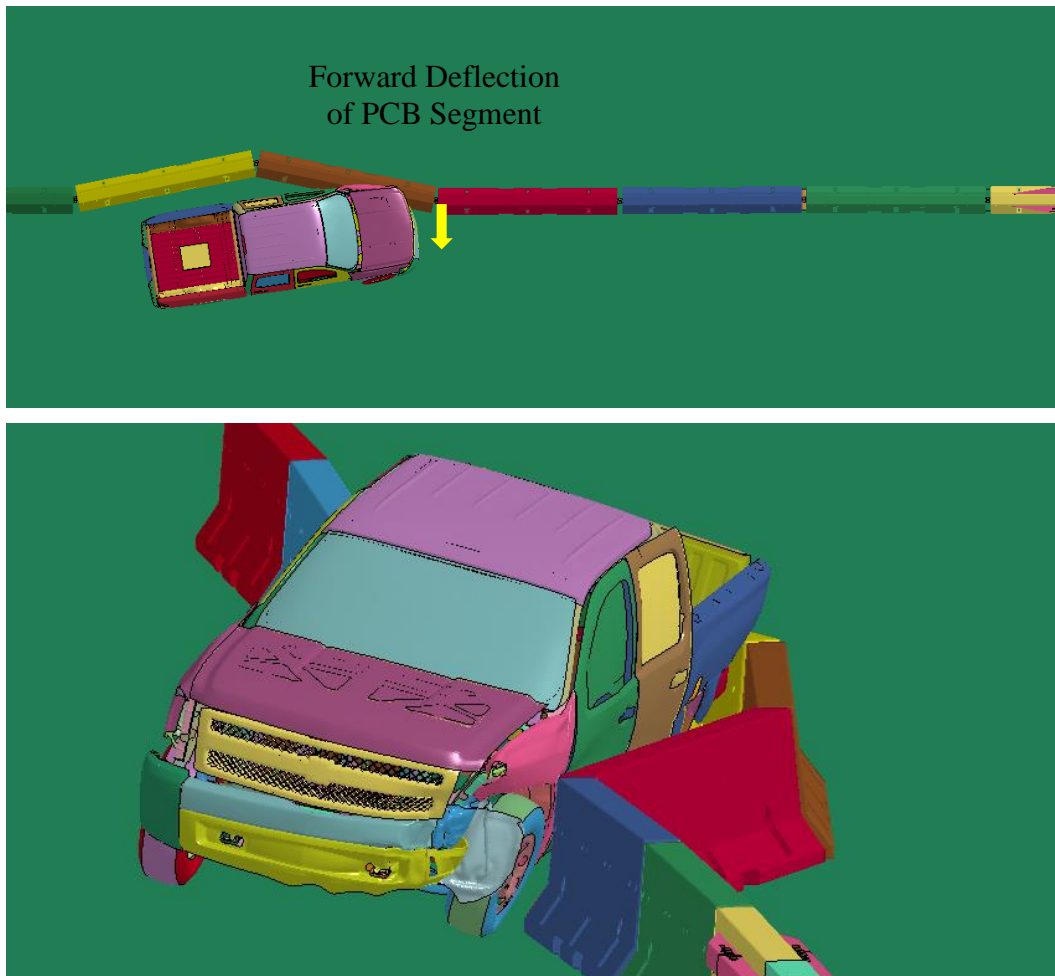


Figure 39. Knee Contact – Impact Point 669.3 in. (17,000 mm) Upstream from Transition Joint

Table 10. Summary of Simulation Results – HSS 3½x3½x¾ Single Tube at Joints Nos. 1 and 2

Simulation No.	Impact Point in. (mm) Upstream Joint No.1	Lat. OIV ft/s (m/s)	Long. OIV ft/s (m/s)	Lat. ORA g's	Long. ORA g's	Roll deg.	Pitch deg.	Lat. Barrier Deflection in. (mm)	Increase in Vertical Bumper Height in. (mm)
1	17.7 (450)	-20.3 (-6.2)	22.0 (-6.7)	-11.4	-6.7	-7.6	6.6	60.8 (1,544)	3.5 (89)
2	33.5 (850)	-21.0 (-6.4)	21.7 (-6.6)	-15.0	-5.8	-11	9.8	64.3 (1,633)	6.6 (168)
3	36.6 (930)	-21.0 (-6.4)	21.0 (-6.4)	-16.7	-6.5	-11.1	10	60.3 (1,532)	6.2 (157)
4	51.2 (1,300)	-19.7 (-6)	14.4 (-4.4)	-17.8	-13	-15	11.9	53 (1,346)	7.6 (193)
5	128 (3,250)	-20.3 (-6.2)	13.8 (-4.2)	-15.0	-3.6	-14.9	12.4	44.5 (1,130)	9 (229)
6	194.4 (4,950)	-18 (-5.5)	16.4 (-5)	-17.5	-5.5	-13.6	12.2	66.4 (1,687)	9.2 (234)
7	202.8 (5,150)	-17.1 (-5.2)	16.1 (-4.9)	-16.8	-5	-12	12.4	56.2 (1,427)	7.3 (185)
8	205.1 (5,210)	-17.4 (-5.3)	13.1 (-4)	-19.3	-6.2	-15	11.3	59.4 (1,509)	5.7 (145)
9	217.3 (5,520)	-17.4 (-5.3)	13.8 (-4.2)	-17.9	-4.8	-16	11.6	56.3 (1,430)	6.9 (175)
10	225.6 (5,730)	-18.4 (-5.6)	12.1 (-3.7)	-19.2	-10.4	-17.6	12.4	56.1 (1,425)	7.2 (183)
11	233.5 (5,930)	-18.4 (-5.6)	12.5 (-3.8)	-18	-10.3	-18	13.6	55.4 (1,407)	7.5 (191)
12	272.8 (6,930)	-19.0 (-5.8)	13.8 (-4.2)	-20.3	-5.3	-17.3	13.4	66 (1,676)	9.6 (244)
13	281.9 (7,160)	-20.0 (-6.1)	14.1 (-4.3)	-20.2	-4.5	-17.5	12.3	69.9 (1,775)	10.4 (264)
14	307.1 (7,800)	-19.0 (-5.8)	16.4 (-5.0)	-12.3	-3.2	-16	14	74.7 (1,897)	23 (584)
15	352.0 (8,940)	-18.4 (-5.6)	15.1 (-4.6)	-17.6	-5.9	-13	11.6	80 (2,032)	6.5 (165)
16	359.1 (9,120)	-15.7 (-4.8)	15.1 (-4.6)	-14.6	-5.9	-14.1	10.9	80.5 (2,045)	5.8 (147)
17	430.3 (10,930)	-19.4 (-5.9)	14.1 (-4.3)	-18.8	-6.9	-15.5	15	77.5 (1,669)	9.8 (249)
18	436.0 (11,075)	-20.3 (-6.2)	14.1 (-4.3)	-20.0	5	-16.7	13.7	79.5 (2,019)	10.4 (264)
19	499.2 (12,680)	-17.4 (-5.3)	17.4 (-5.3)	-12	-7.8	-14.4	14	82.8 (2,103)	15.6 (396)
20	511.8 (13,000)*	-16.1 (-4.9)	14.4 (-4.4)	-17.5	-6.7	-17.6	5.8	57.9 (1,471)	9 (229)
21	590.6 (15,000)	-19.4 (-5.9)	13.8 (-4.2)	-22.5	-6.7	-18	15.3	84 (2,134)	10.6 (269)
22	669.3 (17,000)	-16.4 (-5.0)	15.1 (-4.6)	-15.0	-5.6	-18.5	11.4	83 (2,108)	6.7 (170)
23	744.1 (18,900)	-19.7 (-6)	13.8 (-4.2)	-22.5	6.7	-17.4	16.3	89.9 (2,283)	10.9 (277)
24	820.9 (20,850)	-18.4 (-5.6)	15.7 (-4.8)	-16	-9.3	-18	14.6	81.3 (2,065)	8.7 (221)

* Simulation terminated early due to numerical instability

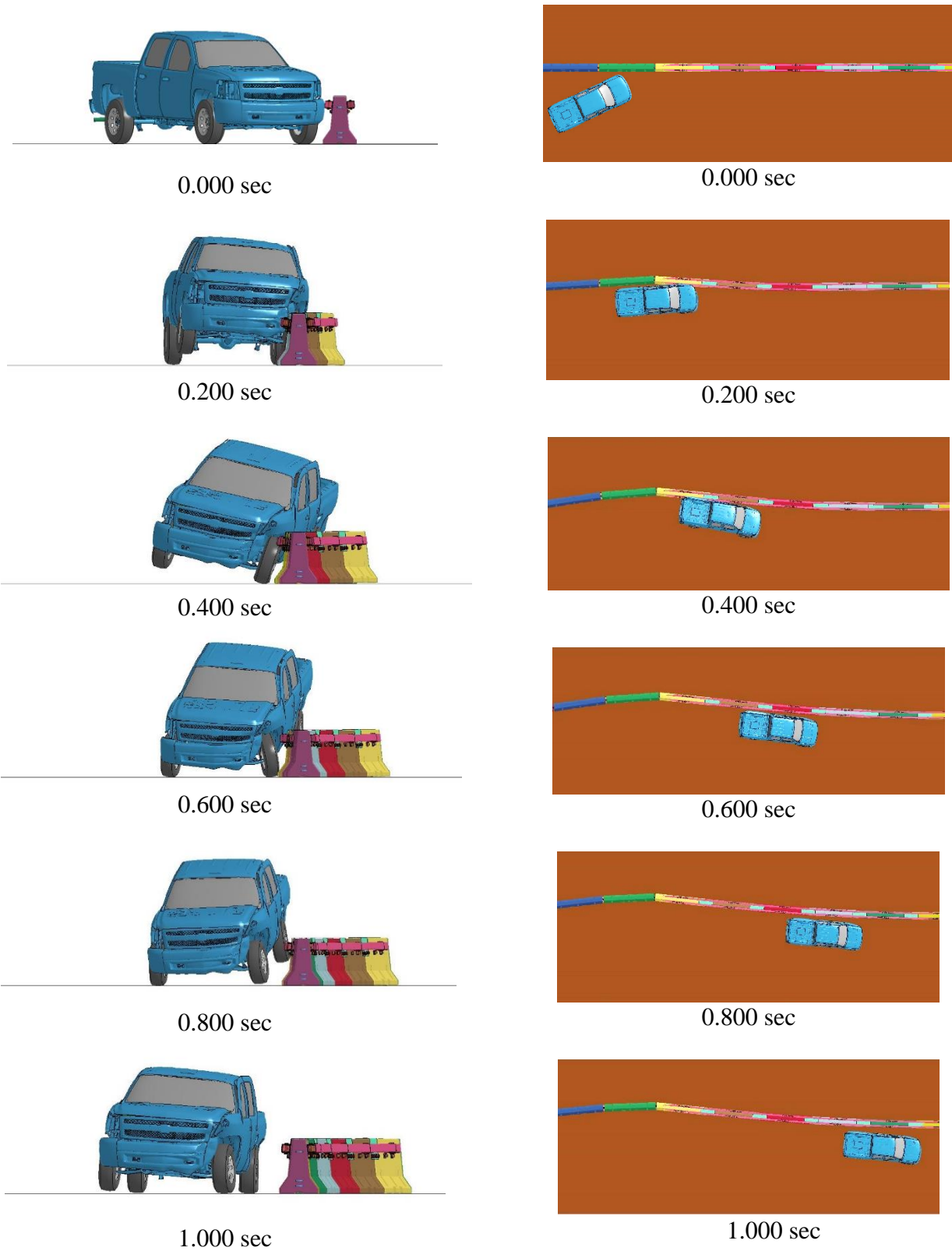


Figure 40. Sequential Photographs: Impact at MASH 2016-Recommended CIP 4.3 ft (1.3 m) Upstream from Transition Joint – 2270P Vehicle

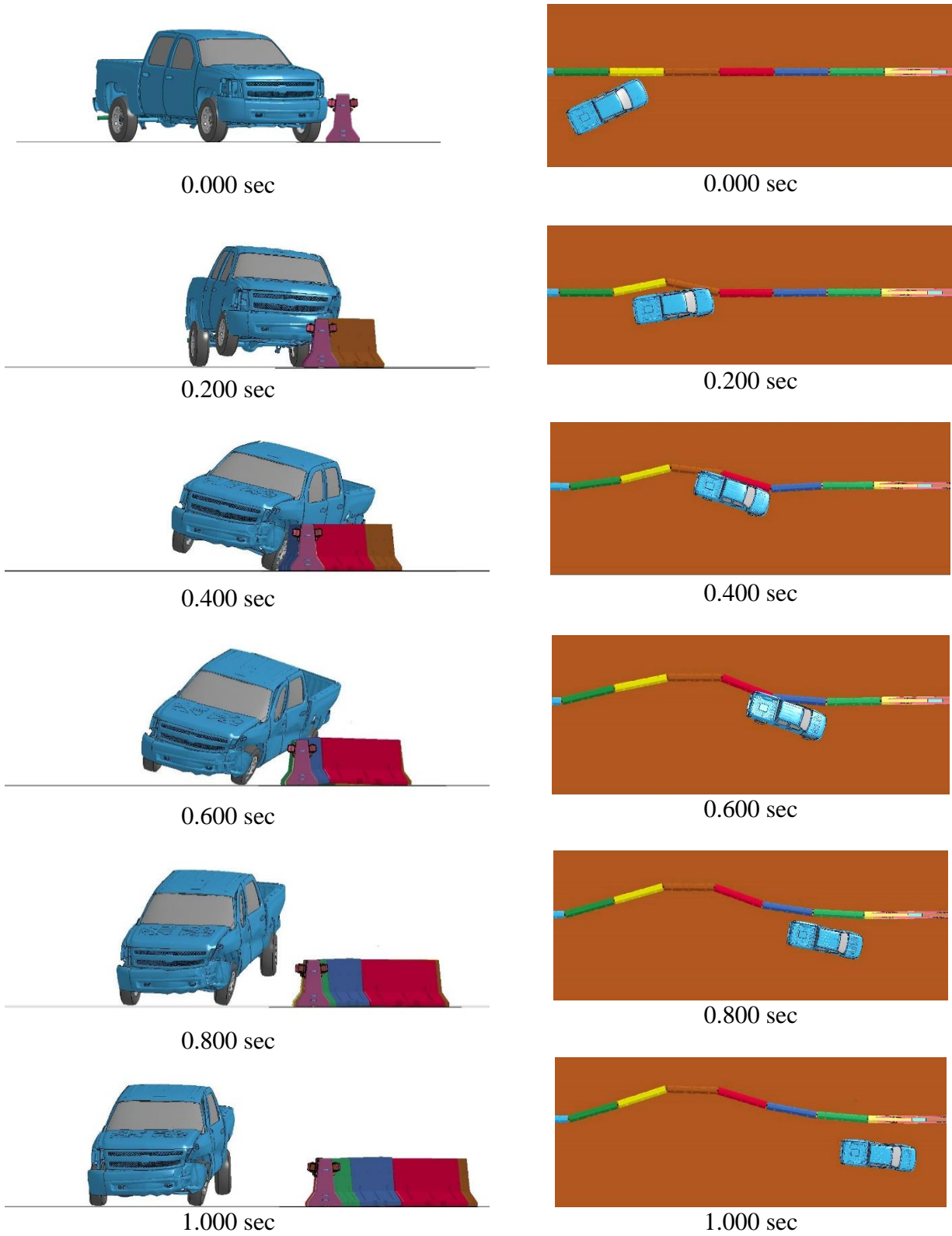


Figure 41. Sequential Photographs: Impact at MASH 2016-Recommended CIP 669.3 in. (17,000 mm) Upstream from Transition Joint – 2270P Vehicle

8.2 Determination of CIP – Test Designation No. 3-20

The numerical analysis primarily focused on the 2270P vehicle due to its higher potential for vehicle snag, climbing, and instability. However, 1100C vehicle impacts on the transition were also evaluated. Simulations were performed using single steel tubes at Joint nos. 1 and 2 with both ¼ in. (6 mm) and ¾ in. (10 mm) thicknesses. For test no. 3-20, MASH 2016 recommends a CIP 3.6 ft (1.1 m) upstream from a joint between adjacent barrier segments. This CIP would evaluate the potential for the small car to snag on the tapered HSS 5x5 tube ends along the reduced-deflection system. Other impact points were not critical, since the knee contact with the vehicle’s door would not be a concern as the PCB deflection in the small car impacts is much lower than the pickup truck, and the small car instability due to knee contact seems unlikely. In addition, other safety concerns, including occupant risk values, barrier deflection, and bumper climb, were not believed to be more critical with other impact points. Thus, the 1100C vehicle impacting at 3.6 ft (1.1 m) upstream from the transition joint and tapered tubes was simulated. The simulation used a Toyota Yaris model developed by NCAC [21] and modified by MwRSF. A summary of the simulation results for 1100C vehicle impacts with one tube (¼-in. (6-mm) and ¾-in. (10-mm) thick tube) at the base of Joint nos. 1 and 2 is provided in Table 11. Sequential photographs for the simulation with the Yaris vehicle model are shown in Figure 42.

Table 11. Summary of Simulation Results – Thick Single Tube and Dual Tubes

Simulation No.	Lat. OIV ft/s (m/s)	Long. OIV ft/s (m/s)	Lat. ORA g’s	Long. ORA g’s	Roll deg.	Pitch deg.	Lat. Barrier Deflection in. (mm)	Increase in Vertical Bumper Height in. (mm)
¼-in. (6-mm) Thick Steel Tubes	0.7 (0.2)	17.1 (5.2)	11.8	-3.3	-19.9	6.9	38.2 (970)	11.9 (302)
¾-in. (10-mm) Thick Steel Tubes	9.2 (2.8)	18 (5.5)	8.5	-3.1	-21.9	7.5	32.8 (833)	11.6 (295)

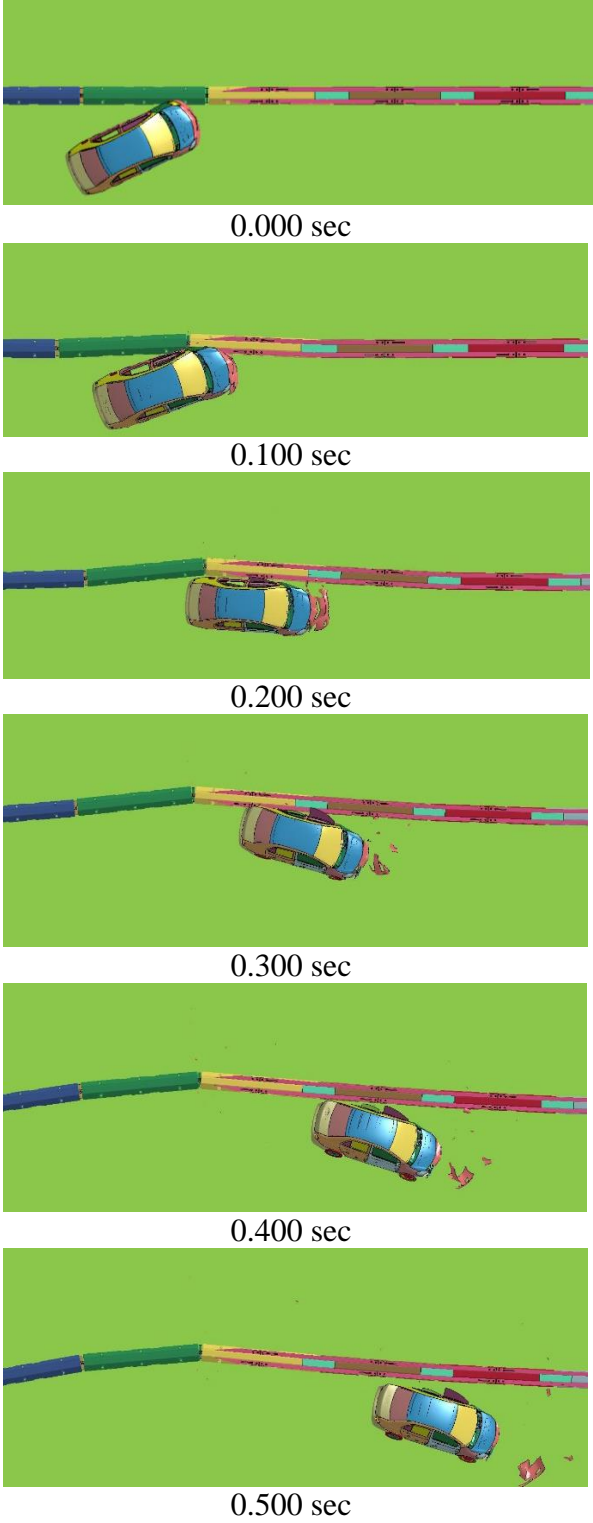
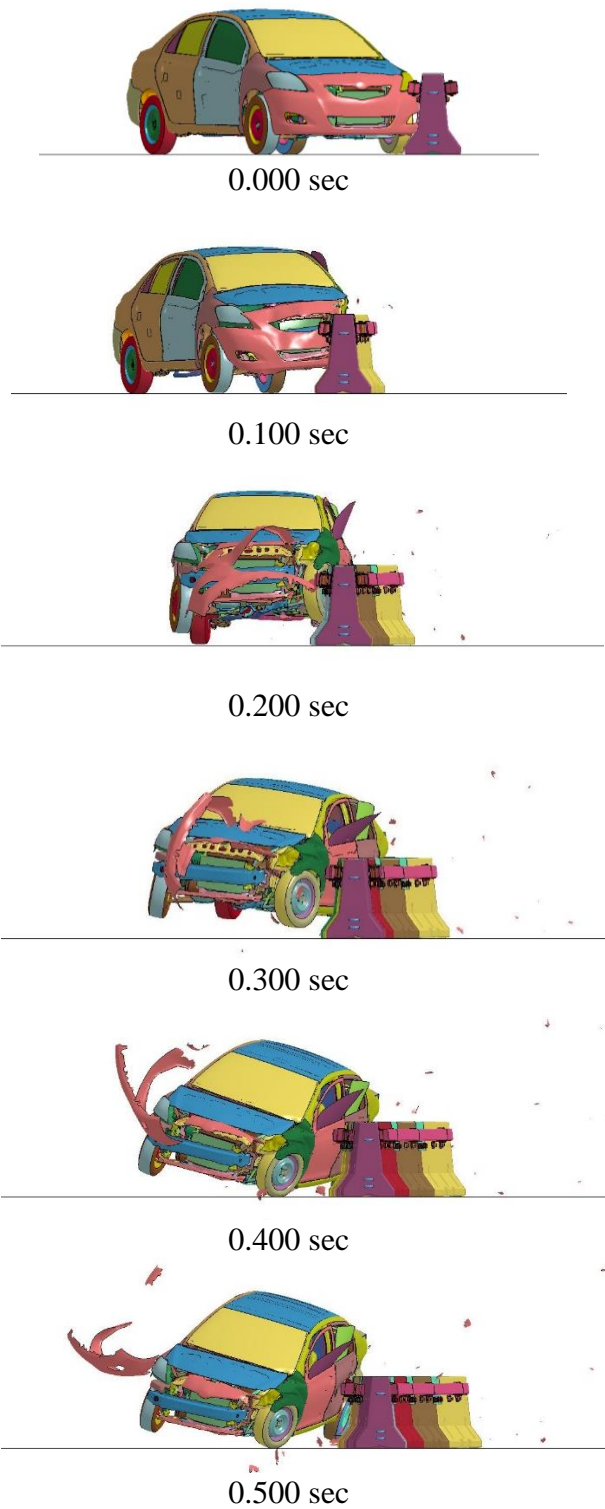


Figure 42. Sequential Photographs: Impact Point at 3.6 ft (1.1 m) Upstream from Transition Joint

8.3 MASH 2016 TL-3 Test Matrix for Evaluation of Transition

As noted previously, the stiffness for reduced-deflection PCB systems and free-standing PCB systems vary significantly. As such, the transition between these two systems incorporates two significant stiffness changes, one from the reduced-deflection PCB to the transition section and the other from the transition section to the free-standing PCB, both of which can increase the potential for pocketing, snag, and vehicle instability. Thus, it is recommended to conduct transition testing at both locations for test no. 3-21 (i.e., upstream from the end of the free-standing PCB and upstream from the reduced-deflection PCB system) at the CIPs obtained from the computer simulation effort.

The MASH 2016-recommended CIP for rigid portable concrete barriers is 4.3 ft (1.3 m) upstream from a joint between adjacent barrier segments. This CIP is recommended based on the shear displacement as the vehicle approaches a joint and the amount of barrier tipping. As such, shear displacement at a joint can lead to snagging and barrier tipping can lead to vaulting and vehicle rollover. The crash testing at this impact point evaluates the structural capacity, vehicle snag, occupant risk, and vehicle stability. Thus, for the current study, a CIP for test designation no. 3-21 was recommended to be 4.3 ft (1.3 m) upstream from a joint between adjacent barrier segments. This impact point also evaluates vehicle snag on tapered tubes.

Moreover, the simulations indicated that the impact point at 669.3 in. (17,000 mm) upstream from the transition joint would induce relatively large forward deflection of PCB segments, knee-formation concern, and a large roll angle. Thus, the second CIP for 2270P vehicle crash testing with test designation no. 3-21 was recommended to be 669.3 in. (17,000 mm) upstream from the transition joint.

Similarly, the MASH 2016-recommended CIP for rigid concrete barriers impacted by an 1100C small car is 3.6 ft (1.1 m) upstream from a joint between adjacent barrier segments to evaluate the vehicle snag and rollover upon approaching a joint between the segments. Thus, for the current study, a CIP for test designation no. 3-20 with an 1100C small car was recommended to be 3.6 ft (1.1 m) upstream from a joint between adjacent barrier segments. This impact point also evaluates vehicle snag on tapered tubes. The MASH 2016 TL-3 test matrix for evaluation of the transition is shown in Table 12.

Table 12. MASH 2016 TL-3 Test Matrix for Evaluation of Transition

Test No.	Vehicle Designation	Speed mph	Angle Deg.	Impact Point
3-21	2270P	62	25	CIP 1- 4.3 ft (1.3 m) Upstream from Transition Joint
3-21	2270P	62	25	CIP 2- 55.7 ft (17 m) Upstream from Transition Joint
3-20	1100C	62	25	CIP 1- 3.6 ft (1.1 m) Upstream from Transition Joint

9 SUMMARY, CONCLUSIONS, AND RECOMMENDATIONS

This research focused on development and analysis of a crashworthy transition between the reduced-deflection PCB and free-standing PCB through engineering analysis and LS-DYNA computer simulation. First, HSS 5x5x $\frac{1}{4}$ tubes along the sides of the reduced-deflection system were tapered down to match the surface of the free-standing PCB segments at a 1:6 lateral-to-longitudinal rate to reduce the potential for vehicle snag. When investigating the transition without proper changes in barrier stiffness, a number of impact points revealed a “knee-shape” that formed in the free-standing PCB system, which allowed a PCB segment to deflect forward and contact the pickup truck’s door. The knee strike on the vehicle’s door showed a tendency to increase vehicle instability as observed in test no. NELON-2 [22]. In this crash test, a knee formed, contacted the vehicle’s door, and induced excessive roll, which was not captured in the Finite Element Analysis (FEA) simulations.

Several design concepts were investigated through LS-DYNA simulations to mitigate the concern of knee formation and provide a safe transition from the reduced-deflection PCB system to the free-standing PCB system. These concepts included: adding one HSS 3 $\frac{1}{2}$ x3 $\frac{1}{2}$ x $\frac{1}{4}$ tube at one joint (Joint no. 1) as well as at two joints (Joint Nos. 1 and 2); adding one HSS 3 $\frac{1}{2}$ x3 $\frac{1}{2}$ x $\frac{3}{8}$ tube at two joints (Joint Nos. 1 and 2); utilizing one HSS 3 $\frac{1}{2}$ x3 $\frac{1}{2}$ x $\frac{1}{4}$ tube with one HSS 2 $\frac{1}{2}$ x2 $\frac{1}{2}$ x $\frac{1}{4}$ tube inside; and using a stack of two HSS 3 $\frac{1}{2}$ x1 $\frac{1}{2}$ x $\frac{1}{4}$ tubes. The simulations with an HSS 3 $\frac{1}{2}$ x1 $\frac{1}{2}$ x $\frac{1}{4}$ tube at two joints had lateral ORAs 10 to 20 percent less than observed in the simulations with a tube at one joint. Adding tubes at two joints created a smoother redirection as more barrier segments were engaged throughout the impact region. Also, concerns for vehicle snag and a knee hitting the vehicle’s door were decreased. Also, based on this numerical study, it was believed that a minimum of eight free-standing barrier segments would be needed upstream from the transition joint (Joint no. 1 first joint with tube).

The concept of adding an increased stiffness (HSS 3 $\frac{1}{2}$ x3 $\frac{1}{2}$ x $\frac{3}{8}$) tube at the base of the two joints located upstream from the reduced-deflection PCB system was selected due to the improved transition performance in terms of less knee contact with the vehicle’s door and decreased barrier deflection as compared to the option with a thinner tube spacer (HSS 2 $\frac{1}{2}$ x2 $\frac{1}{2}$ x $\frac{1}{4}$). Although all concepts of adding one HSS 3 $\frac{1}{2}$ x3 $\frac{1}{2}$ x $\frac{3}{8}$ tube and dual tubes at Joint nos. 1 and 2 indicated a promising improvement in the vehicle and barrier performance in terms of decreased potential of vehicle snag, decreased ORAs, smoother vehicle redirection, and mitigation of knee formation, the option of one tube was preferred over dual tubes due to ease of installation.

Further simulations with different impact points were performed to determine the CIPs for full-scale crash testing of the selected design. The MASH 2016-recommended impact point for test designation no. 3-21 is 4.3 ft (1.3 m) upstream from the joint between adjacent barrier segments to evaluate vehicle snag on both the PCB joint as well as the tapered steel tube. In addition, the impact points farther upstream from the reduced-deflection system, including at 511.8 in. (13,000 mm) through 820.9 in. (20,850 mm), had larger deflections and larger roll and pitch angles. The impact point at 669.3 in. (17,000 mm) upstream from the transition joint had the maximum roll angle (18.5 deg.), a dynamic deflection of 83 in. (2,108 mm), and the knee contacted the vehicle’s door. Based on previous PCB crash testing with a knee forming between adjacent PCBs and the highest roll angle in the simulations, there may be a need to evaluate this impact condition and evaluate the risk of vehicle instability due to the knee contact. For test designation

no. 3-21, two impact locations may be critical, one 4.3 ft (1.3 m) upstream from the transition joint (MASH 2016-recommended CIP) and one 55.7 ft (17 m) upstream from the transition joint. For test no. 3-20 with an 1100C car, the MASH 2016-recommended CIP is 3.6 ft (1.1 m) upstream from a joint between adjacent barrier segments.

Therefore, it was recommended to conduct three full-scale crash tests, two with test designation no. 3-21 using a 2270P pickup truck vehicle with impact points 4.3 ft and 55.7 ft (1.3 m and 17 m) upstream from the joint between adjacent barrier segments and one with test designation no. 3-20 with an 1100C passenger car with an impact point 3.6 ft (1.1 m) upstream from a joint between adjacent barrier segments, as shown in Figure 43.

Based on the numerical study that was performed to develop a transition design between the free-standing PCB and the reduced-deflection PCB system, it is believed that the concept of tapering the end section of the HSS $5 \times 5 \times \frac{3}{16}$ continuous tubes along the reduced-deflection PCB segments and adding an HSS $3 \frac{1}{2} \times 3 \frac{1}{2} \times \frac{3}{8}$ tube at the base of the two joints located upstream from the reduced-deflection PCB system would provide a smooth and safe transition, mitigate the knee contact with the vehicle's door, decrease the barrier deflection, and have high potential to pass the MASH 2016 safety criteria.

Additional research is required to finalize the transition design, including the preparation of details for the spacer tube and connection between the flared box-beam tube and the PCB segments to minimize the vehicle snag.

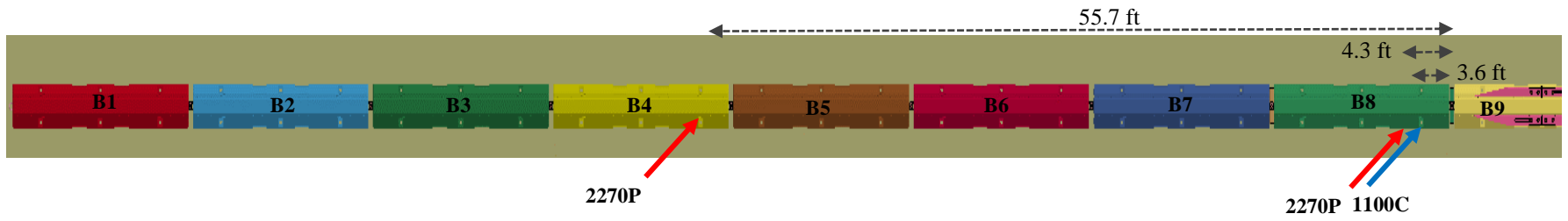


Figure 43. Recommended CIPs – 3.6 ft (1.1 m) Upstream from Transition Joint for 1100C Vehicle Testing (Blue Arrow) and 4.3 ft and 55.7 ft (1.3 m and 17 m) upstream from Transition joint for 2270P Vehicle Testing (Red Arrows)

10 REFERENCES

1. Faller, R. K., Rohde, J. R., Rosson, B. T., Smith, R. P., and Addink, K. H., *Development of a TL-3 F-Shape Temporary Concrete Median Barrier*, Report No. TRP-03-64-96, Midwest Roadside Safety Facility, University of Nebraska-Lincoln, Lincoln, Nebraska, December 1996.
2. Faller, R.K., Rohde, J.R., Rosson, B.T., Smith, R.P., Addink, K.H., *Development of a TL-3 F-Shape Temporary Concrete Median Barrier*, Transportation Research Board Paper No. 97-1207, Washington D.C., December 9, 1996.
3. Polivka, K.A., Faller, R.K., Sicking, D.L., Rohde, J.R., Bielenberg, B.W., Reid, J.D., and Coon, B.A., *Performance Evaluation of the Free-Standing Temporary Barrier – Update to NCHRP 350 Test No. 3-11 (2214TB-1)*, Report No. TRP-03-173-06, Midwest Roadside Safety Facility, University of Nebraska-Lincoln, Lincoln, Nebraska, October 11, 2006.
4. Polivka, K.A., Faller, R.K., Sicking, D.L., Rohde, J.R., Bielenberg, B.W., Reid, J.D., and Coon, B.A., *Performance Evaluation of the Free-Standing Temporary Barrier – Update to NCHRP 350 Test No. 3-11 with 28” C.G. Height (2214TB-2)*, Report No. TRP-03-174-06, Midwest Roadside Safety Facility, University of Nebraska-Lincoln, Lincoln, Nebraska, October 12, 2006.
5. Bielenberg, R.W., Quinn, T.E., Faller, R.K., Sicking, D.L., and Reid, J.D., *Development of a Retrofit, Low-Deflection, Temporary Concrete Barrier System*, Report No. TRP-03-295-14, Midwest Roadside Safety Facility, University of Nebraska-Lincoln, Lincoln, Nebraska, March 31, 2014.
6. Bielenberg, R.W., Schmidt, J.D., Faller, R.K., Reid, J.D., and Emerson, E., *Development of a Retrofit, Low-Deflection Temporary Concrete Barrier System*, Paper No. 16-1596, Presented at the Annual Meeting of the Transportation Research Board and Published in the Compendium of Papers, TRB AFB20 Committee on Roadside Safety Design, Transportation Research Board, Washington, D.C., January 2016.
7. *Manual for Assessing Safety Hardware (MASH), Second Edition*, American Association of State Highway and Transportation Officials (AASHTO), Washington, D.C., 2016.
8. Ross, H.E., Sicking, D.L., Zimmer, R.A., and Michie, J.D., *Recommended Procedures for the Safety Performance Evaluation of Highway Features*, National Cooperative Highway Research Program (NCHRP) Report 350, Transportation Research Board, Washington, D.C., 1993.
9. Bielenberg, R.W., Faller, R.K., Rohde, J.R., Reid, J.D., Sicking, D.L., and Holloway, J.C., *Development of Tie-Down and Transition Systems for Temporary Concrete Barrier on Asphalt Road Surfaces*, Report No. TRP-03-180-06, Midwest Roadside Safety Facility, University of Nebraska-Lincoln, Lincoln, Nebraska, February 23, 2007.
10. *Manual for Assessing Safety Hardware (MASH)*, American Association of State Highway and Transportation Officials (AASHTO), Washington, D.C., 2009.

11. Wiebelhaus, M.J., Terpsma, R.J., Lechtenberg, K.A., Reid, J.D., Faller, R.K., Bielenberg, R.W., Rohde, J.R., and Sicking, D.L., *Development of a Temporary Concrete Barrier to Permanent Concrete Median Barrier Approach Transition*, Report No. TRP-03-208-10, Midwest Roadside Safety Facility, University of Nebraska-Lincoln, Lincoln, NE, July 15, 2010.
12. Sheikh, N.M. and Menges, W.L., *Transition Design for Pinned-Down Anchored Temporary Barrier to Rigid Concrete Barrier*, Report No. 405160-34-1, Texas Transportation Institute, College Station, Texas, November 2012.
13. Halladay, M.L., Federal Highway Administration, *Eligibility Letter No. HAS-10/CC69-b for the Box-Beam Burster Energy Absorbing Single-Sided Crash Cushion (BEAT-SSCC) as an NCHRP Report 350 crash cushion at test level 3*. To Kaddo Kothmann, Road Systems, Inc., Big Spring, Texas, February 22, 2002.
14. Road Systems, Inc., *BEAT SSCC VAR 112707 with photos*, February 13, 2014.
15. Road Systems, Inc., *sscc PI sheet*, February 15, 2013.
16. Baxter, J.R., Federal Highway Administration, *Eligibility Letter No. HAS-10/B-143 for a transition design from a box-beam guardrail to a permanent concrete barrier*. To William Williams, Wyoming Department of Transportation, February 9, 2006.
17. State of New York Department of Transportation, *Box Beam Guide Rail Transition to Concrete Barrier*, Standard Drawing BD-RC3E, January 18, 2008.
18. State of New York Department of Transportation, *Concrete Bridge Barrier Safety Shape Sections & Transition to Box Beam Guide Rail*, Standard Drawing BD-RCB2E, December 23, 2014.
19. Federal Highway Administration, *Guardrail Transitions*, T 5040.26, January 28, 1988, Retrieved online: February 6, 2015, https://safety.fhwa.dot.gov/roadway_dept/policy_guide/road_hardware/barriers/techadvs/archive/t504026/.
20. Hallquist, J.O., *LS-DYNA Keyword User's Manual*, Livermore Software Technology Corporation, Livermore, California, 2007.
21. George Washington University, National Crash Analysis Center, *Vehicle Modeling*, <<http://www.ncac.gwu.edu/research/reports.html>> August 20, 2014. Currently available at: George Mason University, Center for Collision Safety and Analysis, *Research Capability*, <https://www.ccsa.gmu.edu/capability/> August 4, 2017.
22. Bielenberg, R.W., Meyer, D.T., Faller, R.K., and Reid, J.D., *Length of Need and Minimum System Length for F-Shape Portable Concrete Barrier*, Report No. TRP-03-337-17, Midwest Roadside Safety Facility, University of Nebraska-Lincoln, Lincoln, Nebraska, May 3, 2017.

END OF DOCUMENT